*"Life clearly does more than adapt to the Earth. It changes the Earth to its own purposes. Evolution is a tightly coupled dance, with life and the material environment as partners."*

-James Lovelock

*"All the models are wrong, but some of them are useful"*

-George E. P. Box, 1976

# University of Alberta

Stable isotopic fingerprint of resins and ambers: validation of a novel paleoclimatic indicator

by

Gabriela del Pilar González

A thesis submitted to the Faculty of Graduate Studies and Research
in partial fulfillment of the requirements for the degree of

Master of Science

Department of Earth and Atmospheric Sciences



Spring 2014
Edmonton, Alberta

*To my beloved family*

## ABSTRACT

Hydrous and anhydrous thermal maturation experiments were conducted to assess the extent to which diagenetic alteration overprints the primary stable δD and $\delta^{13}C$ isotopic composition of resins. Modern resins recorded an average post-metabolic D exchange <1.9%, compared to only <0.5% for polymerized ambers, and no significant changes were observed in their $\delta^{13}C$. This study also evaluated the seasonal variability of modern resins, to better constrain the primary δD variability of resins. Accordingly, it was observed that in injury-induced resins, the seasonal δD variability could reach up to 80‰, recording short-term climate fluctuations (2–15 days). Moreover, the deuterium fractionation factor between resin and precipitation water ($\varepsilon_{resin\text{-}ppt}$) was found to be -228 ± 19‰. Overall, these results indicate that in resins, D isotopic exchange occurs prior to polymerization, thereby confirming that the stable isotopic composition of their fossilized counterparts constitute a potentially sensitive proxy for paleoenvironmental reconstructions.

## ACKNOWLEDGEMENTS

Foremost, I would like to express my sincere gratitude to my advisor Prof. Dr. Karlis Muehlenbachs, who I personally admire because of his philosophic approach to science. Thanks for your continuous support, patience, scientific motivation, enthusiasm, and immense knowledge. Your guidance and willingness to listen new ideas stimulate my professional creativeness. I could not have imagined having a better advisor and mentor; these lines are not enough to express my gratitude and honor to have worked with you.

Beside my advisor, I would like to thank to the Amber Research Group at the University of Alberta for helping and guiding me in the process of achieving this endeavor. Prof. Dr. Alex Wolfe provided me with constructive critics that led to major improvements of the final manuscript. Dr. Ralf Tappert provided me with critical guidance during my first steps in the lab; with his valuable comments and suggestions he and Dr. Ryan Mckellar significantly helped me in improving this manuscript. My sincere gratitude also goes to all the people that accompanied me during the numerous walks to trap the tree resins on Campus, University of Alberta, and particularly to Dr Muehlenbachs. I also would like to thank my thesis committee, especially Prof. Nadir Erbilgin, for his insightful comments.

I thank my dear friends Olga Levner, with whom I shared great times in and out the stable isotope lab, and Angelina Morales-Izquierdo, a very especial human being, exceptional friend and professional. Thank you both for always being there. Special gratitude to Daniel Petrash, for his continuous support and for stimulating conversations about resins and ambers that somehow ended up on carbonate systems. Last but not least, my deepest gratitude goes to my very supporting and loving family. My parents, Olga de González y Yonny González, for their example of tenacious hard work, positive mind set, and encouragement to accomplish each goal against any adversity. Off course I thank to my best friends and siblings, Olga and Jhonny González for all the good times, and my extended family.

## TABLE OF CONTENT

## LIST OF TABLES

## LIST OF FIGURES

## LIST OF ABBREVIATIONS

ABM: *Abies balsamea* specimen

AT: anhydrous thermal conditions (Thermal gravimetric analysis -TGA)

BS: Black Spruce, *Picea pungens*

$\delta^{13}C_{ppt}$: Carbon isotopic composition of precipitation

$\delta^{13}C_{resin}$: Carbon isotopic composition of resins

DA: Dominican Amber

DA-BE: Dominican amber before experimental treatment

DA-n: Dominican amber after hydrothermal treatment. n (5, 15, 30, 240 and 365 days), represents the number of days that samples were under described conditions.

DOX: 1-deoxy-d-xylulose-5-phosphate pathway

DTG: Derivative of thermal gravimetric weight loss curves

$[D_x]$: Hydrogen isotopic concentration of deuterated waters (x=w) or organic compounds (x= modern or fossil resins) in ppm.

$[D_{w\text{-}resin}]$: Deuterium isotopic exchange between deuterium reach waters and resins (modern or fossil resins) in ppm.

$\delta D_x$: Hydrogen isotopic composition of deuterated waters (x= w), seasonal precipitation (x= ppt) or organic compounds (x= modern or fossil resins).

FTIR: Micro-Fourier-transform infrared spectroscopy

GLA: Grassy lake amber

GLA-BE: Grassy lake amber before experimental treatment

GLA-n: Grassy lake amber after hydrothermal treatment. n (5, 15, 30, 240 and 365 days), number of days that samples were under described conditions.

HT: Hydrous thermal treatment

HC: *Hymenaea courbaril* resins

HC-BE: *Hymenaea courbaril* resins before experimental treatment

HC-n: *Hymenaea courbaril* resins after hydrothermal treatment. n (5, 15, 30, 240 and 365 days), represents the number of days that samples were under described conditions.

IAEA: International Atomic Energy Agency

MG: *Metasequoia glyptostroboides*

MG-BE: *Metasequoia glyptostroboides* before experimental treatment

MG-n: *Metasequoia glyptostroboides* after hydrothermal treatment. n (5, 15, 30, 240 and 365 days), number of days that samples were under described conditions.

MEP: methylerythritol phosphate biosynthetic pathway

MVA: mevalonic acid

PM: *Picea mariana* specimen

TGA: Thermal gravimetric analyses

TOL: *Thuja occidentalis* specimen

VSMOW: Vienna Standard Mean Ocean Water

VPDB: Vienna Pee Dee Belemnite

WUE: Water use efficiency

WS: White spruce, *Picea glauca*

# CHAPTER 1

# General Introduction

## 1.1. Preamble

As part of a survival strategy to adapt to threatening environmental conditions and to deter a variety of herbivores and pathogens, trees have developed a complex defense mechanism based on the production of secondary metabolites (Libby et al., 1976; Levin, 1976; Anderson et al., 1992; Murray et al., 1998; Langenheim, 2003; Nissenbaum et al., 2005). Among the most important secondary metabolites are constitutive and induced resin acids, includes terpenoids, which are copiously produced in response to injuries caused by herbivores or parasites (Trapp and Croteau, 2001). Because the biosynthesis of secondary metabolites occurs in close association with local environmental variables, the stable isotope composition of their polymerization products (henceforth referred to as resins) may preserve valuable paleoclimatic information (Nissenbaum et al., 2005).

Resins are primarily derived from terpenoids (plant isoprenoids), carboxylic acids, and associated alcohols (Langenheim, 1969; Langenheim, 1995; Langenheim, 2003; Bouvier et al., 2005). They polymerize rapidly under exposure to light and air, forming a solid mixture of compounds that may transform into amber after long-term exposure to thermal diagenesis (Langenheim, 2003), and can be found preserved in coal seams and associated thermally immature sediments (Langenheim, 2003). The stable isotopic

composition of resin reflects in part the primary pool of source water accessed by the plant, in addition to fractionation during biosynthesis (Yakir and DeNiro, 1990; Sessions et al., 1999; Schmidt et al., 2003; Sessions et al., 2006; Diefendorf et al., 2012; Tappert et al., 2013).

By further evaluating this idea, it has been observed that amber seems to preserve most of the chemical, and perhaps also isotopic, features of its immature resin precursor (Simoneit et al., 1986; Nissenbaum and Yakir, 1995; Stout, 1995; Tappert et al., 2013). Furthermore, despite the effects of polymerization, volatile losses, and in many cases coalification, in terms of chemical composition, amber is likely equivalent to modern resins (Grimalt et al., 1988). Thus, ambers are increasingly considered pristine geological time capsules from which it is possible to constrain the evolution of terrestrial climates and their associated biota, not only by using their stable chemical and isotopic compositions (*i.e.*, Dal Corso et al., 2013), but also by evaluating their organic inclusions, which provide valuable paleoecological data, useful to constrain the evolution of terrestrial biota (*e.g.*, McKellar et al., 2008; 2011). Moreover, because of their wide geographic and limited temporal distribution, it has been suggested that a more extended use of amber in paleoclimatic studies would enable reliable global-scale environmental correlations (*i.e.*, Nissenbaum and Yakir, 1995; Nissenbaum et al., 2005; McKellar et al., 2008).

However, because the diagenetic pathways of terpenoids and other compounds comprising resins are still poorly constrained (Schimmelmann et al. 1999, 2001, 2006; Sessions et al., 2004; DeBond et al., 2012), and since resins

may have undergone a series of diagenetic reactions involving isotopic exchange prior to preservation in the geological record (Nissenbaum et al., 2005), there is a strong need to assess the extent of deuterium and carbon isotope exchangeability during burial. This will allow us to firmly establish their paleoclimatic potential, and determine whether their deuterium composition reflects ambient conditions at the time of resin exudation, or has been reset due to fluid-rock interactions.

In this chapter, I first provide a brief review of the nature of resins, from their exudative stage to their deposition into host rocks, where they can be diagenetically transformed into amber. Then, I summarize the analytical approach pursued in this thesis, which combines experimental and seasonal observations on the δD and $\delta^{13}C$ of modern resins in order to assess the relative importance of various post-depositional factors in exerting a major control over the hydrogen and carbon isotope variability reported in some amber deposits (*i.e.*, Mckellar et al., 2008). A better understanding of the natural isotopic variability of resin precursors and the extent of post-depositional hydrogen exchange during maturation is essential for using δD and $\delta^{13}C$ of amber in paleoclimate reconstructions.

### 1.2. Rationale

Previous studies on the stable isotope composition of amber deposits have shown that their δD, $\delta^{13}C$, and $\delta^{18}O$ isotopic ratios may be useful parameters for paleoenvironmental correlations (*i.e.*, Nissenbaum and Yakir, 1995; Murray et al., 1998; Nissenbaum et al., 2005, McKellar et al., 2008; Gaigalas and Halas, 2009;

Dal Corso et al., 2011; Tappert et al., 2013). In this regard, Nissenbaum et al. (2005) first envisioned the potential of combining hydrogen and oxygen isotopes of amber, as a strategy for sensitive reconstructions of past climates, ecological states, and hydrological regimes. They stressed, however, that is not entirely clear to what extent amber δD is diagenetically altered (Nissenbaum et al., 2005); this is because it has been noticed that within a single amber deposit, samples affected by weathering usually exhibit higher degrees of deuterium isotopic variability than unaltered specimens (see Nissenbaum and Yakir, 1995). Hence, amber, as other organically derived compounds preserved in the geologic record, may be affected by isotopic re-equilibration during polymerization and throughout its burial and exhumation history (Nissenbaum et al., 2005; Schimmelman et al., 2006).

The influence of primary biotic factors, such as pine beetle (Coleoptera: Scolytidae) outbreak, on the isotopic composition of induced resins has been addressed in the past (McKellar et al., 2011). Yet, other mechanisms and factors controlling the hydrogen isotopic variability of modern and fossilized resins are still poorly constrained. Thus, there is still a high degree of uncertainty on whether the variability of δD of fossil resins can be used as proxy data for paleohydrological reconstruction. In order to determine the influence of diagenetic alteration on the primary δD of fossil resins, the hydrogen exchangeability between resin and diagenetic fluids needs to be assessed within an experimental framework that allow modeling multiple conditions of maturation under variable burial diagenetic paths.

Aiming to quantify the amount of exchangeable hydrogen in resins and ambers in a range of shallow burial diagenetic conditions, this study implements a multifaceted analytical protocol that includes: (1) hydrous thermal hydrogen isotopic exchange, and (2) sample characterization before and after hydrous alteration, both by thermal gravimetric analysis (TGA) and Fourier-transform infrared spectroscopy (FTIR) (Chapter 2). In a second stage, detailed FTIR spectral analyses were implemented in order to determine compositional changes related with simulated shallow burial diagenetic conditions of hydrous-thermally (HT) and anhydrous-thermally (TGA) treated resin and amber analogue samples (Chapter 3). Finally, a time-series sampling of coniferous trees was conducted, aiming to evaluate the natural variability of δD values of modern resins as a result of seasonal temperature and precipitation changes. The latter is envisioned as a uniformitarian approach useful to constrain the range of seasonal variability of resins, and to what extent the δD of ancient amber reflects such primary variability (Chapter 4)(*e.g.,* Fredlund and Tieszen, 1994).

### 1.3. Overview of relevant biogeochemical processes

This section provides a general outline of the biosynthesis of secondary metabolites, their relation with environmental variables, and the chemical processes that lead to preservation of these compounds in the rock record. From exudation to their preservation and exhumation in geological deposits, resins undergo discrete processes including: (1) polymerization under ambient conditions, (2) deposition in continental sedimentary facies, such as coal seams and associate facies, (3) early diagenetic degradation, and (4) post-depositional

alteration. Each of these steps induces a range of chemical reactions that may involve isotopic exchange and re-equilibriation with deuterium-rich basinal waters as it has been observed in mineral systems (see Cole and Chakraborty, 2001).

### 1.3.1. Resins: primary composition and functions

Resins are secondary metabolic products derived from photosynthetically-produced carbohydrates, which by being progressively broken down throughout different metabolic pathways produce terpenoid and phenolic compounds (Langenheim, 2003). Terpenes are hydrocarbons, whose building blocks have a defined structural formula comprising of C5 units (isoprene) building blocks. The ranges of terpenoid compounds in resins are to some extent taxon-specific, and may vary between families, genera, and species (Anderson and LePage, 1995; Otto and Wilde, 2001; Otto et al., 2002, 2007). Because of their significance as a defense-related mechanism, terpenoid biosynthesis is considered a major ecological evolutionary advantage that allows conifers to cope with the seasonal attack of insects and pathogens (Trapp and Croteau, 2001; Langenheim, 2003; Zulak and Bohlmann, 2010, and references therein).

Trees capable of producing resins have a reticulate system of ducts, which can transport constitutive or induced resins (Trapp and Croteau, 2001; Kolosova and Bohlmann, 2012). Constitutive resins are present in the cortex and stored in plant parenchyma cells and in their resin ducts, whilst induced resins can be produced by *de novo* reaction in the cambium zone and developing xylem (Martin et al., 2004; Hamberger et al., 2011; Kolosova and Bohlmann, 2012). Induced

resin compounds are often secreted through "pitch-out", which activates the defense mechanism of the tree as a physiological response to block the insects' entry tunnel before they reach the cambium zone, where circulation of sap-water and nutrients occurs (*e.g.*, McKellar et al., 2011).

*1.3.1.1. Biosynthesis of terpenes*

Independent studies by Bohlmann et al. (1998), Sessions et al. (1999) and Schmidt et al. (2003), among others, have described the pathways and sequence of reactions that lead to terpenoids biosynthesis. They have shown that the enzymes responsible of terpenoid biosynthesis are taxonomically related and exhibit substrate specificity. Thus, they can be grouped into classes, with some enzymes being able to produce single terpene products, while others are multi-product producers (Bohlmann et al., 1998). Terpenoid compounds can be biosynthesized by two metabolic pathways, namely the mevalonic acid (MVA) and methylerythritol phosphate (MEP) pathways. Monoterpenes are formed via the MEP pathway, whereas sesquiterpenes are biosynthesized via the classical MVA route. However, the compartmental separation of the two pathways and the extent depends on the species and the physiological conditions (Hemmerlin et al. 2003). Both of these pathways first synthesize isopentenyl diphosphate (IPP) and dimethylallyl diphosphate (DMAPP), which are in turn used by prenyltransferases to produce the substrates of monoterpene (geranyl diphosphate, GPP), sesquiterpenes (farnesyl diphosphate, FPP) and diterpene synthases (geranylgeranyl diphosphate, GGPP) (Keeling and Bohlmann, 2006; Zulak and Bohlmann, 2010) (Fig.1-1).

Accordingly, it has also been found that the enzymatic reactions involved in the production of traumatic response terpenoids are capable of synthesizing both volatile (C10 monoterpenes, C15 sesquiterpene), and non-volatile (C20 diterpenes) compounds in relatively short timespans (Zulak et al, 2009). Importantly, of the two-biosynthetic pathways described above, the most crucial seems to be the MEP pathway, throughout deoxy-D-xylulose DOX production (Eisenreich et al., 2001; Bouvier et al., 2005; Zulak et al, 2009) (Table 1-1). Whether monocyclic or polycyclic, the mixtures of terpenoid acids polymerizes under oxygen and sunlight exposure, to produce more complex molecular structures that form solid resins (Langenheim, 2003; Bouvier et al., 2005) (Fig. 1-1).

*1.3.1.2. Biotic and abiotic factors influencing the stable isotopic composition of resins*

The variability in stable isotope composition of biochemical compounds produced by land plants can be influenced by a number of abiotic and biotic factors (*e.g.*, Terwilliger and DeNiro, 1995). Among the most important abiotic factors are the isotopic compositions of source pools. In the case of carbon isotopic composition of resins, atmospheric $CO_{2(g)}$ is the primary source of carbon for plants (Diefendorf et al., 2010; Diefendorf et al., 2012). Recent studies have shown that the bulk carbon isotopic composition of resins could be compared with that of bulk leaf material (Stout, 1995; Diefendorf et al., 2012; Tappert et al., 2013 and reference therein). Conversely, different water sources and processes can influence the primary hydrogen isotopic composition of resins. These include

ground water, surface water and precipitation (Craig and Gordon, 1965; Dawson et al., 1998); as well as local humidity and temperature variations (Dawson et al., 2002). Such factors are related to: (1) regional climate (Nissenbaum and Yakir, 1995), which controls isotopic composition of seasonal environmental waters; and (2) seasonal changes (*i.e.*, Sessions, 2006).

Similarly, there are a number of biotic factors that regulate the incorporation of deuterium and carbon isotopes into plant-derived molecules, among them are: (1) genetic code (Trapp and Croteau, 2001; Martin et al., 2002; Zulak and Bohlmann, 2010); and (2) stress source during growth, such as beetle and pathogen attacks (Lorio and Sommers, 1986; McKellar et al., 2011). However, in terms of the hydrogen isotope, the most important is the biosynthetic pathway that produces terpene compounds (Chikaraishi, 2004; Chikaraishi et al., 2004; Sessions et al., 1999; Sessions, 2006). It has been found that the synthesis of terpenes in different organelles within the cells induces specific hydrogen isotope fingerprints (Schmidt, 2003). Thus, it has been suggested that the MVA-pathway operates in the cytosol or mitochondria; whilst MEP/DOX-pathway occurs in the plastids or chloroplast, and also that this difference is capable of producing compounds with different deuterium isotope compositions (Rohmer, 1999; Lichtenthalet, 1999; Schmidt et al., 2003).

With respect to ambient waters, it has been suggested that resins are depleted by approximately -150‰ to -200‰ (Estep and Hoering, 1980; Nissenbaum and Yakir, 1995; Bouvier et al., 2005; Nissenbaum et al., 2005). An early study by Yakir and DeNiro, (1990) experimentally isolated the production

of photosynthate, and reported that the first products of photosynthesis were depleted in deuterium by ~ -171‰ relative to cell water (see also Bouvier et al., 2005; Hayes, 2001). Several new approaches have been applied to determine isotopic fractionation of terpene compounds. These have shown that the magnitude of D-depletion of terpenes produced via the MVA pathway relative to the water source is approximately 200–250‰ (Chikaraishi et al., 2004; Li et al., 2009; Sessions et al., 1999). On the other hand, polymerizable terpenoids, such as diterpenes produced via MEP/DOXP (2-C-methyl-D-erythritol 4-phosphate/1-deoxy-D-xylulose 5-phosphate), have a larger D depletion, which range from -238‰ to -303‰ (Chikaraishi et al., 2004). More recently, estimates of cellulose deuterium fractionation (228–230‰) have been applied to well-preserved fossil resins showing that terpenoid resin acids may be less depleted that previously thought (Wolfe et al., 2012). Yet, the deuterium fractionation between environmental waters and resin remains to be constrained and the relation between the primary deuterium source pool and the final deuterium fingerprint of secondary metabolites is poorly known.

Both biotic and abiotic factors are responsible of the magnitude of D isotopic fractionation. Thus, those variables constraining the geographic distribution and evolution of resin producing tree species, such as temperature, precipitation, latitude, and altitude seem to be important controls on the final fractionation value (*e.g.*, Poinar and Poinar, 1999). These variables may also influence the hydrogen isotopic fractionation variability caused by different effects, including growth rate and growth stage (see Sachse et al., 2012). In this

regard, different empirical studies simulating water-stress (*i.e.*, Rennenberg et al., 2006), light-stress (*i.e.*, Vogg et al., 1998; Yang et al., 2009) and temperature changes (*i.e.*, Vogg et al., 1998; Rennenberg et al., 2006; Zhou et al., 2011) have demonstrated that such stress factors may drastically affect the isotopic values of different trees' biosynthetic compounds (Yang et al., 2009). Seasonal abiotic factor changes can be considered as the main determinant factor inducing D variability in plant resin (Sachse et al., 2012).

In conifer trees, the dynamics of constitutive against defensive resin production depends on seasonality. Defensive terpenoid biosynthesis is the most dynamic process, as it allows continuous synthesis and storage of resins, affecting the rates of carbon allocation from growth-reproduction to defense-related processes. The allocation is physiologically controlled by outbreaks of pathogens, pests, and other selective stress sources (Levin, 1976; Lorio and Sommers, 1986). Accordingly, as a response to insect reproductive cycles, trees initiate stages of enhanced production of secondary metabolites, and thus insect outbreaks, in association with climate, could indirectly control the isotopic fingerprint of resins (Lombardero and Ayres, 2000; McKellar et al., 2011).

By extrapolating the modern conditions of resin production into the geological past, a clear relation between ancient insect attack and trees' physiological response emerges, and as previously observed in copal (an incompletely polymerized resin) and Baltic amber deposits containing anomalously high accumulations of particular insect assemblages, the accumulation of amber may reflect seasonal insects' reproductive cycles (*e.g.*,

Richardson et al., 1989). However, it is important to investigate further how depositional process may affect the chemical and isotopic composition of fossil resins to more precisely establish the framework for evaluating paleoenvironmental models.

### 1.3.2. Amber production: thermally induced reactions in resins and their preservation

Resins are produced by all families of conifers (*e.g.*, Pinaceae, Araucariaceae and Cupressaceae), and by many families of angiosperms including Fabaceae, Burseraceae, Dipterocarpaceae, and Hamamelidaceae (Langenheim, 1995; Stefanovic et al. 1998; Nel et al., 2004). More recently, gene expression and its relation with the biosynthesis of resin acids have been phylogenetically related (Hamberger et al., 2011). However, relatively few of these modern resin-producing families have been conclusively identified in the fossil record.

Even though some distinctive species may be related through specific biochemical components, which exhibit fingerprints easily identifiable via FTIR analyses (Grimalt et al., 1988; Tappert et al., 2011), and the distribution of resinites' compound pattern allow chemosystematic family identification (*i.e.*, Otto and Wilde, 2001), the presence of some biomarkers and changes in functional groups often indicate secondary molecular modification. Thus, during diagenesis, some reactions induced by changes on temperature, oxygen content and pressure of the diagenetic environments could produce modification of organic functionalities, and therefore changes in FTIR spectral bands.

For instance, it is believed that resins containing a relatively low proportion of volatile constituents are more resistant to oxidative degradation or dehydrogenation, and thus are preferentially preserved in the rock record (Anderson et al., 1992; Langenheim, 1995). Accordingly, ambers preserved under aerobic shallow burial diagenetic conditions are characterized by high unsaturations, polyunsaturated and aromatic compounds (Qin et al., 2010; Otto et al., 2007). These secondary products result from oxidative degradation, which promotes reactions such as decarboxylation, demethylation and dehydrogenation (Otto et al., 2001, 2007; Qin et al., 2012). Aerobic resin degradation can also significantly alter other primary resin constituents, such as abietic and pimaric acids, which form secondary products such as Abieta-6, 8, 11, 13-tetraenoic acid, 7-Oxodehydroabietic acid, simonellite, tetrahydroretene, and norabietatrienes (Simoneit and Mazurek, 1982; Otto et al., 2001, 2002, 2007). Over geologic time, reductive preservation may lead to cross-linking, with this molecular alteration process being particularly pronounced after prolonged exposure to relatively high temperatures (Anderson et al., 1992; Murae et al., 1995; Lambert et al., 2008).

### 1.3.3. Evidence of shallow burial diagenetic alteration

Copious amounts of resinites have been preserved in thermally-immature sediments, principally coal seams having vitrinite reflectance ($R_o$) ranging from 0.2–1.0 %, and inferred temperatures between 50–145 °C (Cornford, 2005; Menor-Salván et al., 2010). Many occurrences were formed under warm climate conditions in wet coastal forest. Other amber occurrences have been found within secondary deposits in sandstone, shale, and glauconite (Langenheim, 2003;

McKellar et al., 2008). Post-depositional processes such as weathering and reworking may also cause differential alteration of amber (McKellar et al, 2011).

It has been observed that chemical alteration of the original resin composition can also lead to: (i) changes in color due to oxidation and hydrolysis (Poinar and Mastalerz, 2000; Pastorelli et al., 2011, 2012, 2013); (ii) molecular rearrangement accompanied by a decrease in hydrogen containing functional groups and an increase in aromatized groups with increasing age (*e.g.*, Murae et al., 1995; Yamamoto et al., 2006; Wolfe et al., 2009), together with the appearance of biomarkers not associated with specific biochemical processes (Anderson et al., 1992; Otto et al., 2001, 2002, 2007); and (iii) possible changes in the original δD composition as a results of isotopic exchange reactions with basinal waters during burial diagenesis (*i.e.*, Schimmelmann et al., 1999, 2001, 2006). All of these diagenetic changes support the possibility that thermal maturation may have induced hydrogen isotopic exchange with both meteoric and formation-aged waters.

### 1.4. Objectives

The purpose of this research is to test the reliability of amber δD as a reliable proxy for the composition of paleoenvironmental waters. Accordingly, I first evaluated the percentage of hydrogen in resins and ambers that undergo exchange with deuterated waters during maturation, determining also the magnitude of secondary isotopic exchange. Secondly, I determined the range of modern resin δD variation and its relation to seasonal changes in temperature and

precipitation by conducting an empirical study of the δD isotopic ratios of resins produced by coniferous trees in the vicinity of the University of Alberta campus and their response to yearly-based environmental stress conditions.

### 1.5. Organization of the study

With the exception of the first and last chapters, each of the following chapters was designed to be a self-contained research paper with results being placed in the context provided by previous studies in that subject area. By applying a range of laboratory experiments, Chapter 2, entitled "*Deuterium exchangeability between deuterium enriched waters, modern and fossil resins at 50 and 90°C*", shows the range of exchangeability of deuterium between resins – ambers and deuterium-rich waters as a function of temperature and time. On the other hand, Chapter 3, entitled "*Fourier transform infrared (FTIR) spectroscopic characterization of modern and fossil resins after long-term hydrous and anhydrous thermal treatments*", provides a novel approach to estimate the maturation conditions of resins based on FTIR analysis. Finally, Chapter 4, entitled "*Seasonal stable isotopic composition of modern conifer resins: implications for the use of amber stable isotopes in paleoclimatic reconstruction*", offers a modern model that indicates the seasonal changes of δD within resins produced by coniferous trees. These were analyzed in order to provide insights about the temporal variability in the deuterium composition of resins, and its relation to environmental conditions, more specifically seasonal changes of precipitation δD, and variable rates of $CO_2$ uptake.

Chapter 5 places results in a more general context, providing a discussion that draws together the disparate lines of evidences into a general working model that permit describing the timing and nature of deuterium exchange in resin, and their physicochemical behaviour with increasing burial. Results are thus placed in the context of amber as a reliable paleoclimatic indicator. This chapter also includes a series of recommendations for future studies.

Table 1-1. List of diterpene resin acids with chemical formulas and reference code used in figure 1-1. (see Sodhi et al., 2013 for details).

| Resin acid name | Formula | Code |
|---|---|---|
| Dehydroabietic acid | $C_{20}H_{28}O_2$ | A |
| Abietic acid | $C_{20}H_{30}O_2$ | B |
| Neoabietic acid | $C_{20}H_{30}O_2$ | C |
| Isopimaric acid | $C_{20}H_{30}O_2$ | D |
| Levopimaric acid | $C_{20}H_{30}O_2$ | E |
| Sandaracopimaric acid | $C_{20}H_{30}O_2$ | F |
| Pimaric acid | $C_{20}H_{30}O_2$ | G |
| Communic acid | $C_{20}H_{30}O_2$ | H |
| Dihydroisopimaric acid | $C_{20}H_{32}O_2$ | I |
| 8(14)-Abietenic acid | $C_{20}H_{32}O_2$ | J |
| 8- Abietenic acid | $C_{20}H_{32}O_2$ | K |
| 7- Oxodehydroabietic acid | $C_{20}H_{26}O_3$ | L |

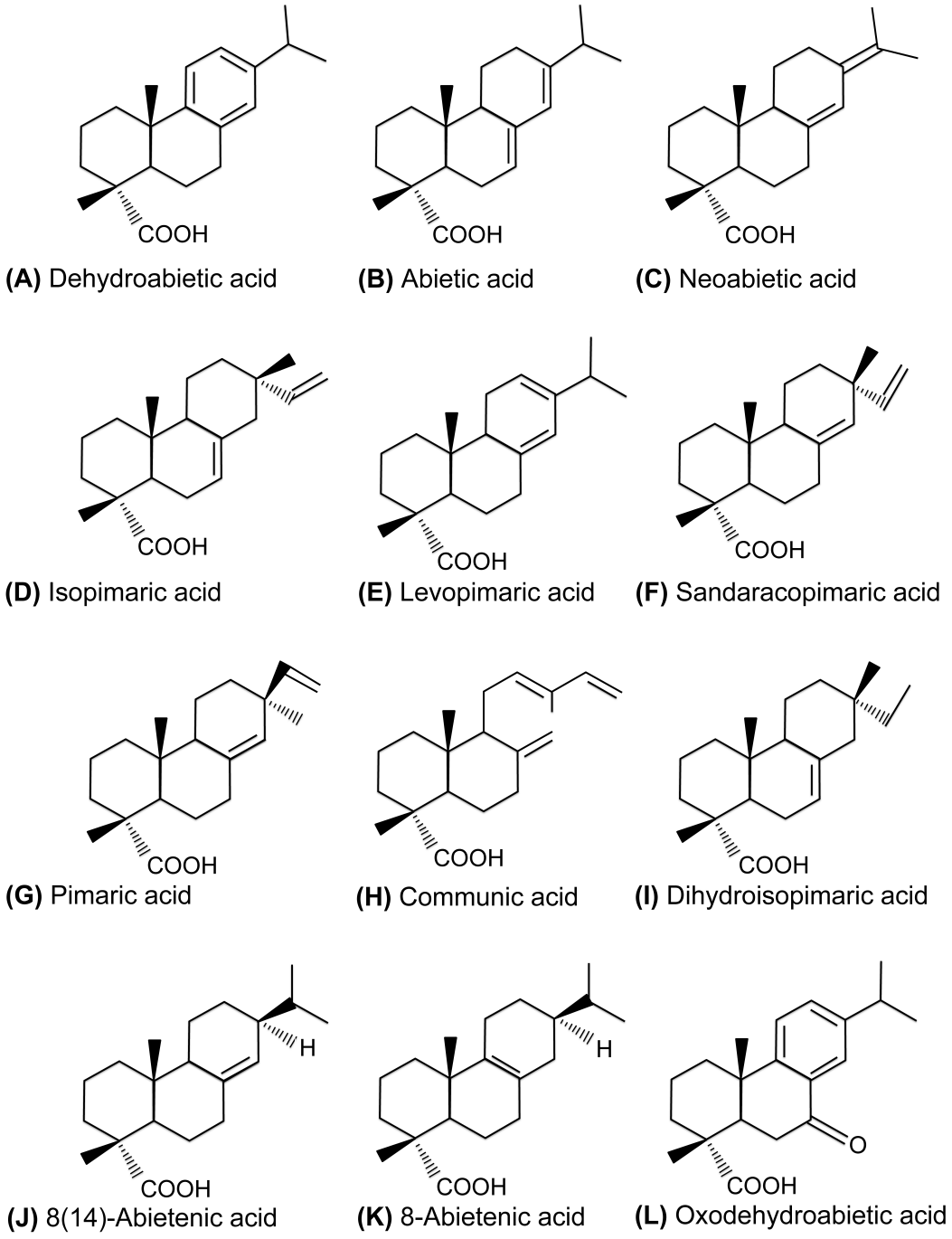


Figure 1-1. Representative structures of some common diterpene (C20) resin acids in confers. The molecules are organize as coded in Table 1-1.

## 1.6. References


Anderson K., Winans, R.E. and Botto, R.E., (1992). The Nature and fate of natural resins in the geosphere. II. Identification, classification and nomenclature of resinites. *Organic Geochemistry*, 18(6), 829–841.

Anderson, K. B. and LePage, B. A., (1995). Analysis of fossil resins from Axel Heiberg Island, Canadian Arctic. *In* Amber, resinite and fossil resins (eds K. B. Anderson & J. C. Crelling), 170–192. Washington, DC: American Chemical Society.

Bohlmann, J., Crock, J., Jetter, R., and Croteau, R., (1998). Terpenoid-based defenses in conifers: cDNA cloning, characterization, and functional expression of wound-inducible (E)-alpha-bisabolene synthase from grand fir (*Abies Grandis*). *Proceedings of the National Academy of Sciences of the United States of America*, 95(12), 6756–6761.

Bouvier, F., Rahier, A. and Camara B., (2005). Biogenesis, molecular regulation and function of plant isoprenoids. *Progress in Lipid Research*, 44(6), 357–429.

Chikaraishi, Y., (2004). Carbon and hydrogen isotopic fractionation during lipid biosynthesis in a higher plant (Cryptomeria japonica). *Phytochemistry*, 65(3), 323–330.

Chikaraishi, Y., Naraoka, H. and Poulson, S. R., (2004). Hydrogen and carbon isotopic fractionations of lipid biosynthesis among terrestrial (C3, C4 and CAM) and aquatic plants. *Phytochemistry*, 65(10), 1369–1381.

Cornford, C., (2005). The petroleum system. Encyclopedia geology. Vol. 3. Elsevier Ltd. 270 p.

Cole, D. R., and Chakraborty, S., (2001). Rates and mechanisms of isotopic exchange, *in Mineralogy and Geochemistry*, 43(1), 83–223.

Craig, H., and Gordon, L.I., (1965). Deuterium and oxygen-18 variations in the ocean and the marine atmosphere. *In*: Tongiorgi, E. (Ed.), Proceedings of the Third Spoletto Conference on Stable Isotopes in Oceanographic Studies and Paleotemperatures, 9–130. CNR-Laboratorio di Geologia Nucleare, London.

Dal Corso, J., Preto, N., Kustatscher, E., Mietto, P., Roghi, G., and Jenkyns, H. C., (2011). Carbon-isotope variability of Triassic Amber, as compared with wood and leaves (Southern Alps, Italy). *Palaeogeography, Palaeoclimatology, Palaeoecology*, 302(3–4), 187–193.

Dawson, T.E., Mambelli, S., Plamboeck, A.H., Templer, P.H., and Tu, K.P., (2002). Stable isotopes in plant ecology. *Annual Review of Ecology and Systematics*, 33(1), 507–559.

Dawson, T.E., Pausch, R.C., Parker, H.M., (1998). The role of hydrogen and oxygen stable isotopes in understanding water movement along the soil–plant-atmospheric continuum. *In*: Griffiths, H. (Ed.), Stable Isotopes: Integration of Biological, Ecological and Geochemical Processes. (Bios Scientific Publishers), 169–183. Oxford, UK.

DeBond, N., Fogel, M.L., Morrill, P.L., Benner, R., Bowden, R., Ziegler, S., (2013). Variable $\delta$ D values among major biochemicals in plants: implications for environmental studies. *Geochimica et Cosmochimica Acta*, 111, 117–127.

Diefendorf, A. F., Freeman, K. H. and Wing, S. L., (2012). Distribution and carbon isotope patterns of diterpenoids and triterpenoids in modern temperate C3 trees and their geochemical significance. *Geochimica et Cosmochimica Acta*, 85, 342–356.

Diefendorf, A. F., Mueller, K. E., Wing, S. L., Koch, P. L. and Freeman, K. H., (2010). Global patterns in leaf $^{13}C$ discrimination and implications for studies of past and future climate. *Procedings of the National Academy of Sciences*, 107, 5738–5743.

Eisenreich W., Rohdich F., and Bacher, A., (2001). Deoxyxylulose phosphate pathway to terpenoids. *Trends in Plant Science*, 6, 78–87.

Estep, M. F., and Hoering, T. C., (1980). Biogeochemistry of the stable hydrogen isotopes. *Geochimica et Cosmochimica Acta*, 44, 1197–1206.

Fredlund, G. G., and Tieszen, L. T., (1994). Modern phytolith assemblages from the North American Great Plains. *Journal of Biogeography*, 21(3), 321–335.

Gaigalas, A., and Halas, S., (2009). Stable isotopes (H, C, S) and the origin of Baltic amber. *Geochronometria*, 33(1), 33–36.

Grimalt, J., Simoneit, B., Hatcher, P., and Nissenbaum, A., (1988). The molecular composition of ambers. *Organic Geochemistry*, 13(4–6), 677–690.

Hayes, J., (2001). Fractionation of carbon and hydrogen isotopes in biosynthetic processes. *Reviews in Mineralogy and Geochemistry*, 43(1), 225–277.

Hamberger, B., Ohnishi, T., Hamberger, B., Séguin, A., and Bohlmann, J., (2011). Evolution of diterpene metabolism: Sitka spruce CYP720B4 catalyzes multiple oxidations in resin acid biosynthesis of conifer defense against insects. *Plant Physiology*, 157(4), 1677–1695.

Hemmerlin, A., Hoeffler, J.F., Meyer, O., Tritsch, D., Kagan, I.A., Grosdemange-Billiard, C., Rohmer, M., Bach, T.J., (2003). Crosstalk between the cytosolic mevalonate and the plastidial methylerythritol phosphate pathways in tobacco bright yellow-2 cells. *Journal of Biological Chemistry*, 278, 26666–26676.

Keeling, C. I., and Bohlmann, J., (2006). Diterpene resin acids in conifers. *Phytochemistry*, 67(22), 2415–2423.

Kolosova, N., and Bohlmann, J., (2012). Growth and defense in plants. *In* Ecological Studies (Matyssek, et al. eds), 220, 85–109. Springer-Verlag Berlin, Heidelberg.

Langenheim, J. H., (1969). Amber: a botanical inquiry. *Science*, 163(3872), 1157.

Langenheim, J.H., (1995). Biology of Amber-producing trees: focus on case studies of *Hymenaea* and *Agathis*. *In* Amber, resinite and fossil resins (eds K. B. Anderson & J. C. Crelling), 170–192. Washington, DC: American Chemical Society.

Langenheim, J.H., (2003). The geologic history and ecology of resins. *In* Plant resins: chemistry, evolution, ecology, and ethnobotany. Timber Press Inc., Portland, Oregon, pp. 201.

Lambert, J. B., Santiago-Blay, J. A., and Anderson, K. B., (2008). Chemical signatures of fossilized resins and recent plant exudates. *Angewandte Chemie*, 47(50), 9608–9616.

Levin, D. A., (1976). The chemical defenses of plants to pathogens and herbivores, *Annual Review of Ecology and Systematics*, *7*(61), 121–159.

Li, C., Sessions, A.L., Kinnamen, F., Valentine, D.L., (2009). Hydrogen-isotopic variability in lipids from Santa Barbara Basin sediments. *Geochimica et Cosmochimica Acta*, 73, 4803–4823.

Libby L., Pandolfi, L., Payton, H., Marshall, J., Giertz-Sienbenlist, V., (1976). Isotopic tree thermometers. *Nature*, 261, 284–288.

Lichtenthaler, H. K., (1999). The 1-deoxy-D-xylulose-5-phosphate pathway of isoprenoid biosynthesis in plants. *Annual Review of Plant Physiology and Plant Molecular Biology*, 50, 47–65.

Lombardero, M., and Ayres, M., (2000). Environmental effects on constitutive and inducible resin defences of *Pinus taeda*. *Ecology Letters*, 1, 329–339.

Lorio P. L., Jr. and Sommers, R.H., (1986). Evidence for competition between growth processes and oleoresin synthesis in *Pinus taeda* L. *Tree Physiology*, 2, 301–306.

Martin, D.M., Faldt, J., and Bohlmann, J., (2004). Functional characterization of nine Norway spruce TPS genes and evolution of gymnosperm terpene synthases of the TPS-d subfamily. *Plant Physiology*, 135, 1908–1927.

Martin, D.M., Tholl, D., Gershenzon, J., and Bohlmann, J., (2002). Methyl jasmonate induces traumatic resin ducts, terpenoid resin biosynthesis, and terpenoid accumulation in developing xylem of Norway spruce stems. *Plant Physiology*, 129, 1003–1018.

McKellar R., Wolfe, A., Tappert, R., Muehlenbachs, K., (2008). Correlation of Grassy Lake and Cedar Lake ambers using infrared spectroscopy, stable isotopes, and palaeoentomology. *Canadian Journal of Earth Sciences*, 45, 1061–1082.

McKellar, R. C., Wolfe, A. P., Muehlenbachs, K., Tappert, R., Engel, M. S., Cheng, T., Sánchez-Azofeifa, G. A., (2011). Insect outbreaks produce distinctive carbon isotope signatures in defensive resins and fossiliferous ambers. *Proceedings. Biological Sciences / The Royal Society*, 278(1722), 3219–24.

Menor-Salván, C., Najarro, N., Velasco, F., Rosales, I., Tornos, F., Simoneit, B. R.T., (2010). Terpenoids in extracts of Lower Cretaceous ambers from the Basque-Cantabrian Basin (El Soplao, Cantabria, Spain): Paleochemotaxonomic Aspects. *Organic Geochemistry*, 41(10), 1089–1103.

Murae, T., Shimokawa, S., and Aihara, A., (1995). Pyrolytic and spectroscopic studies of the diagenetic alteration of resinites. *In* Amber, resinite and fossil resins (eds K. B. Anderson & J. C. Crelling), 76–91. Washington, DC: American Chemical Society.

Murray, A. P., Edwards, D., Hope, J. M., Boreham, C. J., Booth, W. E., Alexander, R. A., and Summons, R. E., (1998). Carbon isotope biogeochemistry of plant resins and derived hydrocarbons. *Organic Geochemistry*, 29(5–7), 1199–1214.

Nel, A., De Ploeg, G., Millet, J., Menier, J. J., Waller, A., (2004). The French amber: a general conspectus and the Lowermost Eocene amber deposit of Le Quesnoy in the Paris Basin. *Geologica Acta*, 2(1), 3–8.

Nissenbaum, A., and Yakir, D., (1995). Stable Isotope Composition of Amber. *In* Amber, resinite and fossil resins (eds. K. B. Anderson & J. C. Crelling), 34–42. Washington, DC: American Chemical Society.

Nissenbaum, A., Yakir, D., and Langenheim, J. H., (2005). Bulk carbon, oxygen, and hydrogen stable isotope composition of recent resins from amber-producing *Hymenaea*. *Die Naturwissenschaften*, 92(1), 26–29.

Otto, A., Simoneit, B. R. T., Lesiak, M., Wilde, V., Worobiec, G., (2001). Resin and wax biomarkers preserved in Miocene Cupressaceae s.1. from Belchatow and Lipnica Wielka, Poland. *Acta Palaeobotanica*, 41, 195–206.

Otto, A., Simoneit, B. R. T., and Wilde, V., (2007). Terpenoids as chemosystematic markers in selected fossil and extant species of pine (*Pinus*, *Pinaceae*). *Botanical Journal of the Linnean Society*, 154, 129–140.

Otto, A., Simoneit, B. R. T., Wilde, V., Kunzmann, L., and Püttmann, W., (2002). Terpenoid composition of three fossil resins from Cretaceous and Tertiary conifers. *Review of Palaeobotany and Palynology*, 120 (3–4), 203–215.

Otto, A., and Wilde, V., (2001). Sesqui-, Di-, and Triterpenoids as chemosystematic markers in extant conifers - A review. *The Botanical Review*, 67, 141–238.

Pastorelli, G., Richter, J., and Shashoua, Y., (2011), Photoageing of Baltic amber – Influence of daylight radiation behind window glass on surface colour and chemistry. *Polymer Degradation and Stability*, 96(11), 1996–2001.

Pastorelli, G., Richter, J., and Shashoua, Y., (2012), Evidence concerning oxidation as a surface reaction in Baltic amber. *Spectrochimica acta. Part A, Molecular and Biomolecular Spectroscopy*, 89, 268–269.

Pastorelli, G., Shashoua, Y., and Richter, J., (2013), Hydrolysis of Baltic amber during thermal ageing--an infrared spectroscopic approach. *Spectrochimica acta. Part A, Molecular and Biomolecular Spectroscopy*, 106, 124–128.

Poinar Jr, G. O., and Poinar, R., (1999). The amber forest: a reconstruction of a vanished world. Princeton, NJ: Princeton University Press. p. 241, Chichester, West Sussex.

Poinar, G.O. Jr., and Mastalerz, M., (2000). Taphonomy of fossilized resins: Determining the biostratinomy of amber. *Acta Geologica Hispanica*, 35(1), 171–182.

Qin, S. J., Sun, Y. Z., Tang, Y. G., (2010). Long term, low temperature maturation of early diagenetic alterations of organic matter from conifers: aliphatic hydrocarbons. *Geochemical Journal*, 44, 247–259.

Qin, S.J., Sun, Y. Z., Tang, Y. G., and Jin, K., (2012). Early diagenetic transformation of terpenoids from conifers in the aromatic hydrocarbon fraction: A long term, low temperature maturation experiment. *Organic Geochemistry*, 53, 99–108.

Rennenberg, H., Loreto, F., Polle, A., Brilli, F., Fares, S., Beniwal, R. S., and Gessler, A., (2006). Physiological responses of forest trees to heat and drought. *Plant Biology (Stuttgart, Germany)*, 8(5), 556–71.

Richardson, D. P., Messer, A. C. S., Greenberg, H. H., Hagedorn, P., Meinwold, J., (1989). Defensive sesquiterpenoids from a dipterocarp (*Dipterocarpus kerrii*). *Journal of Chemical Ecology*. 15(2), 731–747.

Rohmer, M., (1999). A mevalonate-independent route to isopentenyl diphosphate. In: Cane D (ed) Comprehensive Natural Product Chemistry, 2, 45–67. Pergamon Press, Oxford, UK.

Sauer, P.E., Eglinton, T.I., and Hayes, J.M., (2001). Compound-specific D/H ratios of lipid biomarkers from sediments as a proxy for environmental and climatic conditions. *Geochimica et Cosmochimica Acta*, 65(2), 213–222.

Sachse, D., Billault, I., Bowen, G.J., Chikaraishi, Y., Dawson, T. E., Feakins, S.J., Freeman, K.H., R. M., Clayton, McInerney, F.A., van derMeer, M.T.J., Polissar, P., Robins, R.J., Sachs, J.P., Schmidt, H-L., Sessions, A.L., White, J.W.C., West, J.B., and Kahmen, A., (2012). Molecular paleohydrology: interpreting the hydrogen-isotopic composition of lipid biomarkers from photosynthesizing organisms. *Annual Review of Earth and Planetary Sciences*, 40(1), 221–249.

Schmidt, H. L., Werner, R. A., and Eisenreich, W., (2003). Systematics of $^{2}H$ Patterns in Natural Compounds and Its Importance for the Elucidation of Biosynthetic Pathways. *Phytochemistry Reviews*, 2, 61–85.

Schimmelmann, A., Boudou, J. P., Lewan, M. D., and Wintsch, R. P. (2001), Experimental controls on D/H and 13C/12C ratios of kerogen, bitumen and oil during hydrous pyrolysis. *Organic Geochemistry*, 32(8), 1009–1018.

Schimmelmann, A., Lewan, M. D., and Wintsch, R. P. (1999), D/H isotope ratios of kerogen, bitumen, oil, and water in hydrous pyrolysis of source rocks containing kerogen types I, II, IIS, and III. *Geochimica et Cosmochimica Acta*, 63(22), 3751–3766.

Schimmelmann, A., Sessions, A. L., and Mastalerz, M. (2006), Hydrogen Isotopic (D/H) Composition of Organic Matter During Diagenesis and Thermal Maturation. *Annual Review of Earth and Planetary Sciences*, 34(1), 501–533.

Sessions, A., (2006). Seasonal changes in D/H fractionation accompanying lipid biosynthesis in Spartina alterniflora. *Geochimica et Cosmochimica Acta*, 70(9), 2153–2162.

Sessions, A. L., Sylva, S. P., Summons, R. E., and Hayes, J. M., (2004). Isotopic exchange of carbon-bound hydrogen over geologic timescales 1. *Geochimica et Cosmochimica Acta*, 68(7), 1545–1559.

Sessions, A. L., Burgoyne, T. W., Schimmelmann, A., and Hayes, J. M., (1999). Fractionation of hydrogen isotopes in lipid biosynthesis. *Organic Geochemistry*, 30, 1193–1200.

Simoneit, B.R.T., Grimalt, J.O., Wang, T.G., Cox, R.E., Hatcher, P.G., Nissenbaum, A., (1986). Cyclic terpenoids of contemporary resinous plant detritus and of fossil woods, ambers and coals. *Organic Geochemistry*, 10, 877–889.

Simoneit, B. R. T., and Mazurek, M. A., (1982). Organic matter of the troposphere—II. Natural background of biogenic lipid matter in aerosols over the rural western United States. *Atmospheric Environment*, 16(9), 2139–2159.

Sodhi, R. N. S., Mims, C. A., Goacher, R. E., McKague, B., Wolfe, A. P. (2013), Preliminary Characterization of Palaeogene European Ambers Using ToF-SIMS. *Surface and Interface Analysis*, 45(1), 557–560.

Stefanovic, S., Jager, M., Deutsch, J., Broutin, J., Masselot, M., (1998). Phylogenetic relationships of conifers inferred from partial 28S rRNA gene sequences. *American Journal of Botany*, 85, 688–697.

Stout, S. A., (1995). Resin-derived hydrocarbons in fresh and fossil Dammar resins and Miocene rocks and oils in the Mahakam Delta, Indonesia. *In* Amber, resinite and fossil resins (eds K. B. Anderson & J. C. Crelling), 43–75. Washington, DC: American Chemical Society.

Tappert, R., Wolfe, A. P., McKellar, R. C., Tappert, M., and Muehlenbachs, K., (2011). Characterizing modern and fossil gymnosperm exudates using micro-fourier transform infrared spectroscopy. *International Journal of Plant Sciences*, 172(1), 120–138.

Tappert, R., McKellar, R. C., Wolfe, A. P., Tappert, M. C., Ortega-Blanco, J., and Muehlenbachs, K., (2013). Stable carbon isotopes of C3 plant resins and ambers record changes in atmospheric oxygen since the Triassic. *Geochimica et Cosmochimica Acta*, 121, 240–262.

Terwilliger, V.J., and DeNiro, M.J., (1995). Hydrogen isotope fractionation in wood-producing avocado seedlings: biological constraints to paleoclimatic interpretations of δD values in tree ring cellulose nitrate. *Geochimica et Cosmochimica Acta*, 59, 5199–5207.

Trapp, S., and Croteau, R., (2001). Defensive resin biosynthesis in conifers. *Annual Review of Plant Physiology and Plant Molecular Biology*, 52, 689–724.

Vogg, G., Heim, R., Hansen, J., Schäfer, C., and Beck, E., (1998). Frost hardening and photosynthetic performance of Scots pine (Pinus sylvestris L.) needles. I. Seasonal changes in the photosynthetic apparatus and its function. *Planta*, 204(2), 193–200.

Wolfe, A. P., Csank, A. Z., Reyes, A.V.E., McKellar, R.C., Tappert, R., and Muehlenbachs, K. (2012), Pristine Early Eocene wood buried deeply in kimberlite from northern Canada. *PloS One*, 7(9), e45537.

Wolfe, A. P., Tappert, R., Muehlenbachs, K., Boudreau, M., McKellar, R. C., Basinger, J.F., and Garrett A. (2009), A new proposal concerning the botanical origin of Baltic amber. *Proceedings of the Royal Society, Biological Sciences*, 276 (1672), 3403–3412.

Yakir, D., and DeNiro, M. J., (1990). Oxygen and hydrogen isotope fractionation during cellulose metabolism in *Lemna gibba. Plant Physiology*, 93(1), 325–332.

Yamamoto, S., Otto, A., Krumbiegel, G., and Simoneit, B. R. T., (2006). The natural product biomarkers in succinite, glessite and stantienite ambers from Bitterfeld, Germany. *Palaeobotany Palynology*, 140, 27–49.

Yang, H., Pagani, M., Briggs, D. E. G., Equiza, M. A., Jagels, R., Leng, Q., and Lepage, B. A., (2009). Carbon and hydrogen isotope fractionation under continuous light: implications for paleoenvironmental interpretations of the High Arctic during Paleogene warming. *Oecologia*, 160(3), 461–470.

Zhou, Y., Grice, K., Chikaraishi, Y., Stuart-Williams, H., Farquhar, G. D., and Ohkouchi, N., (2011). Temperature effect on leaf water deuterium enrichment and isotopic fractionation during leaf lipid biosynthesis: results from controlled growth of C3 and C4 land plants. *Phytochemistry*, 72(2–3), 207–213.

Zulak, K. G., and J. Bohlmann (2010), Terpenoid biosynthesis and specialized vascular cells of conifer defense. *Journal of Integrative Plant Biology*, 52(1), 86–97.

Zulak, K. G., Lippert, D. N., Kuzyk, M. a, Domanski, D., Chou, T., Borchers, C. H., & Bohlmann, J., (2009). Targeted proteomics using selected reaction monitoring reveals the induction of specific terpene synthases in a multi-level study of methyl jasmonate-treated Norway spruce (*Picea abies*). *The Plant Journal for Cell and Molecular Biology*, 60(6), 1015–30.

## CHAPTER 2

## Deuterium exchangeability between deuterium rich waters, modern and fossil resins at 50 and 90°C

### 2.1. Introduction

Stable isotope ratios of fossilized plant-derived resins have the potential to be used as valuable paleoclimatic and paleoecological proxies. Due to their macromolecular, highly polymerized structure, fossil resins can retain pristine chemical and isotopic signatures over geological timescales (Nissenbaum and Yakir, 1995). Resins, which are produced as defense mechanisms by higher plants, incorporate hydrogen that is primarily derived from environmental waters. The isotopic composition of these environmental waters is thereby largely controlled by the precipitation patterns and by the geographic region (Terwilliger and DeNiro, 1995; Chikaraishi et al., 2004; Sessions, 2006). Although a range of angiosperm and gymnosperm species produce resins, only some of these resins can convert to stable polymers that are resistant to decay and can persist in the geological record as amber (Langenheim et al., 1996).

Most of the work on the isotopic composition of fossil resins has focused on assessing their $\delta^{13}C$ and $\delta^{18}O$ variability for paleoenvironmental reconstructions (*e.g.*, Nissenbaum and Yakir, 1995; Murray et al., 1998; McKellar et al., 2008; Tappert et al., 2013). Only a few studies have addressed the potential significance of their stable hydrogen isotope values (δD) (*i.e.*, Nissenbaum et al., 2005; McKellar et al., 2008; Wolfe et al., 2012). This reflects uncertainties regarding the effects of diagenesis over the primary biosynthetic signature of

deuterium in these plant-derived compounds (Epstein et al., 1976; Nissenbaum and Yakir, 1995), and the likelihood of post-depositional deuterium isotopic exchange with pore waters during burial (Nissenbaum and Yakir, 1995).

Since the early work of Epstein et al. (1976) a number of steps have been taken to address these uncertainties, and a range of plant lipid biomarkers, including alkanes, terpenoids, and fatty acids have been used to constrain the fractionation of deuterium between environmental waters and plant metabolites (*e.g.*, Yakir and DeNiro, 1990; Sessions et al., 1999; Chikaraishi et al., 2004; Sessions, 2006; Chikaraishi et al., 2009; Yang and Leng, 2009). A fractionation of approximately -230 to -192 ‰ relative to source waters is generally accepted for amber (see Nissenbaum et al., 2005; Wolfe et al., 2012, and references therein). Applying this value as a correction factor may allow researchers to use the bulk-amber δD to derive paleo-meteoric water lines (Nissenbaum and Yakir, 1995; Wolfe et al., 2012). Nonetheless, the variable δD composition of detrital fossil resin deposits introduces some difficulty in fully developing this notion, particularly because this can be affected by post-depositional processes that can lead to a degree of deuterium isotopic variability not documented by unaltered resinites, preserved in coal seams (Nissenbaum and Yakir, 1995; McKellar et al., 2008). Also, physical and chemical changes, such as color variation and molecular rearrangement (Grimaldi, 1996; McKellar et al., 2008; Lyons et al., 2009), are associated with a post-depositional decrease in hydrogen-containing functional groups and an increase of aromatic groups with increasing age (Murae et al., 1995; Yamamoto et al., 2006; Wolfe et al., 2009).

Assessing the effects of diagenesis on amber involves modeling complex processes that might have obscured the primary biosynthetic δD signal of their resin precursors, and which includes compositional changes during polymerization, and hydrogen isotope exchange reactions (Epstein et al., 1976; Schimmelmann et al., 1999; Schimmelmann et al., 2006; DeBond et al., 2012). In this study, a number of thermal hydrous isotopic exchange experiments were designed to measure the percentage of deuterium exchange between deuterated waters, resins and ambers, and the effects of increasing temperature. Further analyses included FTIR spectrometry and thermal gravimetry, applied both before and after the thermal exchange experiments for chemical and physical characterization. This analytical approach allows measuring the percentage of exchangeable hydrogen in amber, and precursor resins.

## 2.2. Methods

### 2.2.1. Samples

Modern and fossil resin samples produced by gymnosperm and angiosperm trees were used for the exchange experiments. Modern resins from *Metasequoia glyptostroboides* (MG), a rare deciduous taxodioid conifer of the Cupressaceae family (LePage et al., 2005; Nugue, 2005), were collected from a cultivated specimen at the United States National Arboretum, Washington, D.C., Unite States. Also, modern commercial copal resins from *Hymenaea courbaril* (Fabaceae) (HC) — a widely distribute tropical leguminous tree — were obtained from specimens that naturally grow in Brazil. These trees are widely distributed in

the latitudinal tropical range that includes coastal Africa and Madagascar, northern Mexico and southern Brazil (Langenheim et al., 1996).

The fossil resins included Cretaceous (Campanian) amber from Grassy Lake, Alberta, Canada (GLA), and mid-Oligocene to Miocene ambers from the Dominican Republic (DA). Both GLA and DA ambers are phylogenetically related to the botanical sources of modern resins. The botanical source of Grassy Lake amber is thought to be *Parataxodium*, an extinct genus of the Cupressaceae family (McKellar and Wolfe, 2010), whilst *Hymenaea courbaril* is considered to be a modern equivalent of the extinct *H. protera*: the source tree of Dominican amber (Cunningham et al., 1987; Grimaldi, 1995) (Table 2-1).

GLA samples are associate with coal seams exposed in Southern Alberta, at the margin of the Western Canadian sedimentary basin (McKellar et al., 2008; McKellar and Wolfe, 2010). Samples were collected from within coal seams or from shales directly adjacent to the seams. The amber samples used in this study are dark yellow with dark brown flow line colors, a feature that is typical of mature amber samples. McKellar et al., (2008) provided further details about the physical appearance of Grassy Lake ambers. DA samples are from the northeast Santiago area. These specimens are thought to be Miocene in age, and are found associated with extensively laminated sands, silts, and clays (Grimaldi, 1995). Their color is yellow to deep red, which suggested its degree of maturity (Lambert et al., 1985).

All samples of modern resins and ambers used were translucent with no visible inclusions. Prior to analyses (described below), freshly broken samples, of

about equal size (average 2.0 ± 0.1 mm length, 2.88 ± 0.1 mm wide) and weight (~ 10 mg), were cleaned with distilled water and subsequently dried without additional chemical or physical treatment.

2.2.2. Deuterium thermally induced exchange experiments

The deuterium isotopic exchange experiments were carried out by placing the resin/amber pairs into deuterated water for different periods of time and at temperatures of 50 and 90 °C (Fig. 2-1). Samples of modern resins were placed into 25-cm long and 6-mm diameter quartz glass tubes, which were afterwards placed into an outer silica glass tube (40-cm long with 9-mm diameter) containing an amber sample. The outer tube was later fitted with a special Ultra-Torr ™ vacuum metal fitting that allowed the experimental system to be evacuated for 2 h at 30 mTorr. Following the addition of 0.5 ± 0.1 ml of deuterated water (using a syringe), the resin samples and the water were frozen by placing the outer tube into liquid nitrogen while simultaneously heating those parts of the tube that were not immersed in liquid nitrogen in order to release deuterated $H_2O_{(g)}$ that was possibly adsorbed to the tube surface. After the cryogenic evacuation the outer tube was sealed.

Several experiments testing deuterium exchangeability between resin samples and water were conducted simultaneously under similar conditions, but using waters with different deuterium concentration ($[D_w]$ = 1%, 0.5% and 0.25%). The experiments were conducted at 50 and 90 ± 1 ºC to simulate temperatures that can be reached during shallow burial diagenesis at 2.0 km depth (assuming a geothermal gradient between 20 and 30°C/km); and for different time

intervals (5, 15, 30, 240, and 365 days). Experiments were run in duplicate or triplicate. At the end of each experiment, the samples were dried under vacuum (30 mTorr) at room temperature during over the course of 3 days, followed by δD measurements (Fig. 2-1).

Between 5 and 13 mg of amber or resin was combusted with CuO (1.00 ± 0.001 g), Cu (50 ± 0.01 mg), and Ag (50 ± 0.01 mg) at 800 ºC in vacuum-sealed quartz glass tubes for 4h. Upon cooling the combustion products, $CO_2$ and $H_2O$ were extracted cryogenically. Water was reduced to $H_{2\,(g)}$ using Indiana Zinc at 500 ºC for 25 min (Coleman et al., 1982). The isotope ratios of both $H_{2\,(g)}$ and $CO_{2\,(g)}$ were measured using a dual inlet Finnigan MAT-252 isotope-ratio mass spectrometer. The δ-values are reported relative to VSMOW (Vienna Standard Mean Ocean Water) for deuterium (δD), and VPDB (Vienna Pee Dee Belemnite) for carbon ($\delta^{13}C$).

Deuterium results (in per mil) are expressed in the conventional δ-notation:

$$\delta_{(Sample)} = ((R_{sample}/R_{standard}) - 1)\cdot 10^3, \qquad \text{Eq. 2-1}$$

where R is the D/H ratio of the sample and the standard, respectively.

Because δD is a nonlinear scale relative to the D/H ratio, which introduces small errors on values corresponding to large fractionation factors (Sessions and Hayes, 2005), a conversion factor, based on the relation D/H for $D_{SMOW}$ of water = $1.56\cdot 10^{-4}$, allows to calculate the $[D_{resin}]$ concentration in ppm before and after the exchange experiments:

$$[D_X]_{(ppm)} = 1.56 \cdot 10^{-1}(\delta D_X + 1000), \quad \text{Eq. 2-2}$$

Instrumental non-linearity was calculated to be ~11 %. Reproducibility of measuring the deuterium concentration of samples measured in triplicates was ± 2.4% of the deuterium present.

2.2.3. Thermal gravimetric analysis (TGA)

Amber and resins samples were studied using a TGA-Q500 thermal gravimeter in order to record their weight changes during heating. A mass ranging between 5 and 10 mg of each sample was heated at a constant rate of 5 °C/min, with isotherms at 50 and 90 °C for 60 min (Appendix, 1-1). Furnace temperature was programmed to equilibrate at 30 °C and rise up to 250 ± 0.1 °C at the defined heating rate. The purge gas used was nitrogen of 99% purity, flowing at 60 mL/min. After a nonlinear heating period, the programmed linear rates were achieved. For comparison purposes, the same method was applied for the analyses of both resin and amber samples. Activation energy was calculated with non-isothermal data.

2.2.4. Fourier-Transform Infrared (FTIR) microspectroscopy

Samples were characterized via FTIR in order to identify potential changes in compositional changes due to the experiments (Fig. 2-1). The spectroscopic analyses were conducted before (t = 0) and after (t = 30, and 240 days) the isotopic exchange protocol with 1% [$D_w$] water excess, and also after TGA (TGA – $T_{max}$ = 250 °C) (Fig. 2-1).

FTIR analyses were conducted with a Thermo-Nicolet Nexus 470 bench

spectrometer fitted with a dual-aperture continuum infrared microscope with motorized stage. Samples were first examined with a binocular steriomicroscope and inclusion-free fragments of crushed samples (<5 μm) were selected and mounted directly on a $NaCl_{(s)}$ plate. Beam size was set to 100x100 μm (square aperture) and the spectral resolution to 4 $cm^{-1}$. Spectra were taken between 700 and 4000 $cm^{-1}$ (equivalent to wavelengths of 2.5–15 μm), and for each analysis 200 individual interferograms were co-added. Also, absorbance values were normalized, and spectral regions at 3700–3500 $cm^{-1}$ and 2750–2580 $cm^{-1}$ examined in order to identify changes due to time-dependence in the sequential deuterium exchange experiments and also after TGA treatment.

## 2.3. Results

### 2.3.1. Resins and ambers deuterium exchange at 50 and 90 °C

Table 2-2, 2-3 and Figure 2-2 summarize the results from the experimental deuterium exchange time series. These illustrate the following trends: (1) the deuterium concentration of resin and amber samples subjected to hydrous thermal maturation conditions stabilizes to a constant value after 30 days, both at 50 and 90 °C; (2) after 365 days samples interacting with deuterium-rich waters [$D_w$] showed different responses (Fig. 2-3). As a result, *M. glyptostroboides* resins and Dominican amber showed a decrease in their [$D_{resin}$], from a maximum of 340.4 ± 4.0 and 342 ± 2.0 ppm at 240 days to about 261.0 ± 4.0 and 298.3 ± 0.6 ppm at 365 days, respectively (Table 2-2, and 2-3). During the same time interval, *H. courbaril,* and Grassy lake amber samples increased their deuterium concentrations from their original values to about 50.8 ± 5.6 ppm and 75.8 ± 8.33

ppm, respectively. Importantly, control samples, subjected to similar experiments, but using deionized water in place of deuterated water, showed no variation in [$D_{resin}$] (Table 2-2).

As shown in Figure 2-3, the increase in the deuterium concentration within resin and amber samples subjected to hydrothermal exchange conditions is directly proportional and strongly correlated ($R^2 > 0.90$) with the deuterium concentration in the experimental waters. The intercept value corresponds to the initial [$D_{resin}$] concentration in the untreated material, while the slope of the regression line gives the magnitude of deuterium exchange between the water and samples. Accordingly, the percentage of exchange for resin from *Metasequoia glyptostroboides* is 1.90 ± 0.04%, both at 50 and 90 °C; while resin from *Hymenaea courbaril* produced values of 1.40 ± 0.03% at 50 °C, and 1.90 ± 0.04% at 90 °C.

Dominican amber, on the other hand, showed a deuterium exchange of about 1.10 ± 0.02% and 1.50 ± 0.03% at 50 and 90 °C, respectively. By contrast, Grassy lake amber showed a constant value of 0.50 ± 0.01% at both temperatures, which is notably lower than the deuterium exchange capacity determined for modern resins (Table 2-2 and 2-3). Overall, these results show that the percentage of deuterium exchange is generally very low, *i.e.*, between 0.50 and 1.9% (Fig. 2-3).

*2.3.1.1. Physical changes recorded after the experiments*

After the experiments, the following physical changes in resin and amber samples were observed:

Morphological changes: most of the modern resins changed from their original random tabular shape to spherical forms exhibiting noticeable water inclusions, whereas ambers preserved their shape.

Color: *H.courbaril* resins changed from milky white to yellow-orange; Grassy lake ambers developed a yellowish surface coloration and also the characteristic milky bands described by McKellar et al. (2008). By contrast, resins from *M. glyptostroboides*, and Dominican amber did not show major physical changes (Fig. 2-4).

These changes are associated with an increase in deuterium concentration of the samples, which is related to two surface processes: (1) hydrous-thermal alteration; and (2) molecular water interaction and surficial sorption by the sample.

2.3.2. TGA

Products of hydrous maturation conditions at 90°C were chosen for TGA analyses, these samples were interacting with deuterium rich waters for 240 days (see Fig. 2-1). Figure 2-5 show their thermal gravimetric weight loss curves and corresponding derivative curves (DTG). After TGA treatment, the chosen resin and amber specimens showed the follow heating behavior:

(1) Modern resins (*M. glyptostroboides*) (MG-240) showed a relatively minor

weight loss at 50.15 °C and 149.95 °C; and two well-defined mass loss steps at 95.2 °C, and 170 °C. The total loss was about 3.25% of the original mass (Fig. 2-5a).

(2) Amber samples (Grassy Lake amber) (GLA-240) exhibited a relative minor weight loss at lower temperatures: 49.51 °C, 89.9 °C, and 120.06 °C. The total loss was 2.02% of the original mass (Fig. 2-5b).

Isothermal experiments up to ~100°C showed weight changes that were likely related to water desorption. Non-isothermal experiments (*e.g.*, Trejo et al., 2010), conducted at 5 °C/min heat rate, allowed estimation of the activation energy. For the modern resins, activation energy estimates were around 19.21 kJ/mol (Fig. 2-5c), whereas those for ambers were around 3.60 kJ/mol (Fig. 2-5d). Interestingly, the deuterium isotope concentrations measured after TGA analyses were lower by 115.00 ± 7.37 ppm compared to those before. This, again, is attributable to a loss of absorbed deuterated water (Table 2-3). The carbon isotopic composition of the modern resins and ambers, on the other hand, did not change during the TGA experiments.

2.3.3. Micro-Fourier-transform infrared (FTIR) spectroscopy

The FTIR spectra of untreated specimens of GLA, DA, HC, and MG were compared to spectra after hydrous thermal exchange experiments lasting for 30 and 240 days in deuterated water ($[D_w]$ = 1%), and at temperatures of 50 and 90 °C. The IR spectra of the untreated material closely resembled those previously documented for GLA (McKellar et al., 2008; McKellar and Wolfe, 2010), and DA (Langenheim and Beck, 1968; Beck, 1986), HC and MG modern resins (Tappert

et al., 2011) (Table 2-4; Fig. 2-6 and 2-7). In general, the spectra of these samples are characterized by a broad peak between 3700 and 3200 $cm^{-1}$, which is typically linked to O-H vibrational modes (Tappert et al., 2011). Strong absorption features in the spectral range 3000–2800 $cm^{-1}$ are typically attributed to stretching modes of terminal methyl- or methylene groups. Additional absorption features in the range 1800–1600 $cm^{-1}$ relate to carbon-carbon or carbon-oxygen double bonds (C=C, C=O). The spectral range below 1500 $cm^{-1}$ typically contains the highest number of absorption features in resin spectra, and is most useful in distinguishing different resin types (fingerprinting area). The absorption features in this range are generally linked to carbon and oxygen single bonds of the various acid and ester components that are present in resins, as well as to poorly constrained skeletal vibrations. (*e.g.*, Langenheim et al., 1969, Wolfe et al., 2009, Tappert et al., 2011, Pastorelli et al., 2011).

The FTIR spectra of resin and amber samples are sensitive not only to changes in their terpenoid constituents (*i.e.*, Murae et al., 1995), but also to deuterium addition in their functional groups (*e.g.*, Flakus and Chemecki, 2002). In this regard, Table 2-4 summarizes and compares the main absorbance bands observed in resins and ambers, their shift after the thermal exchange and thermal gravimetry experiments and the tentative wavelength assignment to organic functional groups. This information complements Figures 2-6 and 2-7, which show the FTIR spectra of the samples and the effects of the hydrothermal maturation process after 30 and 240 days at 50 and 90 °C, respectively. Conversely, Figure 2-8 shows the effects of water sorption-desorption process on

MG and GLA spectra after hydrous treatment and the spectra of final products of samples subjected to anhydrous (TGA) treatment. The following spectral changes were observed:

*2.3.3.1. Spectral region 3600–3080 cm$^{-1}$*

At 50 and 90 °C, the spectra showed an increase in absorbance and a broadening of the hydroxyl peak, which is accompanied by a shift of the primary absorbance band towards higher wavenumbers. This region is related to hydroxyl groups that are associated with free alcohols (*i.e.*, 3650 cm$^{-1}$), phenols (3600–3200 cm$^{-1}$), and intramolecular hydrogen bonds of carboxylic acids (3500–2400 cm$^{-1}$) (Figs. 2-6 and 2-7). The increase in broadness of the hydroxyl band with experimental run-time is related to an increase in water sorption by the resin and amber samples. Although, at 3076 cm$^{-1}$ a medium intensity peak common for resin samples (HC, and MG), and DA was identified, this peak is absent or weak in GLA, possibly due to its maturity (Figs. 2-6 and 2-7) (Table 2-4).

*2.3.3.2. Spectral region 3000–2800 cm$^{-1}$*

The spectral features in this range are characteristic by $sp_3$ and $sp_2$ C-H hybridization. Figure 2-8 shows the resulting spectra of product samples after applying both hydrous- and anhydrous thermal treatments. The intensity of these bands after anhydrous treatment (TGA, up to 250 °C) in GLA-240 spectra decreases and at the same time a broadening occurs. The opposite can be observed in MG-240 spectra. These changes suggest desorption of deuterated molecular water bonding, which is consistent with our deuterium measurements in product

samples (Table 2-4).

*2.3.3.3. Other IR spectral regions*

Other IR spectral variations resulted from long-term exposure to maturation-alteration conditions under hydrous conditions; among them relatively high absorption peaks at 1645 and 887 $cm^{-1}$, and the appearance of distinctive peaks at 1092, and 815 $cm^{-1}$ are related to increase in desaturation ($CH_2$ groups) (see Chapter 3).

## 2.4. Discussion

As with other polymers, resins and ambers incorporate deuterium either by water sorption, which implies both physicochemical resin (amber)–water interactions, or by chemical organic hydrogen substitution (Zhou and Lucas, 1999; Schimelmann et al., 1999). However, a number of factors must be considered in order to evaluate the few physical and chemical changes observed after the hydrous and anhydrous thermal alteration experiments. Within this context, three factors are considered to govern results of the isothermal experimental simulations: (1) the primary chemical composition of resins and ambers undergoing thermal maturation (see Table 2-1); (2) the molecular water sorption/desorption mechanisms; and (3) the rates of deuterium exchange between water and resins (ambers).

As previously described, the deuterium transferability from water-to-resins and from water-to-ambers is 1.90 ± 0.20, and 0.5 ± 0.05%, respectively (Fig. 2-2). The experimental results also suggest that the samples equilibrate with their

common deuterium source water after 30 days (Table 2-2 and 2-3). Some of the analyzed resin samples (HC, and GLA; Fig. 2-4), however, showed an increase in their deuterium concentration after long-term experiments (365 days), which were accompanied by noticeable morphological changes. These changes were most significant in experiments conducted at 90°C, and may indicate an increase in water bonding within the resins (Zhou and Lucas, 1999).

In order to discriminate between molecular water being incorporated within the surface of resins and ambers, and exchangeable hydrogen in these resins, selected product samples from the long-term hydrothermal treatment were subjected to TGA analyses. This technique was also used to elucidate the potential influence of water on the transformation of resins to amber, and to assess the percentage of exchangeable hydrogen in the samples more precisely. TGA treatment of hydrous treated samples caused a mass loss of about 3.25% for resins (MG-240), as compared with 2.02% observed in ambers (GLA-240) (Fig. 2-5 a, b). Isotope analyses of TGA-treated samples and their non-treated counterparts showed that heating of the specimen results in a deuterium depletion of about 44% (*e.g.*, after hydrothermal treatment [$D_{resin}$] = 305 ppm; same sample after TGA [$D_{resin}$] = 171 ppm) and 7.78%, reported as percentage of change, for resins and ambers as part of water desorption (Table 2-3). By contrast, the $\delta^{13}C$ did not show any major changes, and remained approximately constant (Appendix 1-2), with values that are consistent with natural variations (see McKellar et al., 2011; Tappert et al., 2013).

These results have two important implications. First, the $\delta^{13}C$ of resins and ambers is unlikely to change during diagenesis, because chemical reactions with the potential to influence the thermal degradation processes of resins and amber are restricted to temperatures above 250 °C (see Murae et al., 1995). Second, the observed mass loss during TGA can be attributed to water loss, whereby resins appear to be more prone to water loss than ambers. This indicates that during the alteration process of resins and amber, water sorption–desorption mechanisms play an important role. At the same time, the proportion of exchangeable hydrogen in unaltered samples is significantly less than 1.9% in resins, and 0.5% in ambers.

2.4.1. Mechanisms of molecular water sorption-desorption in resins and ambers

The polymeric network of amber and modern plant resins may have some resemblance with those of synthetic polymers (*e.g.*, Bellenger et al., 1989; Zhou and Lucas, 1999). Therefore, the latter can be used to interpret the physicochemical interactions observed in our study. Two distinct models can be invoked to explain the molecular exchange between water and resins: (1) free volume water diffusion, in which water molecules reside in the free volume of the resinous material, and (2) water molecule interactions with hydrophilic functional groups, such as hydroxyl and carboxyl, which may also lead to deuterium exchange (Jeffrey and Jeffrey, 1997; Zhou and Lucas 1999).

Water sorption in resins can also be classified according to their activation energies into: (1) weakly-bound hydrogen — a molecular arrangement, which requires only a small amount of energy (4 to 15 kJ/mol) to remove the single

hydrogen water-resin (amber) bond (Type I); and (2) moderately-bound hydrogen — which requires a higher activation energy (50 to 60 kJ/mol) to remove inter-connected hydrogen-bound water from resin molecules (Type II) (Jeffrey and Jeffrey, 1997). From non-isothermal TGA results, the activation energies were found to be 19.21 and 3.60 kJ/mol for resins and ambers, respectively (Fig. 2-5). Although both mechanisms may have an influence on the diagenetic transformation of resin into amber, it can be concluded that most water molecule-resin interaction occur through weak hydrogen Type I-bonding. This kind of interactions may also be associated with the morphological transformation from chips to spheres observed in resins that were subjected to hydrous thermal treatment. As modern resins are comprised of occluded unpolymerized terpenoids (*e.g.*, triterpenes –Anderson et al., 1992), and functional groups associated with terpenoid acids, they may act as natural plasticizers (Anderson et al., 1992). This can lead not only to morphological changes, but also to minor variations in color (Fig. 2-4).

On the other hand, the polymeric structure of ambers is based on multicyclic saturated and partially aromatized structures that lead to a gradual decrease of electronegative functional groups (*i.e.* Grimalt et al., 1988; Clifford et al., 1997). Results from this study showed that the deuterium concentration is proportional to water sorption, and thus inversely proportional to the maturity of the samples. Therefore, because of their compositional differences and water sorption capacity, DA showed a relatively higher deuterium absorption and thus, concentration when compared with GLA samples (see Table 2-1, Fig. 2-2).

2.4.2. Post-experimental chemical characterization

Most of the information regarding the hydrogen bond dynamics, such as their inter– and intra– molecular interactions and vibrational structure, can be observed in infrared absorption spectra, in the spectral region from 3600 to 2500 cm $^{-1}$ (Figs. 2-6 and 2-7) (He et al., 2004). In this region, all resin samples showed an increase in intensity, absorbance, and broadness proportional to the time they were exposed to hydrothermal conditions. Even though the physical state of the samples (*e.g.*, thickness variability) and environmental conditions during measurement (*e.g.*, humidity) might have some effect on the resulting spectrum (Derrick et al., 1999), their combined effects can be considered minor when compared to the effects of water sorption related to Type I-bonding water. Water bonding on resin and amber were found to alter the entire spectrum. This effect suggests interactions with different hydrophilic functional groups within the resin macromolecules. The amount of surface-bound water molecules increases with time and temperature, and is more prevalent in resins compared to amber samples.

The variability of other features in the infrared spectra of resins and ambers appears to be due to thermal degradation after long-term exposure to the experimental conditions. This assumption is supported by the observed changes of the absorption features at 3070, 1645, and 880 (890) cm $^{-1}$, which are related to an increase of desaturation of $CH_2$ groups (see Chapter 4 for details). However, the lack of peaks in the 2500–2000 cm $^{-1}$ region suggest that changes due to molecular deuterium exchange (Flakus and Chemecki, 2002) may not be readily detectable using FTIR spectroscopy. As shown in Figure 2-8, water sorption-desorption

processes in MG and GLA during the hydrous and after anhydrous (TGA) maturation experiments suggest that these mechanisms are relevant in the resin-to-amber diagenetic alteration process. Also, they do not produce major changes in the deuterium concentration of the samples (Table 2-3). Together these results demonstrate that deuterium concentration in amber provide a robust inland paleoclimatic proxy (Nissenbaum and Yakir, 1995; Wolfe et al., 2012).

2.4.3. Further implications

Ever since the pioneering work of Nissenbaum and Yakir, (1995), the deuterium content of ambers has been envisioned as a possible paleoclimatic indicator. However, insufficient knowledge about resin (amber) and water interaction under shallow burial diagenetic conditions and its effects on the resin's (amber's) primary deuterium content hampered its applicability. As determined in this work, under a range of burial conditions, the deuterium incorporation in resins and ambers is primarily controlled by reversible sorption–desorption water interactions, and only to a minor extent by isotopic exchange. The percentage of deuterium exchange is $< 0.50 \pm 0.01$ for ambers, and $< 1.90 \pm 0.04\%$ for resins (Fig. 2-3). These values indicate that during diagenetic alteration the increase in deuterium content of resins and ambers, which may arise from interaction with pore water in the surrounding rocks, is negligible and unlikely to affect their original bulk deuterium composition. Thus, under early burial conditions the effects of water on resins and ambers do not impart a significant deuterium shift.

Finally, it is important to recall that the experimental conditions reproduced in this work simulated those expected in hydrous environments with

relatively low oxygen, high temperature, and low photic exposure. Therefore, the results presented here can be extrapolated to specimens found within primary deposits. Yet, because reworked fossil resins might undergo additional degradation processes, including photoxidation, and hydrolysis (Pastorelli et al., 2012, 2013), these processes increase the potential for water sorption and alteration in their bulk deuterium composition. Consequently, degraded samples should be analyzed with caution.

### 2.5. Conclusions

This work demonstrates that bulk deuterium composition of amber can be considered as a reliable paleoclimatic indicator. The simulation of hydrous thermal maturation processes in modern resins and amber with deuterated waters indicated that:

1. Secondary deuterium incorporation under isothermal conditions at 50 and 90 °C is insufficient to overprint the natural fingerprint inherited from metabolic processes during resin biosynthesis by living plants.

2. Modern resins (HC and MG) showed a higher percentage of deuterium transference (T= 50 °C, $[D_{w\text{-}MG}]< 1.90 \pm 0.20\%$, $[D_{w\text{-}HC}]= 1.40 \pm 0.15\%$; T=90 °C, $[D_{w\text{-}resin\ (MG - HC)}]< 1.90 \pm 0.20\%$), relative to Dominican (T= 50 °C, $[D_{w\text{-}DA}]< 1.10 \pm 0.12\%$; T= 90 °C, $[D_{w\text{-}DA}]=1.50 \pm 0.16\%$), and Grassy Lake ambers ($[D_{w\text{-}GLA}]< 0.50 \pm 0.05\%$, at 50 and 90 °C).

3. The deuterium isotopic concentration was also related to water sorption-desorption processes; after physical and chemical characterization it was concluded that molecular water in amber is associated with surface-bonded water.

4. Once formed, ambers suffering translocation and diagenesis are likely to preserve their primary deuterium fingerprint.

Table 2-1. Fossil and modern resin samples used to perform experimental diagenetic simulation under hydrous- and anhydrothermal conditions. See text for details.

| **Sample** | **Sample type** | **Source tree** | **Location** | **Age** |
|---|---|---|---|---|
| [(1.1)] HC | Resin | *Hymeneae courbaril* - Copal (commercial sample) | Brazil | Modern |
| [(1.2)] MG | Resin | *Metasequoia glyptostroboides* | National Arboretum, Washington DC. United States | Modern |
| [(2.1)] DA | Amber | *Hymeneae protera* (extinct specimen) | Dominican Republic | Mid-Oligocene – Miocene |
| [(2.2)] GLA | Amber | Cupressaceae genus. *Parataxodium.* | Grassy Lake, Alberta. Canada | Campanian, Cretaceous |

[(1.1)] *Hymeneae courbaril*, [(1.2)] *Metasequoia glyptostroboides*, [(2.1)] Dominican Amber, [(2.2)] Grassy Lake Amber

Table 2-2. Deuterium isotopic concentration in resins and amber under hydrothermal maturation experiments with deuterated waters at 50 °C. Deuterated water concentrations were [$D_w$] = 0.25, 0.5, and 1%. Deuterium content of equivalent samples was included, such as samples interacting with de-ionized water, and samples interacting with the three deuterated waters after 5, 15, 30, 240, and 365 days.

| | | | **Temperature** | | 50 ± 1 °C | | | | | |
|---|---|---|---|---|---|---|---|---|---|---|
| | | | **Deuterated waters** | | [$D_w$] 0.25 % | | [$D_w$] 0.5 % | | [$D_w$] 1 % | |
| **Time (days)** | **Sample** | **Replicates*** | **$\delta D_{resin}$ (V-SMOW) ‰** | **[$D_{resin}$] (ppm)** | **$\delta D_{resin}$ (V-SMOW) ‰** | **[$D_{resin}$] (ppm)** | **$\delta D_{resin}$ (V-SMOW) ‰** | **[$D_{resin}$] (ppm)** | **$\delta D_{resin}$ (V-SMOW) ‰** | **[$D_{resin}$] (ppm)** |
| 0 | HC-BE | 6 | -221.9 | 121.4 | - | - | - | - | - | - |
| | MG-BE | 5 | -278.9 | 112.5 | - | - | - | - | - | - |
| | DA-BE | 10 | -257.6 | 115.8 | - | - | - | - | - | - |
| | GLA-BE | 3 | -290.6 | 110.7 | - | - | - | - | - | - |
| 5 | HC-5.DW | 2 | -234.4 | 119.4 | - | - | - | - | - | - |
| | MG-5.DW | 2 | -308.0 | 108.0 | - | - | - | - | - | - |
| | DA-5.DW | 2 | -225.2 | 120.9 | - | - | - | - | - | - |
| | GLA-5.DW | 2 | -262.0 | 115.1 | - | - | - | - | - | - |
| 5 | HC-5 | 12 | - | - | -128.8 | 135.9 | 32.4 | 161.1 | 340.8 | 209.2 |
| | MG-5 | 15 | - | - | -230.9 | 120.0 | 10.6 | 157.7 | 646.1 | 256.8 |
| | DA-5 | 12 | - | - | -135.2 | 134.9 | -7.3 | 163.8 | 478.7 | 230.7 |
| | GLA-5 | 12 | - | - | -221.0 | 121.5 | -131.0 | 135.6 | 23.4 | 159.6 |
| 15 | HC-15 | 12 | - | - | -31.9 | 151.0 | 124.7 | 175.5 | 1103.5 | 308.1 |
| | MG-15 | 15 | - | - | -200.8 | 124.7 | 70.4 | 167.0 | 779.7 | 277.6 |
| | DA-15 | 13 | - | - | -98.2 | 140.7 | 22.6 | 168.7 | 671.0 | 260.7 |
| | GLA-15 | 15 | - | - | -118.2 | 137.6 | -71.6 | 144.8 | 56.0 | 164.7 |
| 30 | HC-30 | 18 | - | - | -9.0 | 154.6 | 337.7 | 208.7 | 1006.9 | 313.1 |
| | MG-30 | 18 | - | - | -200.0 | 124.8 | 120.6 | 174.8 | 1030.4 | 316.8 |
| | DA-30 | 18 | - | - | -25.7 | 152.0 | 96.3 | 180.9 | 743.5 | 272.0 |
| | GLA-30 | 18 | - | - | -107.2 | 139.3 | -48.8 | 148.4 | 58.3 | 165.1 |
| 60 | HC-60 | 16 | - | - | -3.7 | 155.4 | 348.9 | 210.4 | 1096.1 | 327.0 |
| | MG-60 | 16 | - | - | -197.9 | 125.1 | 122.9 | 175.2 | 1052.8 | 320.2 |
| | DA-60 | 16 | - | - | -20.2 | 152.8 | 128.2 | 186.2 | 752.4 | 273.4 |
| | GLA-60 | 16 | - | - | -102.9 | 139.9 | -25.3 | 152.1 | 81.9 | 168.8 |
| 240 | HC-240 | 19 | - | - | -3.6 | 155.4 | 927.1 | 300.6 | 1108.4 | 328.9 |
| | MG-240 | 19 | - | - | -198.9 | 125.0 | 129.0 | 176.1 | 1076.4 | 323.9 |
| | DAS-240 | 19 | - | - | 121.5 | 174.9 | 298.3 | 202.5 | 876.5 | 292.7 |
| | GLA240 | 19 | - | - | -100.4 | 140.3 | -19.6 | 152.9 | 105.4 | 172.4 |
| 360 | HC-365 | 18 | - | - | 564.6 | 244.1 | 666.1 | 259.9 | 960.9 | 305.9 |
| | MG-365 | 18 | - | - | 176.9 | 183.6 | 169.7 | 182.5 | 169.7 | 182.5 |
| | DA-365 | 18 | - | - | 286.9 | 200.8 | 391.1 | 217.0 | 428.6 | 222.9 |
| | GLA-365 | 18 | - | - | 560.1 | 243.4 | 572.4 | 245.3 | 591.3 | 248.2 |

(*) Total number of samples under experimental conditions per period of time, deuterium rich waters and temperatures (50 and 90 °C). Samples were prepared and analyzed in duplicates per time interval, which represents the number of days by the side of modern and fossil resin specimens.
(-) No samples.

Table 2-3. Deuterium isotopic concentration in resins and amber under hydrothermal maturation experiments with deuterated waters at 90°C. Deuterated water concentrations was $[D_W]$ = 0.25, 0.5, and 1%. Highlighted samples were treated with thermal gravimetric analysis (TGA), and analyzed with fourier transform infrared (FTIR) spectroscopy after long-term hydrothermal maturation experiments. See details in text.

| | 90 ± 1 °C | | | | | | |
|---|---|---|---|---|---|---|---|
| | $[D_W]$ 0.25 % | | $[D_W]$ 0.5 % | | $[D_W]$ 1 % | | Characterization |
| **Sample** | **$\delta D_{resin}$ (V-SMOW) ‰** | **$[D_{resin}]$ (ppm)** | **$\delta D_{resin}$ (V-SMOW) ‰** | **$[D_{resin}]$ (ppm)** | **$\delta D_{resin}$ (V-SMOW) ‰** | **$[D_{resin}]$ (ppm)** | **TGA** $[D_{resin}]$ (ppm)** |
| HC-5 | -220.0 | 121.7 | -8.8 | 154.6 | 493.1 | 232.9 | - |
| MG-5 | -117.9 | 137.6 | 35.5 | 182.7 | 893.1 | 295.3 | - |
| DA-5 | -66.9 | 145.6 | 96.6 | 171.1 | 427.5 | 222.7 | - |
| GLA-5 | -181.0 | 127.8 | -117.9 | 137.6 | 65.7 | 166.2 | - |
| HC-15 | -119.5 | 137.4 | 203.3 | 180.7 | 770.9 | 276.3 | - |
| MG-15 | -32.1 | 151.0 | 113.2 | 198.8 | 947.8 | 303.9 | - |
| DA-15 | -31.6 | 151.1 | 156.5 | 180.4 | 1118.0 | 330.4 | - |
| GLA-15 | -121.6 | 137.0 | -37.1 | 150.2 | 79.7 | 168.4 | - |
| HC-30 | -58.6 | 146.9 | 205.7 | 188.1 | 827.9 | 285.1 | - |
| MG-30 | -1.5 | 155.8 | 106.6 | 202.7 | 952.3 | 304.6 | - |
| DA-30 | 35.7 | 161.6 | 222.2 | 190.7 | 1183.8 | 340.7 | - |
| GLA-30 | -94.7 | 141.2 | 10.2 | 157.6 | 82.1 | 168.8 | - |
| HC-60 | -3.7 | 155.4 | 276.8 | 199.2 | 827.9 | 285.1 | - |
| MG-60 | 0.4 | 156.1 | 114.4 | 210.8 | 973.5 | 307.9 | - |
| DA-60 | 45.9 | 163.2 | 231.8 | 192.2 | 1193.4 | 342.2 | - |
| GLA-60 | -60.7 | 146.5 | 8.3 | 157.3 | 92.6 | 170.4 | - |
| HC-240 | 1.1 | 156.2 | 302.4 | 203.2 | 862.2 | 290.5 | 187.9 |
| MG-240 | 31.3 | 160.9 | 171.4 | 222.9 | 958.7 | 305.6 | 171.3 |
| DAS-240 | 99.5 | 171.5 | 545.4 | 241.1 | 1195.4 | 342.5 | 132.2 |
| GLA240 | -59.6 | 146.7 | 9.5 | 157.5 | 87.8 | 169.7 | 156.5 |
| HC-365 | 336.5 | 208.5 | 471.5 | 229.6 | 819.8 | 283.9 | - |
| MG-365 | 427.8 | 222.7 | 381.4 | 215.5 | 912.6 | 298.4 | - |
| DA-365 | 145.3 | 178.7 | 575.4 | 245.8 | 673.2 | 261.0 | - |
| GLA-365 | -158.6 | 131.3 | 43.8 | 162.8 | 70.3 | 167.0 | - |

(**) Deuterium concentration of samples after TGA analysis and samples analyzed with FTIR.
(-) No samples/ no samples analysis.

Table 2-4. Interferogram analyses of resin and amber samples after time series maturation experiments. The spectroscopic bands were identified, assigned, and described for each sample. Grey shadowed fields indicate bands that showed changes.

| | | | Raw | | | | T= 55 °C, t= 240 days | | | | T= 90 °C, t= 240 days | | | |
|---|---|---|---|---|---|---|---|---|---|---|---|---|---|---|
| **Functional Group** | **Type** | **Frequency**** | **HC** | **MG** | **DA** | **GLA** | **HC** | **MG** | **DA** | **GLA** | **HC** | **MG** | **DA** | **GLA** |
| O-H | Alcohols, phenols free O-H | 3650 | A(w) | A | A | V(w) | A | A | V(w) | V(w) | V(w) | A | V(w) | A |
| | Hydrogen bonded | 3400 | V(br) | V(br) | V(br) | V(br) | W(br) | W(br) | V(br) | W(br) | V(br) | W(br) | V(br) | W(br) |
| | Carboxylic acids R(C=O)O-H | 3076 | S(w) | S(w) | S(w) | A | S(w) | S(w) | S(w) | A | M(w) | M(sh) | M(sh) | V(w) |
| C-H | $sp_2$ hybridization hydrogen | 2960 | S(sh) | S(sh) | S(sh) | S(sh) | V(sh) | S(br) | S(sh) | S(br) | M(sh) | M(sh) | A | shoulder |
| | $sp_3$ hybridized ($R_3$-CH) | 2935 | V(w) | A | A | A | M(sh) | A | A | A | S(sh) | S(sh) | S(br) | S(sh) |
| | | 2858 | S(sh) | M(sh) | S(w) | S(w) | M(w) | V(w) | S(w) | M(sh) | M(sh) | M(sh) | M(sh) | M(sh) |
| | | 2848 | A | M(sh) | M(sh) | V(sh) | A | M(sh) | M(sh) | V(w) | A | M-S(sh) | V(w) | V(w) |
| C=O | esters (R(C=O)R) | 1775 | Shoulder (w) | A | Shoulder (w) | A | Shoulder - V(w) | A | Shoulder (w) | Shoulder (br) | Shoulder - V(w) | A | Shoulder (w) | Shoulder (br) |
| | | 1730 | Shoulder | Shoulder | Shoulder | Shoulder | Shoulder | Shoulder | M(sh) | S-M(sh) | Shoulder | Shoulder | M-V(w) | S-M(sh) |
| | | 1715 | A | S(sh) | A | S(sh) | A | S(sh) | A | A | A | S(sh) | A | A |
| | Acids (R(C=O)H) | 1697 | S(sh) | A | S(sh) | A | S(sh) | A | S(sh) | S-M(sh) | S(sh) | A | M-V(w) | S-M(sh) |
| C=C | $R_2C=CH_2C$ | 1648 | M(sh) | M(sh) | M(sh) | M(w) | M(sh) | M(sh) | M(sh) | Shoulder(w) | S(sh) | M(w) | S-M | Shoulder(w) |
| | $C=C-H_2$ | 1460 | M(sh) | A | M(w) | A | M(sh) | A | M(sh) | A | M(sh) | A | M(w) | M(br) |
| | Aromatic ring C-H, C=C | 1448 | A | S(sh) | A | S(sh) | A | S(sh) | A | S(w) | M(sh) | S | A | S(br) |
| | | 1417 | M(w) | A | M(sh) | A | M(w) | A | M(sh) | A | M(br) | A | M(w) | M(sh) |
| | | 1382 | S(sh) | Doublet | S(sh) | Doublet | S(sh) | Doublet | S(sh) | M(w) | S(sh) | Doublet | S(sh) | M(sh) |
| | stretching $CD_2$ | 1092 | W | W | W | W | W | W | W | M(w) | M | M | M | M |
| | $sp_2$ hybridized C-H($C=CH_2$) | 887 | S(sh) | Doublet | S(sh) | M(sh) | S(sh) | Doublet | S(sh) | M(sh) | S(sh) | M(sh) | S(sh) | V(w) |
| | C-D in plane bending vibration | 815 | A | A | A | A | M | M | M | M | M | M | M | M |

A= absent, W= wide, V= variable, S= strong, M= medium, (sh)= sharp, (br)= broad, (w)= weak

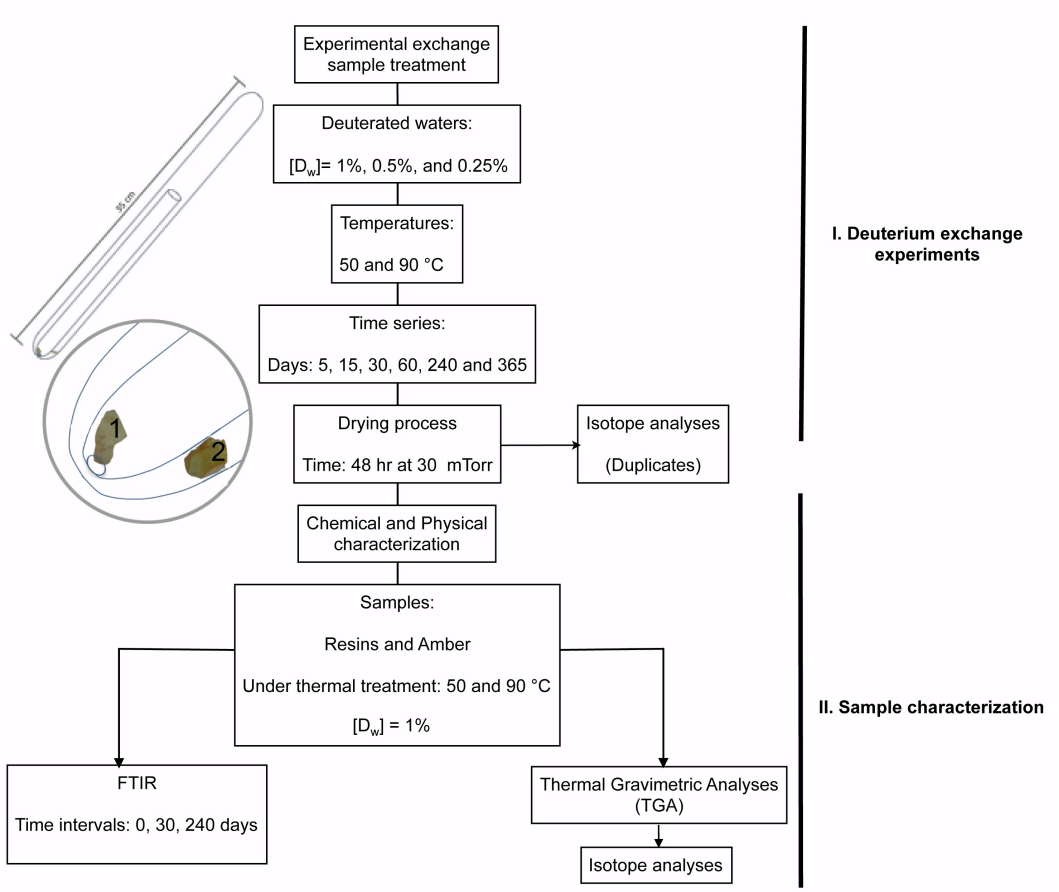


(1) Represent the resins (HC or MG), and (2) the amber (DA or GLA) specimens used for experiments.

Figure 2-1. Conceptual diagram showing the experimental approach applied. The protocol included two stages. First, resin and amber's hydrothermal maturity simulation with three deuterated waters, and their resulting isotopic composition analysis; and second chemical (FTIR) and physical (TGA) characterization of selected samples. As per sample preparation, a first tube (1) containing the resin sample was placed into a second tube (2) containing the amber' sample.

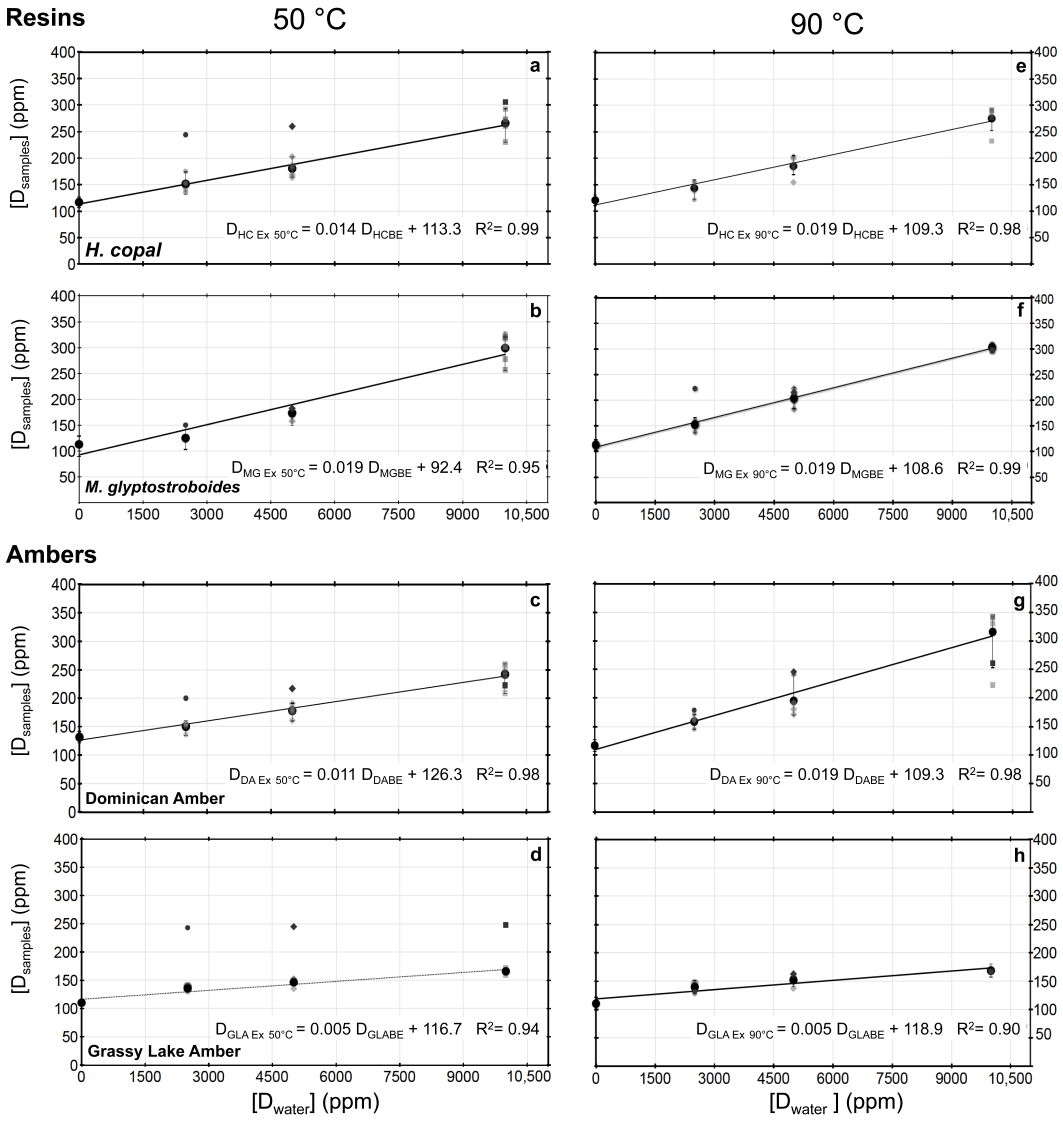


Figure 2-2. Correlation graph between isotopic deuterium concentration of analyzed resin, amber samples, and deuterated waters at 50 °C (a–d) and 90 °C (d–g). The intercept in the linear equation is primary deuterium isotope concentration of raw samples; while the slope represents the percentage of deuterium transferred from the waters to the specimens.

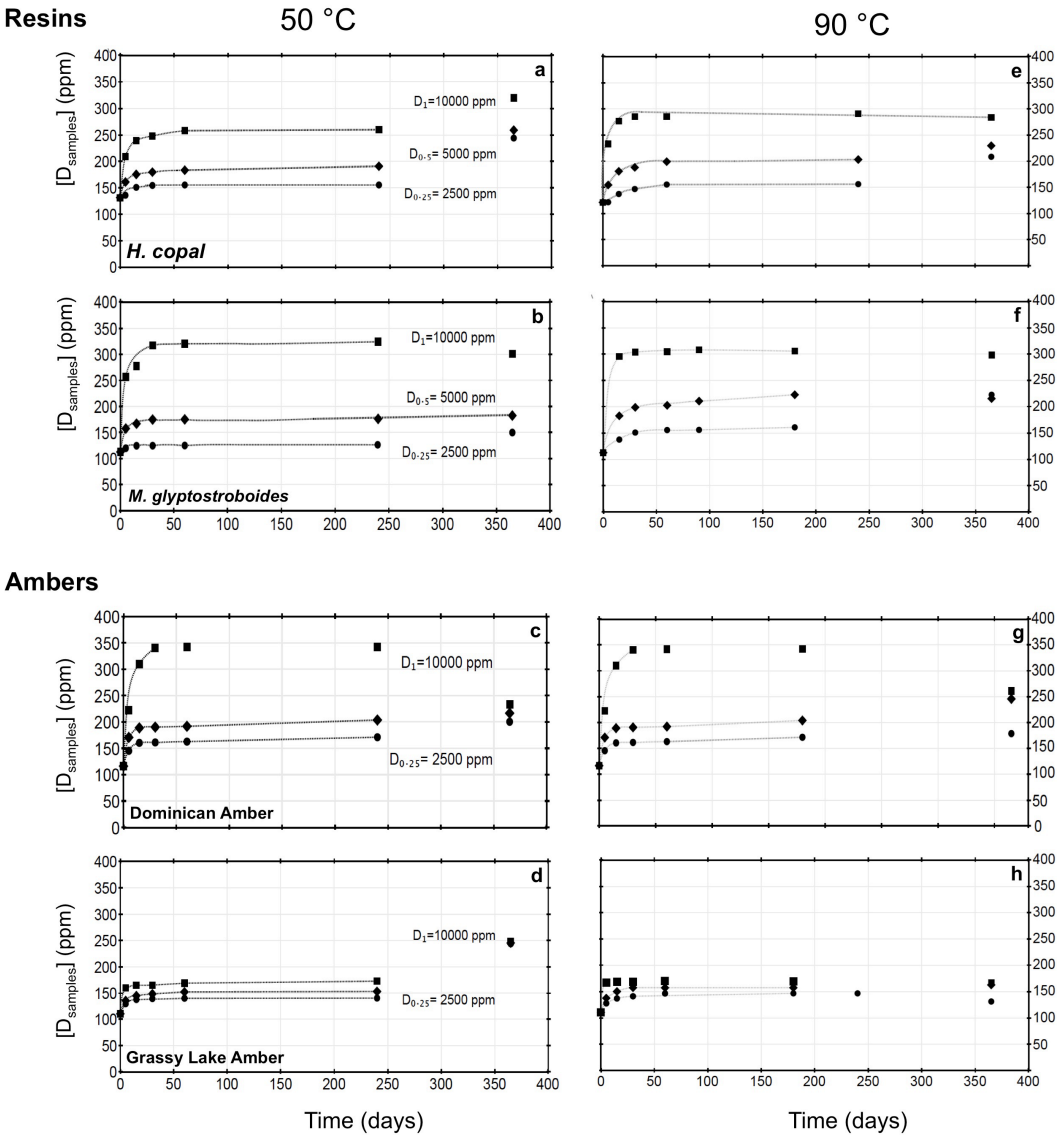


Figure 2-3. Time-series analyses showing the variability of deuterium concentrations in resins and ambers samples exposed to three different deuterated waters at 50°C (a–d) and 90°C (e–h). The standard error bars of the slopes and intercepts show the uncertainties of the regression analyses.

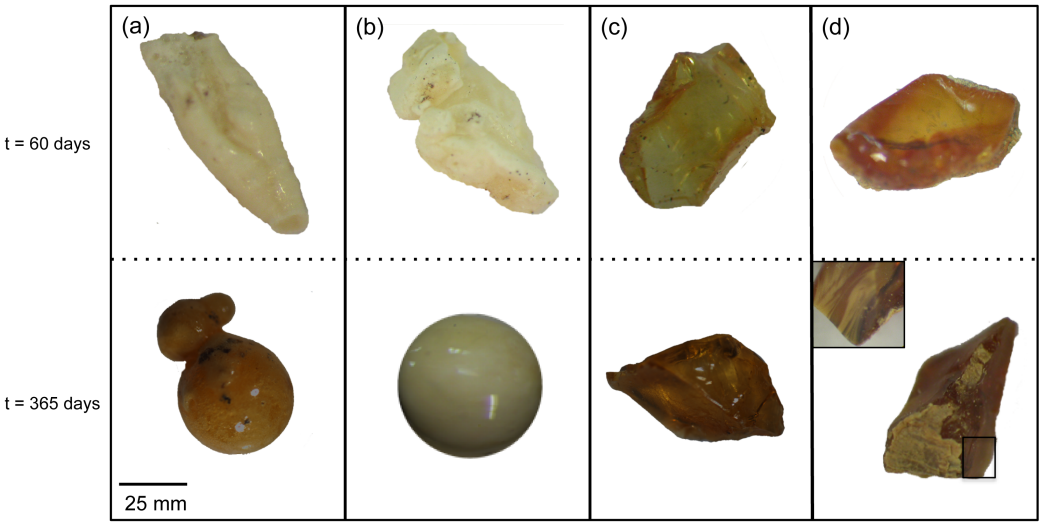


Figure 2-4. Physical variations observed in resins and ambers with time after 60 and 365 days under hydrothermal conditions at 90°C. HC (a) and MG (b) specimens showed significant morphological changes from chips elongate forms after 60 days, and from elongate forms to spheres after 365 days. Also, HC samples showed change in colour from pale-white to dark orange. It was also noticed that DA(c), and GLA (d) samples developed a foam-covered surface, more conspicuous in GLA samples. The colour of amber specimens was darkened after the treatment.

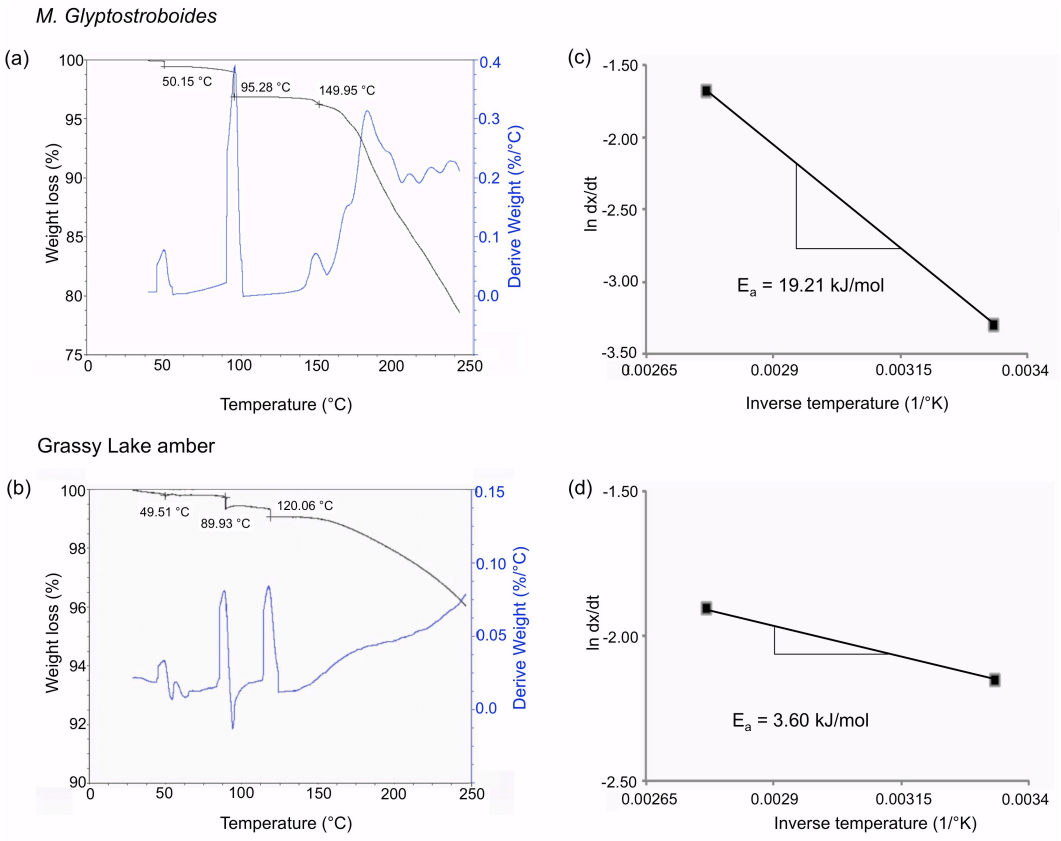


Figure 2-5. TGA and DTG curves (a, b), and calculated activation energy (Ea) from non-isothermal experiments (c, d) for MG-240 and GLA-240 samples. The magnitude of variation from TGA experiments is evidenced by a closer inspection of DTG curve that shows major weight changes at the mentioned temperatures for both samples. The activation energies were calculated from Arrhenius plot in the temperature interval 30 to 50 ˚C.

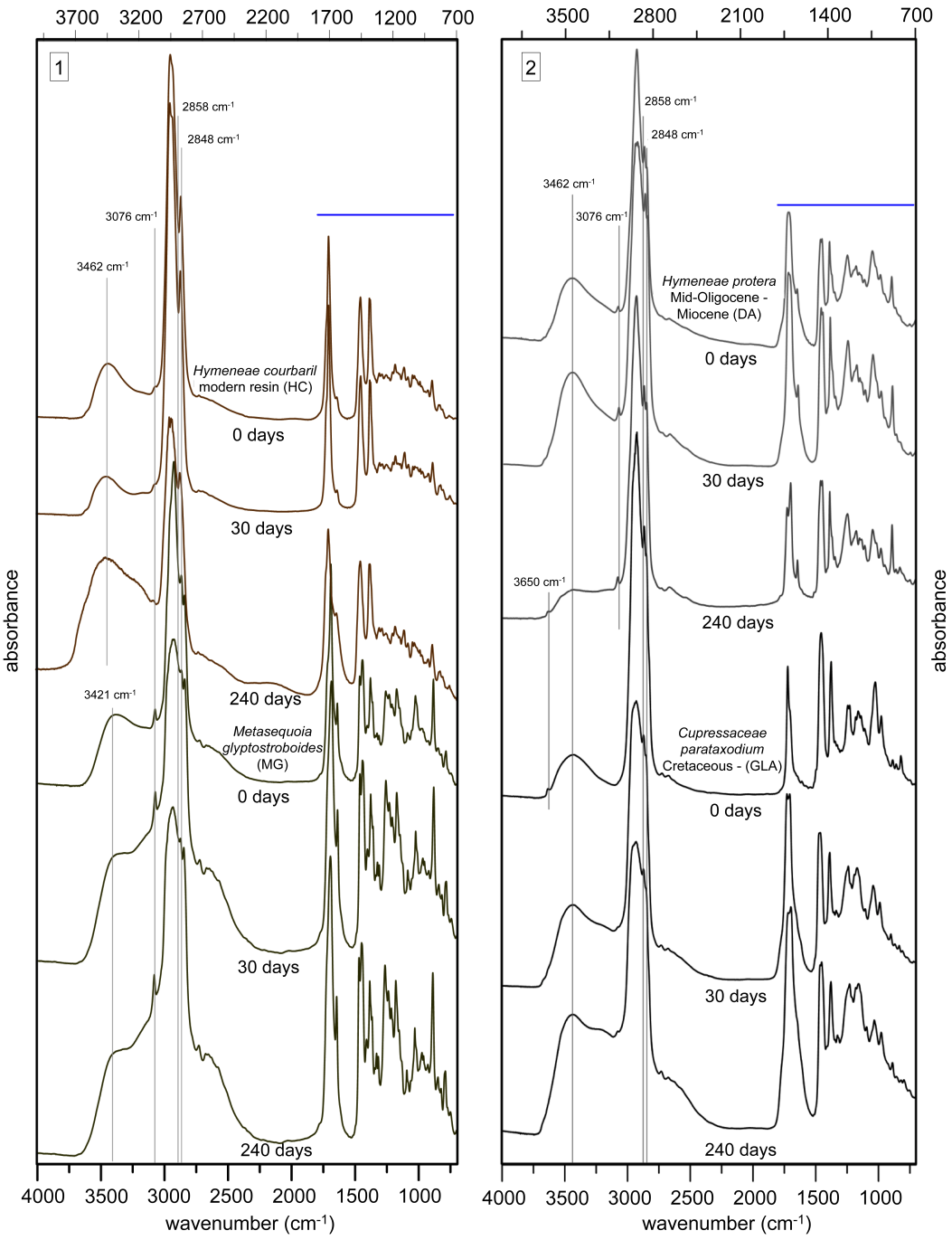


Figure 2-6. FTIR spectra of resin and amber samples after hydrous thermal maturation process at 50 °C. The spectra show untreated (t= 0), and equivalent hydrous-altered (1) resin and (2) amber samples (after 30, and 240 days).

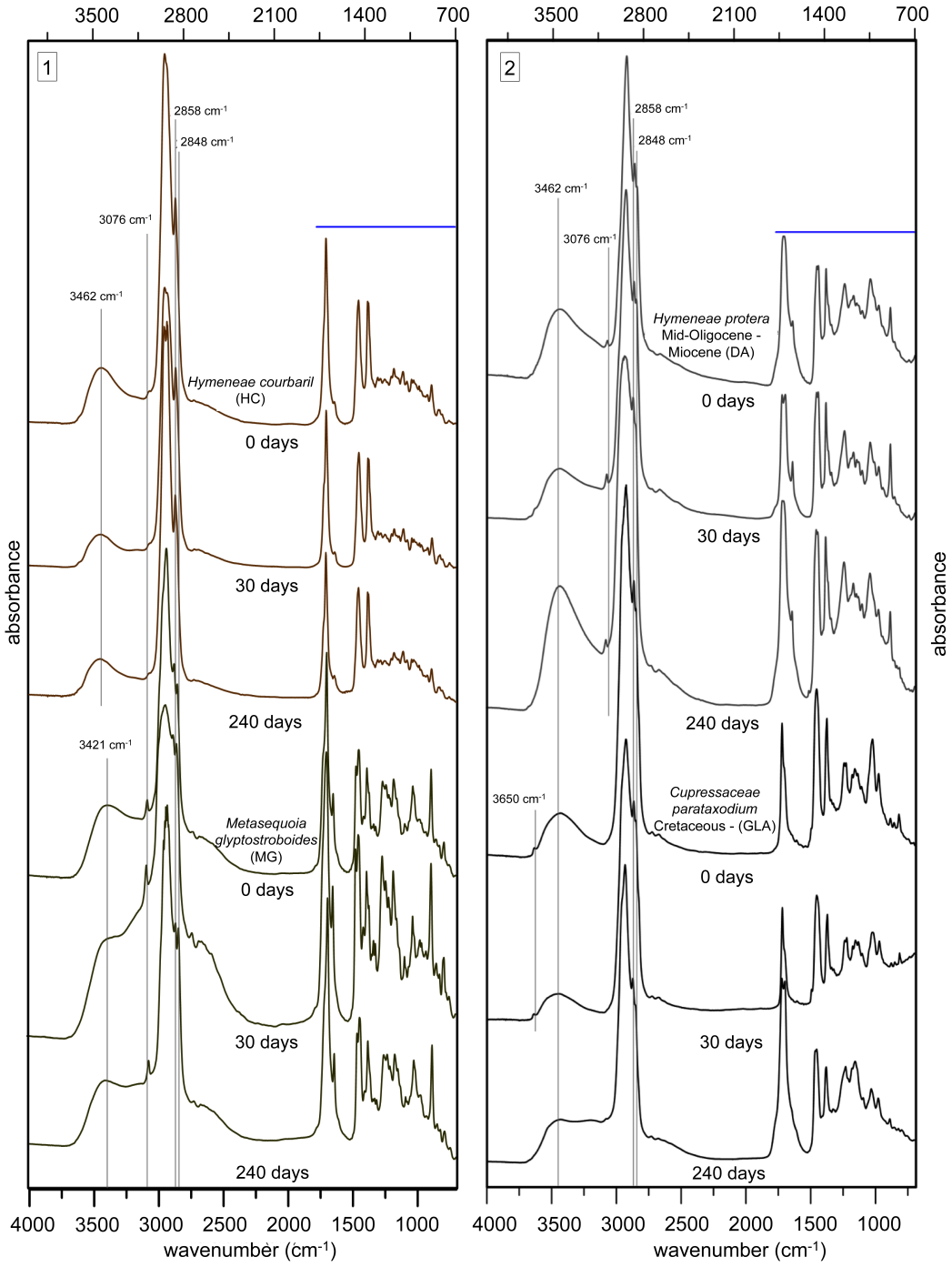


Figure 2-7. FTIR spectra of resin and amber samples after hydrous thermal maturation process at 90°C. The spectra show untreated (t= 0), and equivalent hydrous-altered (1) resin and (2) amber samples (after 30, and 240 days).

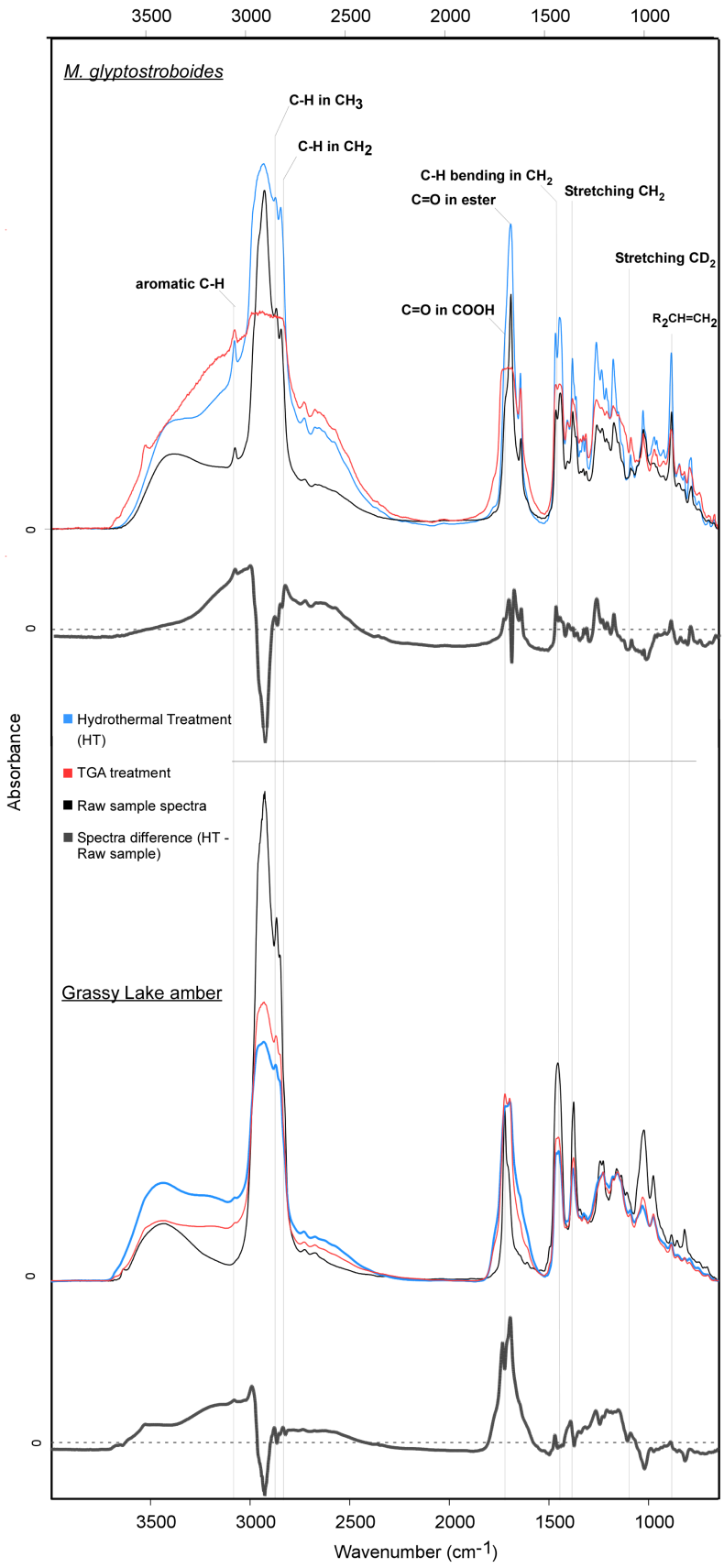
3500
3000
2500
2000
1500
1000
M. glyptostroboides
C-H in CH3
C-H in CH2
C-H bending in CH2
C=O in ester
Stretching CH2
Stretching CD2
aromatic C-H
C=O in COOH
R2CH=CH2
0
0
Hydrothermal Treatment (HT)
TGA treatment
Raw sample spectra
Spectra difference (HT - Raw sample)
Absorbance
Grassy Lake amber
0
0
3500
3000
2500
2000
1500
1000
Wavenumber (cm-1)

Figure 2-8. Spectral FTIR comparison of untreated MG and GLA samples subjected to hydrothermal maturation conditions by 240 days (a-b), and their products after anhydrous thermal treatment (TGA) (c). The subtraction of raw spectra from hydrous-treated spectra (d) reveals significant features induced by the thermal maturation process here implemented.

## 2.6. References


Anderson K., Winans, R.E., and Botto, R.E., (1992). The nature and fate of natural resins in the geosphere. II. Identification, classification and nomenclature of resinites. *Organic Geochemistry*, 18(6), 829–841.

Beck, C.W., (1986). Spectroscopic investigations of amber. *Applied Spectroscopy*, 22, 57–200.

Bellenger, V., Verdu, J., and Morel, E., (1989). Structure-properties relationships for densely cross-linked epoxide-amine systems based on epoxide or amine mixtures. *Journal of Materials Science*, 24(1), 63–68.

Chikaraishi, Y., Naraoka, H., and Poulson, S. R., (2004). Carbon and hydrogen isotopic fractionation during lipid biosynthesis in a higher plant (*Cryptomeria japonica*). *Phytochemistry*, 65(3), 323–330.

Chikaraishi, Y., Tanaka, R., Tanaka, A., and Ohkouchi, N., (2009). Fractionation of hydrogen isotopes during phytol biosynthesis. *Organic Geochemistry*, 40(5), 569–573.

Clifford, D. J., Hatcher, P. G., Botto, R. E., Muntean, J. V., Michels, B., and Anderson, K. B., (1997). The nature and fate of natural resins in the geosphere—VIII. NMR and Py-GC-MS characterization of soluble labdanoid polymers, isolated from Holocene class I resins. *Organic Geochemistry*, 27, 449–464.

Coleman, M. L., Shepherd, T. J., Durham, J. J., Rouse, J. E., Moore, G. R., (1982). Reduction of water with zinc for hydrogen isotope analysis. *Analytical Chemistry*, 54(6), 993–995.

Cunningham, A., Gay, I. D., Oehlschlanger, A. C., and Langenheim, J. H., (1987). $^{13}C$ NMR and IR analyses of the structure, aging and botanical origin of Dominican and Mexican ambers. *Phytochemistry*, (22), 965–968.

DeBond, N., Fogel, M. L., Morrill, P. L., Benner, R., Bowden, R., and Ziegler, S., (2012). Variable δD values among major biochemicals in plants: implications for environmental studies. *Geochimica et Cosmochimica Acta*, 111, 117–127.

Derrick, M. R., Stulik, D., and Landry, J. M., (1999). Infrared spectroscopy in conservation science. *Getty Publications*. 236 p.

Epstein, S., Yapp, C.J., and Hall, J.H., (1976). The determination of D/H ratios of non-exchangeable hydrogen in cellulose extracted from aquatic and land plants. *Earth and Planetary Science Letters*, 30, 241–251.

Flakus, H. T., and Chelmecki, M., (2002). Infrared spectra of the hydrogen bond in benzoic acid crystals: temperature and polarization effects. *Spectrochimica acta. Part A, Molecular and Biomolecular Spectroscopy*, 58(1), 179–96.

Grimaldi, D. A., (1995). The age of Dominican amber. *In* Anderson, K. B. and J. C. Crelling, editors. Amber, resinite, and fossil resins. American Chemical Society Symposium Series 617. 203–217.Washington, DC: American Chemical Sociaty.

Grimaldi, D. A., (1996). Amber: window to the past. *Harry N. Abrams in association with the American Museum of Natural History*, New York, 216 pp.

Grimalt, J., Simoneit, B., Hatcher, P., and Nissenbaum, A., (1988). The molecular composition of ambers. *Organic Geochemistry*, 13(4–6), 677–690.

He, Y., Zhu, B., and Inoue, Y., (2004). Hydrogen Bonds in Polymer Blends. *Progress in Polymer Science*, 29(10), 1021–1051.

Jeffrey, G. A., and Jeffrey, G. A., (1997). An introduction to hydrogen bonding. 12, p. 303, *Oxford University Press*, New York.

Langenheim, J. H., (1969). Amber: a botanical inquiry. *Science*, 163(3872), 1157.

Langenheim, J. H., (1995). Biology of amber-producing trees : focus on case studies of *Hymenaea* and *Agathis*. *In* Amber, resinite and fossil resins (eds K. B. Anderson and J. C. Crelling). 1–31. Washington, D.C.: American Chemical Society.

Langenheim, J.H., and Beck, C.W., (1965). Infrared spectra as a mean of determinig botanical source of amber. *Science*, 149(3679), 52–55.

Lambert J.B., Frye, J.S., and Poinar, G.O., (1985). Amber from the Dominican Republic: analysis by nuclear magnetic resonance spectroscopy, *Archaeometry,* 27, 43–51.

LePage, B., Yang, H., and Matsumoto, M., (2005). The evolution and biogeographic history of Metasequoia. *In* The Geobiology and Ecology of Metasequoia (eds LePage, B. A., Williams, C. J. and Yang, H.), 22, 3–114, *Springer*, Dordrecht.

Lyons, P. C., Mastalerz, M., and Orem, W. H., (2009). Organic geochemistry of resins from modern *Agathis australis* and Eocene resins from New Zealand: Diagenetic and taxonomic implications. *International Journal of Coal Geology*, 80(1), 51–62.

Murae, T., Shimokawa, S., and Aihara, A., (1995). Pyrolytic and spectroscopic studies of the diagenetic alteration of resinites. *In* Amber, resinite and fossil

resins (eds K. B. Anderson & J. C. Crelling), 76–91. Washington, DC: American Chemical Society.

Murray, A. P., Edwards, D., Hope, J. M., Boreham, C. J., Booth, W. E., Alexander, R. A., and Summons, R. E., (1998). Carbon isotope biogeochemistry of plant resins and derived hydrocarbons. *Organic Geochemistry*, 29(5–7), 1199–1214.

McKellar, R. C., Wolfe, A.P., Tappert, R., Muehlenbachs, K., (2008). Correlation of Grassy Lake and Cedar Lake ambers using infrared spectroscopy, stable isotopes, and palaeoentomology. *Canadian Journal of Earth Sciences*, 45, 1061–1082.

McKellar, R. C., Wolfe, A. P., Muehlenbachs, K., Tappert, R., Engel, M. S., Cheng, T., and Sánchez-Azofeifa, G. A., (2011). Insect outbreaks produce distinctive carbon isotope signatures in defensive resins and fossiliferous ambers. *Proceedings Biological Sciences/The Royal Society*, 278, 3219–3224.

McKellar, R. C., and Wolfe, A. P., (2010). Canadian Amber. *In* Biodiversity of fossils in amber from the major world deposits (ed. D. Penney), 96–113, *Siri Scientific Press*, Manchester.

Nissenbaum, A., and Yakir, D., (1995). Stable Isotope Composition of Amber. *In* Amber, resinite and fossil resins (eds. K. B. Anderson & J. C. Crelling), 34–42. Washington, DC: American Chemical Society.

Nissenbaum, A., Yakir, D., and Langenheim, J. H., (2005). Bulk carbon, oxygen, and hydrogen stable isotope composition of recent resins from amber-producing *Hymenaea*. *Die Naturwissenschaften*, 92(1), 26–29.

Nugue, C., (2005). Cultivars of *Metasequoia glyptostroboides*. *In* The Geobiology and Ecology of Metasequoia (eds LePage, B. A., Williams, C. J. and Yang, H.), 22, 361–366, *Springer*, Dordrecht.

Pastorelli, G., Richter, J., and Shashoua, Y., (2011). Photoageing of Baltic amber – Influence of daylight radiation behind window glass on surface colour and chemistry. *Polymer Degradation and Stability*, 96(11), 1996–2001.

Pastorelli, G., Richter, J., and Shashoua, Y., (2012). Evidence concerning oxidation as a surface reaction in Baltic amber. *Spectrochimica Acta. Part A, Molecular and Biomolecular Spectroscopy*, 89, 268–269.

Pastorelli, G., Shashoua, Y., and Richter, J., (2013). Hydrolysis of Baltic amber during thermal ageing - an infrared spectroscopic approach. *Spectrochimica Acta. Part A, Molecular and Biomolecular Spectroscopy*, 106, 124–128.

Sessions, A., (2006). Seasonal changes in D/H fractionation accompanying lipid biosynthesis in *Spartina alterniflora*. *Geochimica et Cosmochimica Acta*, 70(9), 2153–2162.

Sessions, A. L., Burgoyne, T. W., Schimmelmann, A., and Hayes, J. M., (1999). Fractionation of hydrogen isotopes in lipid biosynthesis. *Organic Geochemistry*, 30, 1193–1200.

Sessions, A. L., and Hayes, J. M., (2005). Calculation of hydrogen isotopic fractionations in biogeochemical systems. *Geochimica et Cosmochimica Acta*, 69(3), 593–597.

Schimmelmann, A., Lewan, M. D., and Wintsch, R. P., (1999). D/H isotope ratios of kerogen, bitumen, oil, and water in hydrous pyrolysis of source rocks containing kerogen types I, II, IIS, and III. *Geochimica et Cosmochimica Acta*, *63*(22), 3751–3766.

Schimmelmann, A., Sessions, A. L., and Mastalerz, M., (2006). Hydrogen isotopic (D/H) composition of organic matter during diagenesis and thermal maturation. *Annual Review of Earth and Planetary Sciences*, 34(1), 501–533.

Tappert, R., McKellar, R. C., Wolfe, A. P., Tappert, M., Ortega-Blanco, J., and Muehlenbachs, K., (2013). Stable carbon isotopes of resin exudates record responses of C3 plants to changes in atmospheric oxygen since the Triassic. *Geochimica et Cosmochimica Acta*, 121, 240–262.

Tappert, R., Wolfe, A. P., McKellar, R. C., Tappert, M., and Muehlenbachs, K., (2011). Characterizing modern and fossil gymnosperm exudates using micro-Fourier transform Infrared Spectroscopy. *International Journal of Plant Sciences*, 172(1), 120–138.

Trejo, F., Rana, M. S., and Ancheyta, J., (2010). Thermogravimetric determination of coke from asphaltenes, resins and sediments and coking kinetics of heavy crude asphaltenes. *Catalysis Today*, 150(3–4), 272–278.

Terwilliger, V.J., and DeNiro, M.J., (1995). Hydrogen isotope fractionation in wood-producing avocado seedlings: biological constraints to paleoclimatic interpretations of δD values in tree ring cellulose nitrate. *Geochimica et Cosmochimica Acta*, 59, 5199–5207.

Wolfe, A.P., Csank, A.Z., Reyes, A.V.E., McKellar, R.C., Tappert, R., and Muehlenbachs, K., (2012). Pristine Early Eocene wood buried deeply in kimberlite from northern Canada. *PloS One*, 7(9), e45537.

Wolfe, A. P., Tappert, R., Muehlenbachs, K., Boudreau, M., McKellar, R. C., Basinger, J. F., and Garrett, A., (2009). A new proposal concerning the

botanical origin of Baltic amber. *Proceedings. Biological sciences / The Royal Society*, 276(1672), 3403–3412.

Yakir, D., and DeNiro, M. J., (1990). Oxygen and Hydrogen Isotope Fractionation during Cellulose Metabolism in *Lemna gibba. Plant physiology*, 93(1), 325–332.

Yamamoto, S., Otto, A., Krumbiegel, G., and Simoneit, B. R. T., (2006). The natural product biomarkers in succinite, glessite and stantienite ambers from Bitterfeld, Germany. *Review of Palaeobotany Palynology*, 140, 27–49.

Yang, H., and Leng, Q., (2009). Molecular hydrogen isotope analysis of living and fossil plants—*Metasequoia* as an example. *Progress in Natural Science*, 19(8), 901–912.

Zhou, J., and Lucas, J. P., (1999). Hygrothermal effects of epoxy resin. Part I : the nature of water in epoxy. *Polymer*, 40, 5505–5512.

## CHAPTER 3

## Fourier transform infrared (FTIR) spectroscopic characterization of modern and fossil resins after long-term hydrous and anhydrous thermal treatments

### 3.1. Introduction

The Fourier-Transform Infrared (FTIR) spectra of resins and amber have been widely used as a tool for their biochemical characterization, establishing their botanical source and determining their maturity (*i.e.*, Brody et al., 2001, Tappert et al., 2011; Wolfe et al., 2012). Although a number of studies have investigated the effects of thermal exposure in the FTIR spectral response of resins, demonstrating that their constitutive functional groups can be affected by oxidation, hydrolysis, and polymerization (*i.e.*,Wolfe et al., 2012; Pastorelli et al., 2013), and the effects of shallow to intermediate burial diagenesis are still outstanding issues (see Gonzalez et al., 2012).

In this study, I simulate a range of fluid-resins interactions during burial, aiming to evaluate how these factors affect the FTIR spectra of matured resins and their fossilized counterparts, amber. The experimental simulations were coupled with post-experimental FTIR analyses and assessed the effects of (1) conditions associated with weathering (*e.g.*, Pastorelli et al., 2011, 2012, 2013), (2) pyrolysis (*e.g.*, Anderson et al., 2006; Lyon et al., 2009), (3) physicochemical thermal alteration (*e.g.*, Dal Corso et al., 2013), and (4) potential alteration of early diagenetic compounds within resins (*e.g.*, Qin et al., 2012 and references therein).

As it has been demonstrated that ambers subjected to complex geological histories preserve most of their original spectral FTIR signatures (*e.g.*, Grimalt et

al., 1988; Murae et al., 1995; Lyons et al., 2009; Dal Corso et al., 2013), with this experimental approach it would be possible to demonstrate whether or not ambers undergo major chemical changes at relatively low temperatures. Also, these results may allow reconstructing the diagenetic history and maturation stages of amber, in order to determine the conditions that led to amber preservation.

## 3.2. Methodology

### 3.2.1. Samples

This study evaluates modern resins from phylogenetically related *Metasequoia glyptostroboides* (Cupressaceae) (MG), and *Hymenaea courbaril* (Fabaceae) (HC), with phylogenetically related fossilized resinites from Late Cretaceous (Campanian) Grassy Lake amber (GA) (McKellar et al., 2008; McKellar and Wolfe, 2010), and mid-Oligocene to Miocene Dominican amber (DA) (Grimaldi, 1995). Samples were subjected to hydrothermal maturation experiments using deuterated water ($[D_w]$ = 1%) at 50 ˚C and 90 ˚C, and were subsequently treated via an anhydrous thermal maturation process at temperatures up to 250 ˚C (TGA).

### 3.2.2. Fourier Transform Infrared (FTIR) microspectroscopy

FTIR analyses were conducted using a Thermo-Nicolet Nexus 470 bench spectrometer, fitted with a dual-aperture continuum infrared microscope with a motorized stage. Fresh, inclusion-free, crushed samples less than 5 μm in size were mounted directly on $NaCl_{(s)}$ disc. Before spectroscopic analyses, the infrared microscope in its visual mode was used to search for even surfaces in areas free of

impurities; this step was particularly important in modern resin samples subjected to the experimental treatment described above, because the treatment produced vacuoles or fluid inclusions. Beam size was set at either 50 or 100 μm, and for each analysis 200 scans were accumulated at a spectral resolution of 4 $cm^{-1}$, resulting in 869 absorption values over the 4000 – 700 $cm^{-1}$ interval (equivalent to wavelengths of 2.5–15 μm).

Raw and thermally altered resins and ambers were analyzed in order to compare and identify their chemical changes after simulated maturation and deuterium isotope exchange. Absorbance values were normalized to unity, and their regions at 3700–3500 $cm^{-1}$ and 2750–2580 $cm^{-1}$ were examined in order to identify possible changes in their OH- and OD-stretching frequencies, respectively. In addition, the presence of hydrogen-bonded fractions of carboxylic acid groups (1699–1700 $cm^{-1}$) associated with ester functional groups and aromatic carbon double bonds (1525 $cm^{-1}$) were examined in an attempt to identify possible changes due to simulated time-dependent hydrous maturation. Spectra of raw untreated samples were subtracted from those of equivalent samples that were subjected to hydrothermal treatment (90 °C, 240 days), in order to determine band changes. Spectral band ratios (3400 $cm^{-1}$/3088 $cm^{-1}$, 1646 $cm^{-1}$ /1450 $cm^{-1}$, and 924 $cm^{-1}$/887 $cm^{-1}$) were calculated and plotted.

3.2.3. Multivariable statistical analyses

Changes in the spectral bands resulting from the experimental treatment were identified using a minimum-variance hierarchical clustering, which also permitted recognition of correlation between resin-amber and resin acid

chemomarkers. The latter are important for determining specific molecular arrangements that produce a given spectral fingerprint region. In other words, the compounds that induce thermal polymerization and chemical functional group variability were analyzed within a cluster framework that included bands characteristic of resin acids, common bands identified in sample products of hydrous and anhydrous treatment (resin and amber). Bands with significant absorbance values were selected in order to reduce the number of null values and ensure a robust dataset. Band ratios (n= 7) comparison was used as input method (*e.g.*, Wolfe et al., 2009). The scale of differences was corrected by standardizing the data set prior to cluster analysis. Cluster analyses were performed using the statistical package MVSP (Kovach Computing Services).

### 3.3. Results

The dynamics of the alteration-preservation process of resins and ambers were analyzed by contrasting the FTIR spectra of natural samples with those subjected to long-term isothermal hydrous alteration. The latter showed changes in absorbance peaks that can be attributed to chemical alteration related to water molecules interactions, thermal alteration, both under anoxic and oxic condition, and to a minor extent, deuterium incorporation. The observed trends are described below.

#### 3.3.1. Control vs. hydrothermal treated samples

After 240 days, hydrothermally treated resins showed an increase of peak broadness within the 3600–3080 $cm^{-1}$ absorbance region. This region is related to

hydrogen bond hydroxyl groups associated with free alcohols (*i.e.*, 3650 $cm^{-1}$), phenols (3600 – 3200 $cm^{-1}$), and carboxylic acid's intramolecular hydrogen bonds (3500–2400 $cm^{-1}$) (Grimalt et al., 1988; Tappert et al., 2011). This feature, however, was not observed in Dominican amber (DA) (see Fig. 3-1, Table 3-1). The FTIR spectrum of DA showed a common peak at 3076 $cm^{-1}$ associate to $sp^2$– hybridized C-H bonds, which is absent or weak in Grassy Lake amber (GLA) (Langenheim, 1969; Grimalt et al., 1988; Tappert et al., 2011)(Fig. 3-1).

The absorption bands at 2960–2935 $cm^{-1}$ and 2850–2840 $cm^{-1}$ are characteristic of $sp^3$– and $sp^2$– C-H hybridization (Fig 3.1a). The 1722–1690 $cm^{-1}$ region, which is attributed to carboxyl functional groups, remained unchanged for MG and HC. These exhibited a sharp peak at 1715 $cm^{-1}$, which is generally attributed to carbonyl groups (Langenheim, 1969; Tappert et al., 2011; Pastorelli et al., 2013). However, both DA and GLA showed the carbonyl bands attributed to the carboxylic acids (1693 $cm^{-1}$), and non- hydrogen-bonded carbonyl groups ("free" C=O at 1722 $cm^{-1}$). LGH, MG, and DA also exhibited a sharp peak related to dienes at 1648 $cm^{-1}$, but this peak is notably absent in GLA (Fig. 3-1).

Bands at 1495 $cm^{-1}$ ($CH_2$ bending), 1392 (1250) $cm^{-1}$, and 1170 $cm^{-1}$, assigned to C-O bonds in acid and ester functional groups, remained unchanged in resin and DA samples, but GLA showed both a decrease in intensity and sharpness that could be related to products of thermal alteration (Fig. 3-1). In general, the fingerprint region remained unchanged for all of the samples, but DA showed an increase in absorbance in the 885 $cm^{-1}$ band. On the other hand, a peak shift was observed when comparing GLA-BE and GLA-240 in the 1228 - 1108

$cm^{-1}$ spectra region. Comparing the band ratio of 1468/1093 of GLA-BE (1468/1092=2.54) and GLA-AT (1468/1092=2.13), by their subtraction its shift was determine to be about 0.47 (Table 3-1). Also, the identification of a distinctive peak at 1093 $cm^{-1}$ may represent the effects of deuterium exchanges (Tashiro et al., 1994).

Changes on the spectral response of carboxylic functional groups, under hydrous- and TGA conditions (Fig. 3-1) were observed in the intensity of the peak at 1720 $cm^{-1}$ (C=O stretching of esters) and at 1698 $cm^{-1}$ (C=O stretching carboxylic acid). Interestingly, by subtracting the spectra of untreated samples from the spectra of thermally altered samples, it was revealed that 1720 $cm^{-1}$ peak absorbance increase and 1698 $cm^{-1}$ peak decrease (Fig. 3-2). Similarly, changes in bands assigned to vibrations due to equilibration of the central methylene groups interacting with neighbouring methylene groups (1451 $cm^{-1}$), and interactions of the methylene groups with adjacent oxygen atoms (1464 $cm^{-1}$) seem reversible (Fig. 3-2).

GLA showed intensity changes in peaks that are assigned to C-O bonds in acid and ester functional groups at 1495, 1382 (1250), and 1170 $cm^{-1}$, respectively (Fig. 3-1 c2.2). Resins and DA, on the other hand, did not show major changes in this region, but exhibited a decrease in intensity and sharpness of these peaks. This also may be due to the formation of alteration products (Fig. 3-1 c2.1). Between 1170–700 $cm^{-1}$ are regions related to C-O (1170–1025 $cm^{-1}$), alkenes (C=C-H, 980–700 $cm^{-1}$), and C-H ring vibrations (900–700 $cm^{-1}$) that were consistently found to vary in all samples.

3.3.2. Control vs. anhydrous treated (TGA) samples

For TGA treated samples, the major spectral FTIR changes were associated to bands at 3080 (3070), 1645, and 890 cm $^{-1}$. An increase in absorption within these bands, which are assigned C-H stretching vibrations of the =CH-R structure (conjugate double bond), and C=C and $CH_2$ vibrations of olefinic groups, reflect unsaturation and conversion of single bonds into double bonds, which is the inverse process of polymerization (Anderson et al., 1992). In most compounds with a labdane skeleton, the 3080 cm $^{-1}$ band can be correlated to C-H stretching vibration of the exomethylene bond (Grimalt et al., 1988; Anderson et al., 1992; Wolfe et al., 2009; Tappert et al., 2011). The appearance of this band in GLA after anhydrous-isothermal treatment, and the observed increase in intensity in younger ambers and resins, together with an increase in the peak located at ~1645 cm $^{-1}$ (stretching C=C within exocyclic methylene) (Grimalt et al. 1988), and a decrease in the peak at ~1450 cm $^{-1}$ (bending modes in C-H), are both consistent with augmented in unsaturation (Fig. 3-2 c). As previously observed, mature ambers show an inverse relation between the peaks listed above, and an absence of absorption peak at 3080 cm$^{-1}$ that result from their depletion of exocyclic methylene during post-depositional polymerization (*e.g.*, Brody et al., 2001; Tappert et al., 2011). In mature ambers, non-variability or slight increases on the out-of-plane peak C-H deformation at 880 – 890 cm $^{-1}$ were also observed.

### 3.3.3. Changes in band ratios

#### *3.3.3.1. Sample product of hydrothermal alteration*

Variability in the absorbance band ratios of samples subjected to hydrous isothermal conditions reflects changes that are likely to occur during their maturation process upon resin burial. As shown in Table 3-2, relative changes in intensity of band ratios with increasing temperature is evident in HC, DA and GLA samples subjected to hydrous maturation condition (Fig. 3-3). These specimens exhibited variations in the absorbance intensity of OH-stretching (3400 $cm^{-1}$) and asymmetric C-H stretching of terminal alkene (3088 $cm^{-1}$), resulting in peak ratios (3400/3088) showed a trend of progressive decrease from 50 to 90 °C (Fig. 3-3). A similar trend was observed in HC and GLA, for band ratios including those associated with stretching non-conjugated C=C (1646 $cm^{-1}$), and bending terminal $CH_2$ and $CH_3$ (1450 $cm^{-1}$). By contrast, the FTIR spectra of MG and DA samples show an increase in the 1646/1450 ratio from 50 to 90 °C. This was also observed in their phylogenetically related resins (MG and GLA), which showed a positive correlation with increasing temperature in the 1460/1448, 1448/1385 band ratios. By contrast, DA and HC showed negative trends (Fig. 3-3 b).

#### *3.3.3.2. TGA treatment of hydrothermal alteration products*

For fossilized resins, a decrease within 924/887 and 823/791 band ratios was observed with increasing temperature. The same effect was also observed in the HC and MG spectra in the 924/887 band ratio. But in MG, the 823/791 band

ratio has a characteristic positive trend (Table 3-2). After AT treatment (TGA), amber samples showed a decrease in 1646/1450, 1448/1385 and 823/791 band ratios. GLA also showed a decrease in 924/887 ratio, whilst DA samples showed no variation. For samples GLA and DA, the 1722/1693 ratio reflected no change after anhydrous thermal maturation (Table 3-2). In contrast, MG resin showed a decrease in 3400/3088, 1460/1448, and 1448/1385, but an increase in 1646/1450, 924/887, and 823/791. MG and GLA showed similarities in their 1448/1385 and 823/791 band ratios; this trend was also observed in HC and DA samples (Table 3-2, Fig. 3-3).

The decrease of the band ratios 3400/3088, 1722/1693 and 924/887, and the increase of the ratio 1646/1450 ratio identified in the spectra of resins indicates the progress of the decomposition due to oxidation and hydrolysis. Amber samples, however, showed an opposite trend. DA showed an increase in absorbance within the 885 $cm^{-1}$ band that can be attributed to the presence of an exocyclic methylene group (Beck, 1986).

### 3.3.4. Thermally treated samples and resin acids spectra

Figure 3-4 describes two major clusters, one cluster reflects the association between the resin acids and amber, and the other that of resin acids and the low maturity resins (Fig. 3-4a,b). Accordingly, group “a1” represents the relation between abietic acid and GLA, whilst group “a2” shows the relation between 7-oxodehydroabietic acid and MG resins (Fig. 3-4a). The grouping between DA and HC showed less discrimination upon the clustering with resin acids. This can be correlated with less alteration to their primary structure (Fig. 3-4b). Resins and

ambers derived from Fabaceae species are prone to show a spectral signature characteristic of abietane and sandaracopimarene (see Table 3-1). By contrast, Cupressaceae-derived resins show a characteristic spectrum that combines that of abietene, pimarene and sandaracopimarene, and allow comparison with that of resin acids (Table 3-1) (Anderson et al., 2006; Tappert et al., 2011).

### 3.4. Discussion

Although, the physicochemical response of resinites was temperature dependent, some minor but significant spectral variations were observed in samples altered under hydrothermal (HT) rather than under anhydrothermal (AT) conditions. Most spectral changes occurred above 50 °C, providing insights into the evolution of functionalities during burial diagenesis. However, and in agreement with previous research, no major alteration in primary skeletal structure was observed during both long-term thermal treatment and anhydrous-thermal stress (Otto et al., 2001, 2002, 2007; Tappert et al., 2011). This indicates that, in general, the primary biomolecular structure of resins remains unchanged during early to shallow burial diagenesis. Furthermore, this shows that the FTIR absorbance variability is an useful proxy for determining the maximum thermal exposure of amber specimens.

The high activation energy required for triggering major molecular changes in resins can be reflected in significant variations of the amber' spectra that typically occurs at temperatures exceeding 250 °C (Murae et al., 1995). Thus, at relatively low temperatures, resins transform progressively into amber without major skeletal changes induced by process such as isomerization, decaboxylation

and aromatization (Anderson et al., 1992; Murae et al., 1995). However, it is possible to identify spectral changes associated with chemical modifications to functional groups, which result in variability on their relative absorbance and depends on whether the environmental conditions of maturation are oxic or dysoxic. The spectral differences identified can therefore be grouped in those resulting from (1) long-term hydrous thermal treatment at isotherm condition (50 and 90 °C) under low oxygen concentration (hydrothermal conditions), and (2) thermal treatment at open atmosphere conditions (TGA).

3.4.1. Spectral IR changes after hydrothermal maturation simulation

One of the most relevant changes observed during the hydrothermal maturation process is an increased intensity in distinctive peaks that can be related to an increase in unsaturation of exomethylene ($CH_2$) in diterpenoids, as well as a decrease in peaks representative of the lost or re-equilibration of oxygenate functional groups as carbonyl. For instance, a relative decrease of 1722 $cm^{-1}$, concomitant with an increase in absorbance at 1450 $cm^{-1}$, cannot be regarded as a decarboxylation reaction (Murae et al., 1995). Since the isothermal experiments were conducted at relatively low temperatures, and also because only minor changes were observed in bands representing carbon bonding (*i.e.*, between 2933 $cm^{-1}$ and 2652 $cm^{-1}$) (Table 3-1; Fig. 3-1). On the other hand, the production of aromatic terpenoid functionalities better explain a greater proportion of observed peak changes (*e.g.*, 3400/3080, 1646/1450 and 924/887 band ratios) in samples subjected to isothermal treatment (Table 3-1-2, Fig. 3-1 and 3-2).

The 3005–3076 $cm^{-1}$ region represents conjugated double bonds (R=C-

H)(Roach et al., 2002), and the 3076 $cm^{-1}$ band is commonly observed in immature samples, such as DA, HC and MG resinites (Fig. 3-1)(Langenheim, 1969; Grimalt et al., 1988; Lambert and Frye, 1982; Lambert et al., 2008; Tapper et al., 2011). Changes in these band intensities and ratios with increasing temperature under limited oxygen concentrations are also related to reactions that induce aromatization and dehydrogenation in terpenoid compounds (Simoneit et al., 1986; Dehmer 1995). This effect was also observed in mature samples, such as GLA specimens, that are characterized by the lack of peaks at 3076 $cm^{-1}$, suggesting that increased unsaturation is not exclusive of thermally mature samples, and is a process derived from shallow burial diagenetic reactions (see Qin et al., 2010; Qin et al., 2012), which may in turn result in different alteration pathways (Otto et al., 2001; 2002; 2007).

Oxidative maturation conditions under moderate burial temperatures may induce the loss of hydrogen, cleavage of acid groups and demethylation, also producing aromatic hydrocarbons functionalities (*e.g.*, Otto et al., 2001; 2002; 2007). The products of these reactions can be associated with both an increase in unsaturation related to $CH_2$, $CH_3$ and conjugated rings bending (~1644, 1515, 1445 $cm^{-1}$), and side chains (~1400–1300 $cm^{-1}$). Therefore, the degradation of amber and resins under hydrous conditions seems to produce functional group rearrangement and an auto-oxidation reaction. These effects have been also observed in mature resins (Otto et al., 2007; Pereira et al., 2009).

The combination between oxidative and reductive processes leads to a re-equilibration in the 1730–1700 $cm^{-1}$ region, attributed to carboxyl functional

groups (Tappert et al., 2011; Pastorelli et al., 2012). Although these peaks remained unchanged for resins with hydrogen-bonded carbonyl groups (Table 3-1 and 3-2), DA and GLA showed the same absorbance intensity in both carbonyl bands and in non-hydrogen-bonded carbonyl groups (Tappert et al., 2011, see Table 3-2). This effect was also observed in amber occluded within fossil wood that was found in a kimberlite pipe and preserved as a result of fast reaction under high temperature, and anoxic environmental conditions (Wolfe et al., 2012). This suggests that changes in the 1730–1700 $cm^{-1}$ region result from a temperature-induced equilibrium reaction involving carboxylic acid dimers and monomers (*i.e.*, Lee et al., 1988).

However, over geologic time, resins exposed to moderate temperatures can lose their ring unsaturation and exomethylene functionalities (Anderson et al., 1992). Maturation reactions of resin acids, such as isomerization, polymerization and defuntionalization, would explain the loss of unsaturated functionalities such as oleofinic carbons and monomers (Anderson et al., 1992; Clifford and Hatcher, 1995), whilst the cross-linking reaction of diterpene acids is related to the exponential decrease with age of exocyclic methylene signals. Interestingly, an opposite effect was observed in our hydrous-maturation experiments, suggesting that the kinetic aspect of these processes is complex and thus worthy of furture analysis.

3.4.2. Spectral IR changes of hydrothermally aged samples after anhydrous thermal treatment (TGA)

Besides the spectral influence of molecular water, changes in the carbonyl region, identified when comparing untreated samples and thermally altered GLA samples spectra, suggest an increase in intensity in C=O stretching of esters and a decrease in the C=O stretching of acid bands. In this regard, an increase in intensity in the 1698 $cm^{-1}$ (C=O stretching, esters), and a decrease in the 1720 $cm^{-1}$ (C=O stretching, carboxylic acid) bands is quite evident (cf. Pastorelly et al., 2013). Interestingly, after TGA treatment, the spectrum shows a relative increase of the 1698 $cm^{-1}$ band as compared with the 1720 $cm^{-1}$ band, indicating a temperature dependent reversible process that is also documented by 1451–1464 $cm^{-1}$ bands.

However, it has been shown that under isothermal conditions changes in pressure can also produce aromatic ring instability (Pruzan et al., 1990). Thus, in addition to classic polymerization theories (Anderson et al., 1992), the exposure to lithospheric pressure would also explain the lack of aromatic functional groups and unsaturation in ancient amber (see Pruzan et al., 1990). Also, based on the experimental conditions, the higher temperature clearly produced dehydration reactions, which combined with variable oxygen concentrations, induced a visible change in the functional group FTIR imprint (Table 3-2). Upon calibration, this can be potentially used to determine the maximum depth of burial under a given geothermal gradient and identify the conditions of preservation.

### 3.4.3. Possible alteration of primary resin acids polymers

The primary molecular structures of the tricyclic oleoresins that constitute diterpenoid resin acids have been divided in three groups: abietanes, pimaranes and dehydroabietanes (Keeling et al., 2011; Hamberger et al., 2011). However, the FTIR characterization conducted before and after thermal treatment showed that the changes within the spectra at 50 and 90 °C under hydrous conditions and limited oxygen led to an auto-oxidation reaction, which induces degradation and an increase in unsaturations.

By clustering the spectra of diterpene resin acids and related compounds with that of resins and ambers permit the identification of botanical affinities (*i.e.*, Wolfe et al., 2009), but also their relation with alteration products. In this regard, altered resin and amber samples correlate with the appearance of 7-oxodehydroabietic, dehydroabietic and communic acid appearance (Fig. 3-5a-b). This is an association that is in turn comparable with the products derived from the abietane-type diagenetic pathway identified in a variety of amber deposits (Yamamoto et al., 2006; Otto et al., 2007; Qin et al., 2012) (Fig. 3-5). The presence of dehydroabietic acid may therefore be used to constrain this association, as observed when comparing the increase in unsaturations in the spectra of Cupressaceae-derived organic matter and their early diagenetic products (Simoneit and Mazurek, 1982; Qin et al., 2012). Also, the thermally-treated resins correlated with non-treated ambers, which suggest a possible unexplored pathway for transforming resins into ambers (*e.g.*, Fig. 3-4a).

3.4.4. Deuterium incorporation: case study GLA

As hydrous thermal experiments were conducted with deuterated waters, the spectral analyses allowed identification of peak shifts resulting from hydrogen substitution by deuterium. These shifts, reported to occur in the 2500–2000 cm $^{-1}$ band (Flakus and Chemecki, 2002), are difficult to evaluate using FTIR analyses, mostly because of the deuterium exchange in resins and amber is <1.9% (González et al., 2012). Also, the effects of deuterium exchange in resins and amber could be superimposed on the vibration of various chemical species and thus remain imperceptible into FTIR spectra (Lukas and Chemecki, 2002). However, the characteristic changes on the spectral features of GLA amber at 1092 cm $^{-1}$ (stretching $CD_2$), and 815 cm $^{-1}$ (C-D in-plane bending vibration) have been associated in the past with the incorporation of deuterium into polyethylene blends (*i.e.* Tashiro et al., 1994). The band shift of 1468/1093 band ratio for GLA-BE and GLA-AT evidenced the low magnitude and effect of the deuterium incorporation in modern and fossil samples (Table 3-1; Fig. 3-4).

## 3.5. Conclusions

FTIR spectroscopy provides relevant information that not only reveals the phylogenetic relation with the resin's source tree, but also the diagenetic conditions under which resins were preserved and transformed into amber. The spectral response seems particularly sensitive to the maximum burial temperature to which resin and ambers were subjected, and also to the D isotope composition of pore waters. Accordingly, our concluding remarks are:

1.- Resins and ambers subjected to hydrothermal burial diagenetic condition showed an increase in functionalities related to unsaturation and a decrease in oxygenated functional groups. This was evidenced by 3400/3080, 1646/1450 and 924/887 band ratios.

2.- The appearance of a characteristic aromatic functional group at 3076 $cm^{-1}$ in HC, MG and DA, together with an increase in unsaturation, and correlation of altered samples with dehydroabitic acid, suggest the presence of early diagenetic abietene derived polyunsaturated compounds.

3.- DA and GLA showed increase and decrease in intensity of the 1730–1699 $cm^{-1}$ carbonyl functional groups that lead to an equilibrium between acids and esters. Thus, samples under hydrous conditions showed predominance of the acids, which is related to hydrolysis and autoxidation; whilst samples altered under anhydrous thermal treatment indicated relative prevalence of the esters, which is related to dehydration and oxidative reactions.

4.- Evidence of deuterium incorporation in GLA can be observed after the shift of peaks related to $CH_2$ stretching (1090 $cm^{-1}$; 1468 $cm^{-1}$), evidencing the effect of deuterium exchange between amber and deuterated water under hydrous thermal conditions. Band ration between 1468 $cm^{-1}$/1093 $cm^{-1}$ confirmed the low rate of deuterium incorporation.

Table 3-1. Bands identified in the infrared (IR) spectra of resins and fossil resins. Raw samples were compared with equivalent hydrothermally treated (240 days) samples at 50 ˚C and 90 ˚C. Also, the IR spectra of products after hydrothermal and subsequently thermal gravimetric analysis (TGA) treatment were also included. Samples of resins (1) and amber (2) were separated based on their phylogenetic association with Fabaceae (*i.e.*, 1.1; 2.1) or Cupressaceae (*i.e.*, 1.2; 2, 1). The grey highlighted samples' spectra are represented in Figure 3-1.

| Family | [1]Fabaceae | | | | | | | [2]Cupressaceae | | | | | | | |
|---|---|---|---|---|---|---|---|---|---|---|---|---|---|---|---|
| Resins and ambers samples | **HC $_{Raw}$** | **HC $_{50°C}$** | **HC $_{90°C}$** | **DA $_{Raw}$** | **DA $_{50°C}$** | **DA $_{90°C}$** | **DA-AT** | **MG $_{Raw}$** | **MG $_{50°C}$** | **MG $_{90°C}$** | **MG-AT** | **GLA $_{Raw}$** | **GLA $_{50°C}$** | **GLA $_{90°C}$** | **GLA-AT** |
| | | | | 3711.46 | | | 3634.03 | | | | 3731.30 | 3636.25 | | | |
| | 3456.38 | 3477.08 | 3426.13 | 3427.82 | 3491.76 | 3446.70 | 3443.78 | 3375.74 | | 3441.06 | 3523.50 | 3437.64 | 3439.20 | 3499.06 | 3449.01 |
| | | | | | | | | | 3298.78 | | | | 3242.89 | | 3208.33 |
| | | 3078.46 | 3078.35 | 3076.81 | 3079.06 | 3078.08 | 3077.77 | 3078.38 | 3079.13 | 3079.14 | 3078.85 | | 3077.39 | | |
| | 2962.16 | 2951.91 | | | | | | | | | | | | | |
| **I** | | 2929.33 | 2930.22 | | 2930.47 | 2933.48 | 2931.16 | 2930.28 | 2932.29 | 2929.85 | | 2926.24 | 2930.62 | 2927.40 | 2930.47 |
| | 2869.02 | 2868.61 | | 2866.32 | 2866.08 | 2868.03 | 2866.63 | 2871.09 | 2873.86 | 2870.60 | | 2867.30 | 2873.16 | 2869.42 | 2870.03 |
| | | | 2843.59 | | 2848.01 | 2843.64 | 2848.22 | 2847.17 | 2847.43 | 2847.23 | | | | | |
| | | | 2728.02 | | 2725.74 | | | 2727.74 | 2729.05 | | 2731.44 | 2728.01 | 2730.65 | 2726.58 | 2728.92 |
| | | | | 2662.21 | | | 2667.94 | | 2676.12 | | 2676.09 | 2677.81 | 2675.06 | 2671.69 | 2677.04 |
| | | | | | 2648.64 | | | | | | 2631.21 | | | | |
| **II** | 1706.06 | 1706.39 | | 1715.51 | 1725.07 | 1726.34 | 1725.47 | | | | | 1722.16 | 1720.03 | 1723.08 | 1721.74 |
| | | | 1688.89 | | 1695.16 | 1720.12 | 1697.45 | 1693.59 | 1693.36 | 1693.33 | | 1704.79 | 1698.33 | 1699.25 | 1698.78 |
| | | 1641.48 | 1643.63 | 1644.05 | 1642.01 | 1644.32 | 1643.21 | 1643.70 | 1644.61 | 1643.94 | 1644.88 | | | | |
| | | | | | | | | | | | | 1609.24 | | | |
| | | | | | 1511.38 | | | | | | | 1542.81 | | | |
| | | | 1469.34 | | 1458.14 | 1458.09 | 1458.12 | 1467.48 | 1468.50 | 1467.54 | 1467.91 | | | | |
| | 1454.41 | 1453.62 | 1448.38 | 1456.59 | 1444.72 | | 1444.87 | 1444.91 | 1448.42 | 1448.61 | 1449.83 | 1455.30 | 1451.68 | 1453.38 | 1453.25 |
| | | | | | | | | 1408.10 | 1409.35 | | 1408.50 | | | | |
| | 1385.19 | 1385.64 | 1383.92 | 1385.30 | 1385.28 | 1386.64 | 1385.98 | 1382.83 | 1383.65 | 1383.58 | 1384.40 | 1375.83 | 1377.91 | 1377.53 | 1377.44 |
| | | | | | | | 1343.55 | | | | | | | | |
| | | | | | | | | | 1330.45 | | | | 1326.23 | 1326.16 | 1326.32 |
| | 1306.26 | 1305.64 | | | | | | 1315.58 | 1316.88 | 1315.88 | 1317.19 | | | | |
| | | | 1264.10 | | | | | 1261.94 | 1263.87 | 1260.94 | 1265.19 | | | | |
| | 1253.02 | 1252.46 | | | | | | | | | | | | | |
| | | | 1236.87 | 1243.07 | 1246.93 | 1243.98 | 1242.47 | 1235.56 | 1237.35 | 1234.68 | 1236.03 | 1242.95 | | | |
| | | | | | | | | | | | | 1227.61 | 1229.56 | 1228.05 | 1228.55 |
| **III** | 1200.98 | 1200.36 | | | | | | 1213.66 | 1214.55 | 1213.90 | | | | | |
| | 1181.13 | 1181.15 | 1178.57 | 1172.59 | 1175.53 | 1172.24 | 1172.66 | 1176.48 | 1179.01 | 1176.55 | 1179.79 | 1180.76 | 1180.76 | | 1180.46 |
| | | | 1152.67 | | 1147.53 | 1134.27 | 1147.11 | | | | | 1160.36 | 1159.27 | 1154.87 | 1156.95 |
| | 1080.66 | 1080.38 | 1091.71 | | | | | 1091.13 | 1092.06 | 1091.73 | 1091.19 | | 1093.32 | 1093.03 | 1093.26 |
| | 1044.46 | 1044.37 | | 1042.64 | 1042.31 | 1043.98 | 1044.87 | | | | | | | | |
| | 1028.74 | 1029.50 | 1029.28 | | | | | | | | | | | | |
| | 986.17 | 986.66 | 973.33 | 977.88 | 974.65 | 978.44 | 977.84 | 974.65 | 973.24 | 972.88 | 973.51 | 976.13 | 977.67 | 976.04 | 976.93 |
| | 890.27 | 889.60 | 887.35 | 887.10 | 887.36 | 887.64 | 887.85 | 887.13 | 887.56 | 886.68 | 888.38 | 885.15 | 888.06 | 886.61 | 887.54 |
| | | | 847.13 | | 855.13 | | 856.11 | 852.59 | | | 846.91 | 857.25 | 857.84 | 852.50 | 854.55 |
| | | | | | | | | | 847.29 | 847.47 | | | | | |
| | 827.83 | 828.23 | 822.97 | | 824.25 | | | | 823.10 | 822.94 | 822.92 | 819.48 | 820.83 | 820.95 | 820.91 |
| | | | 794.96 | | | | | 787.99 | 788.88 | 788.93 | 797.23 | 705.70 | 796.45 | | 796.60 |
| | 755.38 | 754.56 | 747.78 | 743.55 | 739.38 | | 744.72 | 749.18 | 749.11 | 747.62 | 746.74 | | | | |
| | | | 699.27 | | 696.94 | 696.99 | 698.28 | | | | | | | | |
| | | | 673.18 | | | | | 673.94 | 670.61 | | 670.94 | | 678.76 | | |

Table 3-2. Fourier transform infrared spectra band ratios calculated using values of absorbance for resins (HC, MG) and ambers (DA, GLA), and their associated resin acids. The grey highlighted bands are key to evaluate changes under different alteration conditions after 240 days (see Figure 3-2).

| | [1.1] *H. copal* | | | [2.1] Dominican amber | | | | [1.2] *M. glyptostroboides* | | | | [2.2] Grassy Lake amber | | | |
|---|---|---|---|---|---|---|---|---|---|---|---|---|---|---|---|
| Wavelenght ratios | HC $_{Raw}$ | HC $_{50°C}$ | HC $_{90°C}$ | DA $_{Raw}$ | DA $_{50°C}$ | DA $_{90°C}$ | DA-AT | MG $_{Raw}$ | MG $_{50°C}$ | MG $_{90°C}$ | MG-AT | GLA $_{Raw}$ | GLA $_{50°C}$ | GLA $_{90°C}$ | GLA-AT |
| 3400 $cm^{-1}$ / 3088 $cm^{-1}$ | - | 2.72 | 0.33 | 1.75 | 0.68 | 0.16 | 0.85 | 0.92 | 0.59 | 1.51 | 0.42 | - | 1.17 | - | - |
| 1722 $cm^{-1}$ / 1693 $cm^{-1}$ | - | 2.20 | 0.07 | 2.33 | 0.82 | 2.27 | 1.01 | - | - | 2.56 | - | 1.54 | 0.97 | 0.98 | 1.02 |
| 1646 $cm^{-1}$ / 1450 $cm^{-1}$ | 1.60 | 0.61 | 2.35 | 0.54 | 0.33 | 0.51 | 0.37 | 0.76 | 0.74 | 0.72 | 0.97 | 0.08 | 1.45 | - | 1.27 |
| 1460 $cm^{-1}$ / 1448 $cm^{-1}$ | - | - | - | 1.01 | 1.02 | 0.04 | - | 0.88 | 0.93 | 1.13 | 1.00 | - | - | - | - |
| 1448 $cm^{-1}$ / 1385 $cm^{-1}$ | - | 1.09 | 0.76 | 1.04 | 1.20 | 1.00 | 1.09 | 1.16 | 1.24 | 1.28 | 1.11 | 1.21 | 1.15 | 1.35 | 1.16 |
| 924 $cm^{-1}$ / 887 $cm^{-1}$ | 0.70 | 0.54 | 0.25 | 1.10 | 0.44 | 1.11 | 0.43 | 0.56 | 0.45 | 0.38 | 0.68 | 2.27 | 1.69 | 3.36 | 1.83 |
| 823 $cm^{-1}$ / 791 $cm^{-1}$ | 1.39 | 1.78 | 1.00 | - | - | - | 3.23 | - | 0.74 | 0.84 | 0.93 | 3.57 | 1.01 | 2.27 | 1.27 |

| | Chemomarkers | | | | | | | | | | | | Band ratio assigment |
|---|---|---|---|---|---|---|---|---|---|---|---|---|---|
| Wavelenght ratios | Abietic acid | 7-Oxodehydroabietic acid | 8-Abietic acid | Dehydroabietic acid | Communic acid | 8(14) Abietic acid | Dehydroisopimaric acid | Isopimaric acid | Levopimaric acid | Neoabietic acid | Pimaric acid | Sandaracopimaric acid | |
| 3400 $cm^{-1}$ / 3088 $cm^{-1}$ | - | 0.03 | - | 0.08 | - | - | 0.65 | - | - | 1.79 | - | - | OH stretching/asymmetric CH stretching of terminal alkene |
| 1722 $cm^{-1}$ / 1693 $cm^{-1}$ | - | 0.91 | - | - | 0.07 | - | - | 0.12 | - | - | - | 1.91 | C=O carbonil esters / C=O carboxylic acids |
| 1646 $cm^{-1}$ / 1450 $cm^{-1}$ | 2.50 | - | 3.11 | 2.74 | 0.34 | 2.61 | 3.18 | 0.80 | 0.43 | 1.06 | 0.77 | 0.94 | Stretching C=C (non-conjugated)/bending $CH_2$, $CH_3$ |
| 1460 $cm^{-1}$ / 1448 $cm^{-1}$ | - | 1.30 | 1.43 | - | 0.97 | - | 0.75 | 1.00 | 1.10 | - | 0.97 | 1.14 | Interactions of the methylene groups adjacent to oxygen atoms/central methylene groups interacting with neighbouring methylene groups |
| 1448 $cm^{-1}$ / 1385 $cm^{-1}$ | 0.87 | 0.91 | 0.68 | - | 1.62 | 1.40 | 1.00 | 1.55 | 1.08 | 2.38 | 1.12 | 0.91 | Bending modes in C-H methylene group/bending $CH_2$, $CH_3$ modes |
| 924 $cm^{-1}$ / 887 $cm^{-1}$ | 0.91 | 1.24 | 1.10 | 1.19 | 0.34 | 2.18 | 2.19 | 1.85 | 1.20 | 0.49 | 0.52 | 1.05 | C-C stretching/out of plane termical methylene |
| 823 $cm^{-1}$ / 791 $cm^{-1}$ | 1.32 | - | 1.65 | - | 1.01 | 2.44 | 2.78 | 2.06 | 0.79 | 2.52 | 1.19 | 3.71 | Rocking $CH_2$/Stretching CC modes |

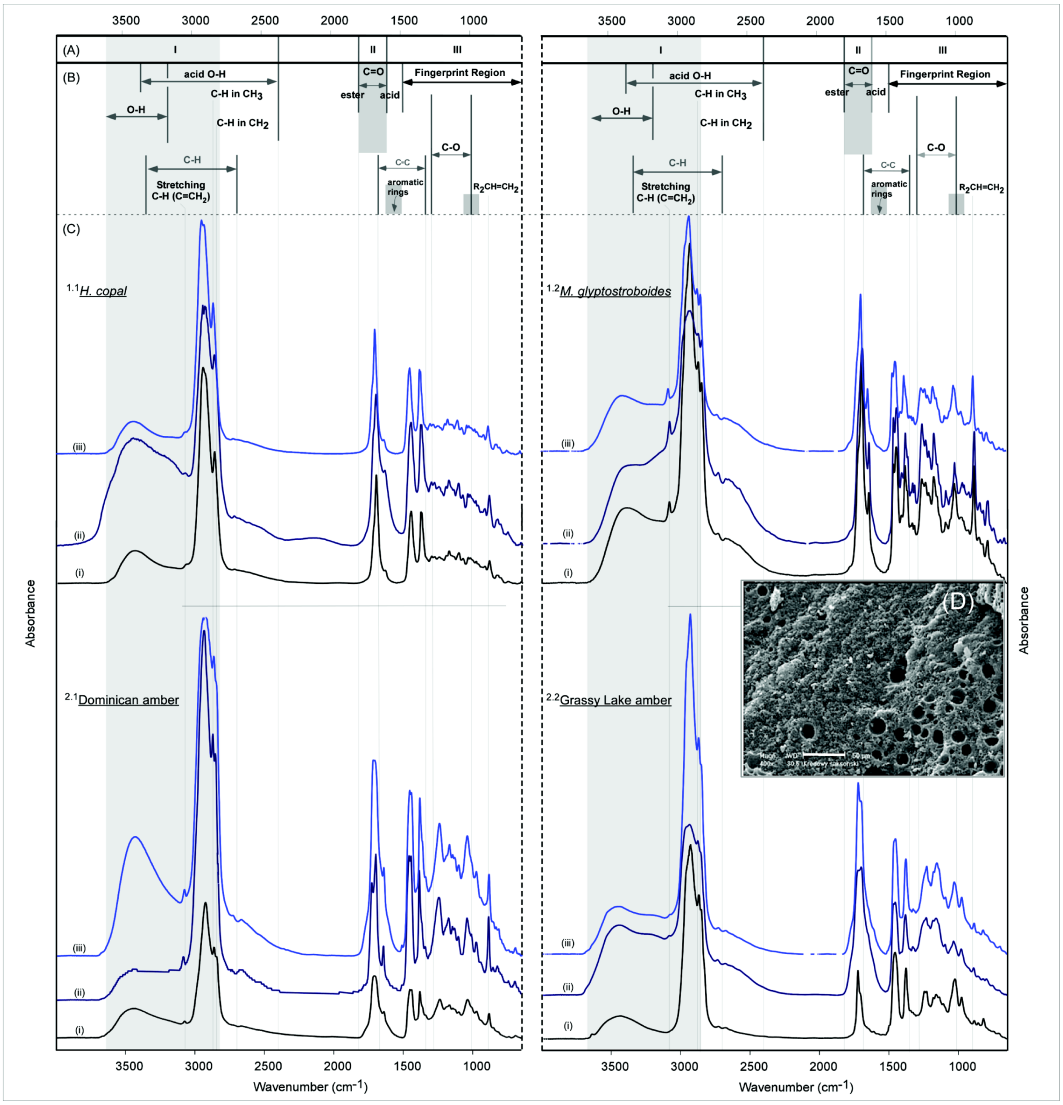


Figure 3-1. Stacked FTIR spectra of control (1.1) and hydrothermally altered resin (1.2) and amber (2.1 and 2.2) samples. (A) Spectra regions are as described in Table 3-1. Band assignment and interpretation (B). Samples' spectra (C) are as follows–control samples (i); samples under hydrothermal conditions after 240 days at 50 ˚C (ii) and 90 ˚C (iii). Example of a scanning electron microscopy image of Baltic amber showing degradation surfaces (D). These features form on ambers altered under hydrous thermal treatment (scale bar is 50 µm)(modified from Kosmowska-Ceranowicz, 2006).

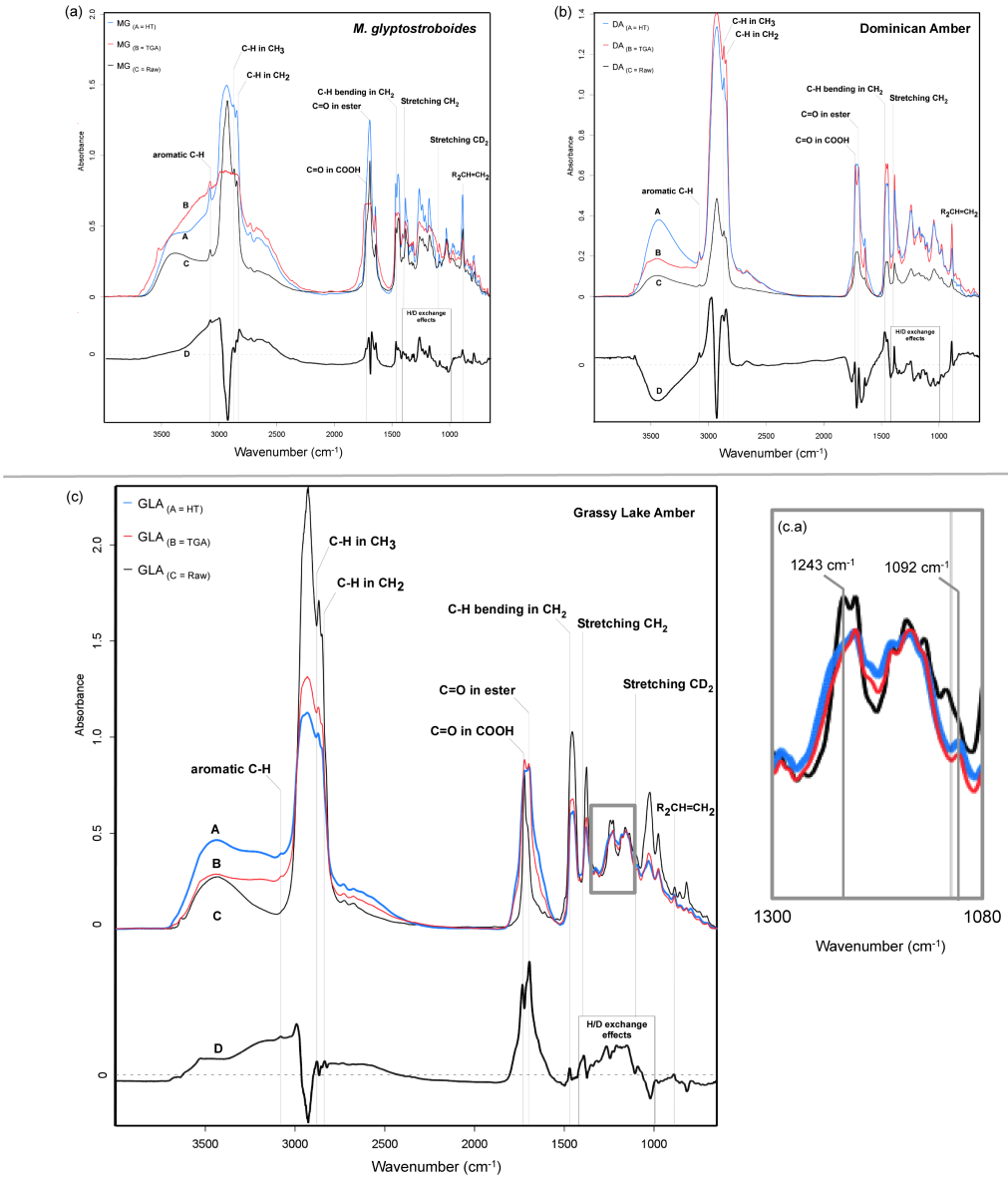


Figure 3-2. Spectral FTIR comparison of untreated (a), hydrothermally treated (b), and anhydrous thermally treated (c) samples after 240 days. The spectroscopic subtraction of raw from hydrothermally treated samples (d) reveals features associated with thermal maturation. These spectra represent (a) *Metasequoia glyptostroboides* resin (MG), (b) Dominican amber (DA), and (c) Grassy Lake amber (GLA). The inset shows a more detailed frame of IR spectra showing absorbance shifts representative of deuterium incorporation (1092 $cm^{-1}$) (c.a.).

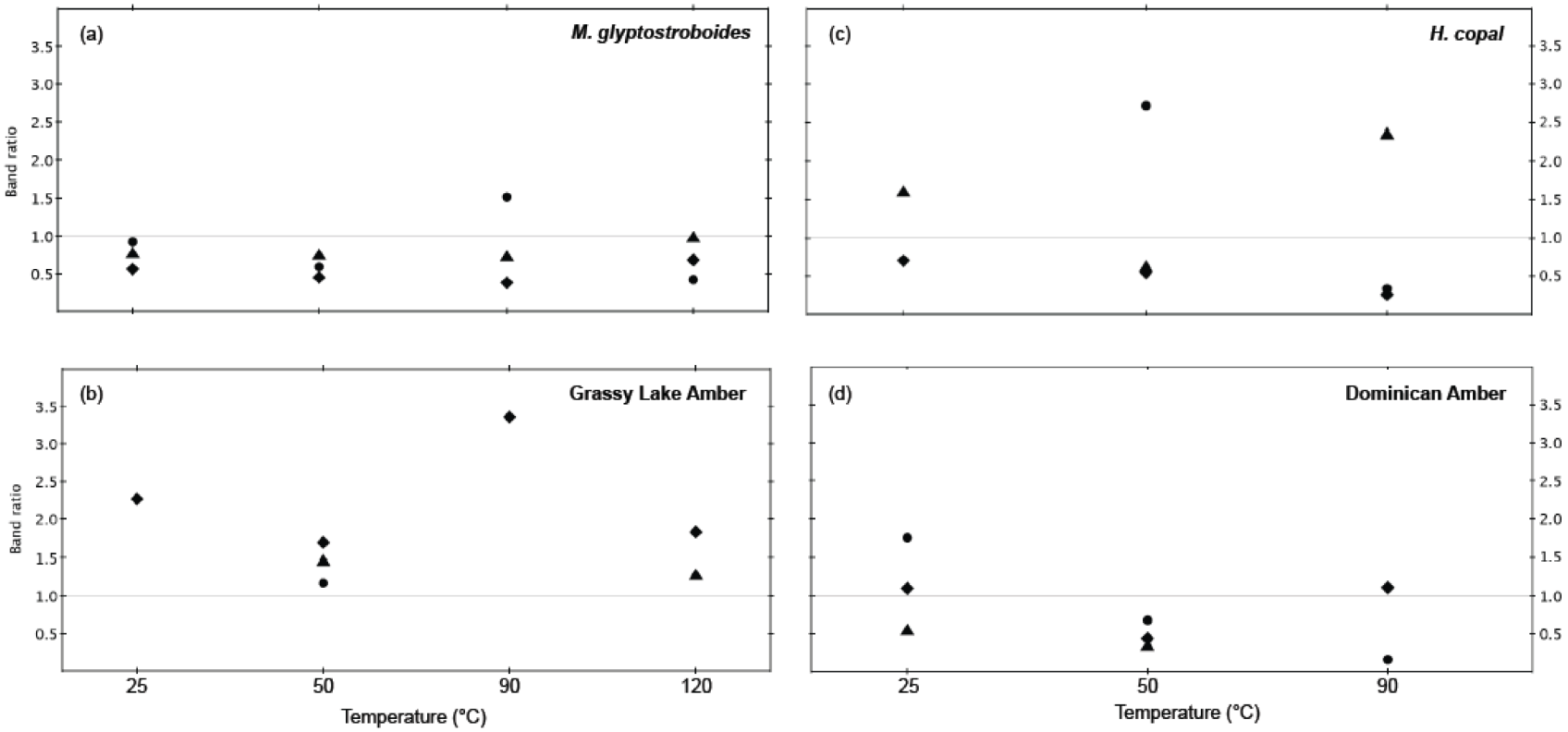
(a)
M. glyptostroboides
(c)
H. copal
(b)
Grassy Lake Amber
(d)
Dominican Amber
Band ratio
Band ratio
3.5
3.0
2.5
2.0
1.5
1.0
0.5
25
50
90
120
Temperature (°C)
Temperature (°C)
● 3400 cm-1 / 3088 cm-1
▲ 1646 cm-1 / 1450 cm-1
◆ 924 cm-1 / 887 cm-1

Figure 3-3. Scatter plot of FTIR absorbance peaks ratios 3400 $cm^{-1}$ / 3088 $cm^{-1}$, 1646 $cm^{-1}$ / 1450 $cm^{-1}$, and 924 $cm^{-1}$ / 887 $cm^{-1}$ and their variation with increasing temperature. (a,b) Control and hydrous altered samples of *Metasequoia glyptostroboides* resin (MG-240) and Grassy Lake amber (GLA-240) at 50 ˚C, and 90˚C (see text for details). GLA-240 products were also subject to anhydrous thermal treatment (AT-TGA) up to 250 ˚C. (c,d) Control and hydrous altered samples of *Hymeneae courbaril* resin (HC-240) and Dominican amber (DA-240) at 50 ˚C, and 90˚C (see text for details).

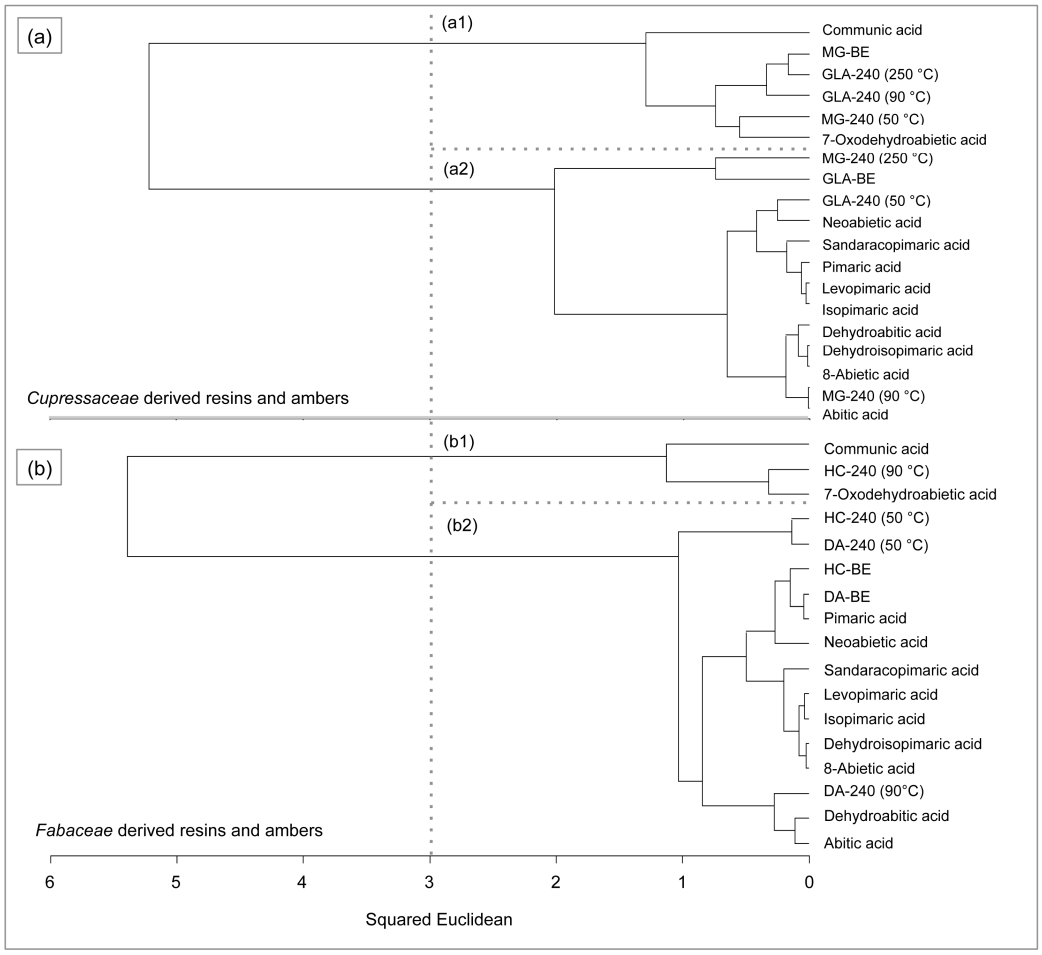


Figure 3-4. Hierarchical clustering of resin acids and thermally treated amber and resin samples. (a) Represents the grouping of Cupressaceae-derived resins and resin acids. The first group (a1) contains GLA and MG under hydrous and anhydrous thermal conditions with communic and 7-oxodehydroabietic acids. The second (a2) cluster contains altered samples, such as MG-240 (250 ˚C) with GLA-BE raw sample, GLA-240 (50 ˚C) with neoabietic acid, and MG-240 (90 ˚C) with abietic, dehydroabietic, and dehydroisopimaric acids. (b) Represents resin and amber samples derived from *Fabacea* specimens and their clustering with primary and secondary constitutive resin acids. Accordingly, (b1) shows clustering of HC-240 (90 ˚C) with communic and 7-oxodehydroabietic acids, whilst (b2) groups samples equivalent to HC-240 (50 ˚C) and DA-240 (50 ˚C), raw resin (HC-BE) and amber (DA-BE) with pimaric acid, and DA-240 (90 ˚C) with dehydroabietic acid.

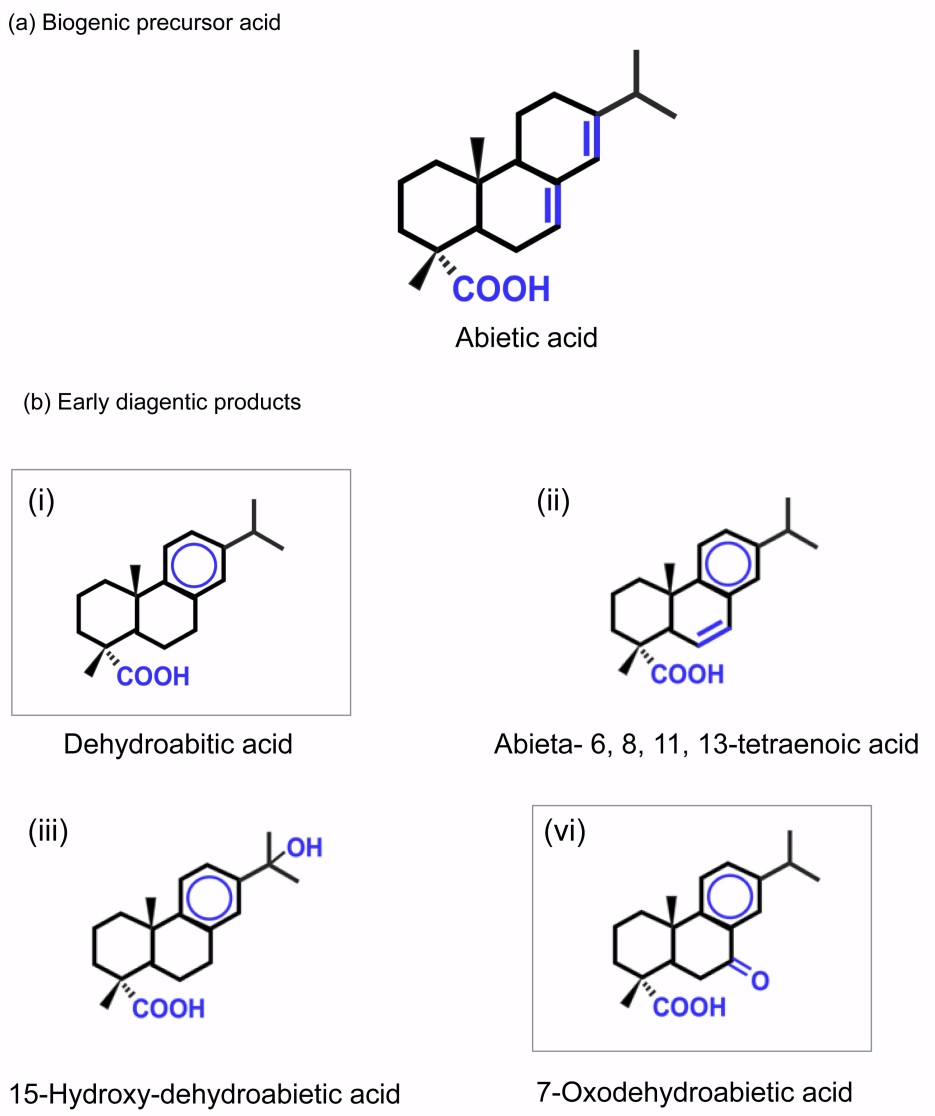


Figure 3-5. Abietic acid (a) and early diagenesis derived compounds (with their associated functionalities). (b) These early diagenetic derived compounds represent the possible products of hydrous and anhydrous thermal treatment of resins and ambers, and were ordered following the diagenetic reaction pathway proposed by Otto et al. (2007). Grey squares represent the main acid clusters after the resin and amber maturation experiments. Blue color functionalities represent those functional groups in the molecule that are prone to change as a result of the experimental protocol, as identified by changes in the samples' FTIR spectral response.

### 3.6. References


Anderson, K. B. (2006), The nature and fate of natural resins in the geosphere. XII. Investigation of C-ring aromatic diterpenoids in Raritan amber by pyrolysis-GC-matrix isolation FTIR-MS. *Geochemical Transactions*, 7(1), 1–9.

Anderson K., Winans, R.E., and Botto, R.E., (1992). The nature and fate of natural resins in the geosphere. II. Identification, classification and nomenclature of resinites. *Organic Geochemistry*, 18(6), 829–841.

Beck, C.W., (1986). Spectroscopic investigations of amber. *Applied Spectroscopy*, 22, 57–200.

Brody, R. H., Edwards, H. G., and Pollard, M., (2001). A study of amber and copal samples using FT-Raman spectroscopy. *Spectrochimica Acta. Part A, Molecular and Biomolecular Spectroscopy*, 57(6), 1325–1338.

Clifford, D. J., and Hatcher, P. G., (1995). Maturation of Class Ib (Polylabdanoid) resinites. *In* Amber, resinite and fossil resins (eds K. B. Anderson & J. C. Crelling), 92–104. Washington, DC: American Chemical Society.

Dal Corso, J, Roghi, G., and Ragazzi E., (2013). Physico-chemical analysis of Albian (Lower Cretaceous) amber from San Just (Spain): Implications for palaeoenvironmental and palaeoecological studies. *Geologica Acta*, 11, 359–370.

Dehmer, J., (1995). Petrological and organic geochemical investigation of recent peats with known environments of deposition. *International Journal of Coal Geology*, 28, 111–138.

Flakus, H. T., and Chelmecki, M., (2002). Infrared spectra of the hydrogen bond in benzoic acid crystals: temperature and polarization effects. *Spectrochimica Acta. Part A, Molecular and Biomolecular Spectroscopy*, 58(1), 179–196.

González, G., Tappert, R., Wolfe, A. P., Muehlenbachs, K., (2012). Is the deuterium isotope composition of amber a reliable inland paleoclimatic indicator?. *Mineralogical Magazine*, 76, 1773.

Grimaldi, D., (1995). The age of Dominican amber. *In* Amber, resinite, and fossil resins. (eds K. B. Anderson & J. C. Crelling), 203–217. Washington, DC: American Chemical Sociaty.

Grimalt, J., Simoneit, B., Hatcher, P., and Nissenbaum, A., (1988). The molecular composition of ambers. *Organic Geochemistry*, 13(4–6), 677–690.

Hamberger, B., Ohnishi, T., Hamberger, B., Séguin, A., and Bohlmann, J., (2011). Evolution of diterpene metabolism: Sitka Spruce CYP720B4 catalyzes

multiple oxidations in resin acid biosynthesis of conifer defense against insects. *Plant Physiology*, 157(4), 1677–1695.

Keeling, C. I., Madilao, L. L., Zerbe, P., Dullat, H. K., Bohlmann, J., (2011). The primary diterpene synthase products of *Picea abies* levopimaradiene/ abietadiene synthase (PaLAS) are epimers of a thermally unstable diterpenol. *Journal of Biological Chemistry*, 286, 21145–21153.

Kosmowska-Ceranowicz, B., (2006). Amber microworlds. *Academia. Research in Progress Geology*, 1(9), 29–31.

McKellar, R. C., and Wolfe, A. P., (2010). Canadian Amber, *in* Biodiversity of fossils in amber from the major world deposits (ed. D. Penney), *Siri Scientific Press*, Manchester, 96–113.

McKellar R. C., Wolfe, A.P., Tappert, R. and Muehlenbachs K., (2008). Correlation of Grassy Lake and Cedar Lake ambers using infrared spectroscopy, stable isotopes, and palaeoentomology. *Canadian Journal of Earth Sciences*, 45, 1061–1082.

Murae, T., Shimokawa, S., and Aihara, A., (1995). Pyrolytic and spectroscopic studies of the diagenetic alteration of resinites. *In* Amber, resinite and fossil resins (eds K. B. Anderson & J. C. Crelling), 76–91. Washington, DC: American Chemical Society.

Lambert, J. B., and Frye, J. S., (1982). Carbon functionalities in amber. *Science*, 217, 55–57.

Lambert, J. B., Santiago-Blay, J. A., Anderson, K. B., (2008). Chemical signatures of fossilized resins and recent plant exudates. *Angewandte Chemie International Edition*, 47, 9608–9616.

Langenheim, J. H., (1969). Amber: a botanical inquiry. *Science*, 163(3872), 1157.

Lee, J.Y., Painter, P. C., and Coleman, M. M., (1988). Hydrogen bonding in polymer blends. 3. Blends involving polymers containing methacrylic acid and ether groups. *Macromolecules*, 354(12), 346–354.

Lyons, P. C., Mastalerz, M., and Orem, W. H., (2009). Organic geochemistry of resins from modern *Agathis australis* and Eocene resins from New Zealand: diagenetic and taxonomic implications. *International Journal of Coal Geology*, 80(1), 51–62.

Otto, A., Simoneit, B. R. T., Lesiak, M., Wilde, V., Worobiec, G., (2001). Resin and wax biomarkers preserved in Miocene Cupressaceae s.1. from Belchatow and Lipnica Wielka, Poland. *Acta Palaeobotanica*, 41, 195–206.

Otto, A., Simoneit, B. R. T., and Wilde, V., (2007). Terpenoids as chemosystematic markers in selected fossil and extant species of pine (*Pinus* , *Pinaceae*). *Botanical Journal of the Linnean Society*, 154, 129–140.

Otto, A., Simoneit, B. R.T, Wilde, V., Kunzmann, L., and Püttmann, W., (2002). Terpenoid composition of three fossil resins from Cretaceous and Tertiary conifers. *Review of Palaeobotany and Palynology*, 120(3-4), 203–215.

Pastorelli, G., Richter, J., and Shashoua, Y., (2011). Photoageing of Baltic amber – Influence of daylight radiation behind window glass on surface colour and chemistry. *Polymer Degradation and Stability*, 96(11), 1996–2001.

Pastorelli, G., Richter, J., and Shashoua, Y., (2012). Evidence concerning oxidation as a surface reaction in Baltic amber. *Spectrochimica acta. Part A, Molecular and Biomolecular Spectroscopy*, 89, 268–269.

Pastorelli, G., Shashoua, Y., and Richter, J., (2013). Hydrolysis of Baltic amber during thermal ageing - An infrared spectroscopic approach. *Spectrochimica Acta. Part A, Molecular and Biomolecular Spectroscopy*, 106, 124–128.

Pereira, R., De Souza Carvalho, I., Simoneit, B. R.T., and De Almeida Azevedo, D., (2009). Molecular composition and chemosystematic aspects of Cretaceous amber from the Amazonas, Araripe and Recôncavo basins, Brazil. *Organic Geochemistry*, 40(8), 863–875.

Pruzan, P. H., Chervin, M. M., Thiery, J. P. I., Besson, J. M. (1990). Tranformation of benzene to a polymer after static pressurization to 39 GPa. *Journal of Chemical Physics*, 92(11), 6910–6915.

Qin, S. J., Sun, Y. Z., Tang, Y. G., (2010). Long term, low temperature maturation of early diagenetic alterations of organic matter from conifers: aliphatic hydrocarbons. *Geochemical Journal*, 44, 247–259.

Qin, S.J., Sun, Y. Z., Tang, Y. G., and Jin, K., (2012). Early diagenetic transformation of terpenoids from conifers in the aromatic hydrocarbon fraction: A long term, low temperature maturation experiment. *Organic Geochemistry*, 53, 99–108.

Roach, J. A. G., Mossoba, M. M., Yurawecz, M. P., and Kramer, J. K. G., (2002). Chromatographic separation and identification of conjugated linoleic acid isomers. *Analytica Chimica Acta*, 465(1–2), 207–226.

Simoneit, B.R.T., Grimalt, J., Wang, T., Cox, R., Hatcher, P., and Nissenbaum, A., (1986). Cyclic terpenoids of contemporary resinous plant detritus and of fossil woods, ambers and coals. *Organic Geochemistry*, 10(4–6), 877–889.

Simoneit, B.R.T., and Mazurek, M.A., (1982). Organic Matter of the troposphere—II. Natural background of biogenic lipid matter in aerosols over the rural western United States. *Atmospheric Environment* , 16(9), 2139–2159.

Tappert, R., Wolfe, A. P., McKellar, R. C., Tappert, M., and Muehlenbachs, K., (2011). Characterizing modern and fossil gymnosperm exudates using micro-Fourier Transform Infrared Spectroscopy. *International Journal of Plant Sciences*, 172(1), 120–138.

Tashiro, K., Izuchi, M., Kaneuchi, F., Jin, C., Kobayashi, M., Stein, R. S., (1994). Cocrystallization and phase segregation of polyethylene blends between the D and H species. 6. Time-resolved FTIR Measurements for Studying the Crystallization. *Macromolecules*, 27, 1240–1244.

Wolfe, A. P., Csank, A. Z., Reyes, A. V., McKellar, R. C., Tappert, R., and Muehlenbachs, K., (2012). Pristine Early Eocene wood buried deeply in kimberlite from northern Canada. *PloS One*, 7(9), e45537.

Wolfe, A. P., Tappert, R., Muehlenbachs, K., Boudreau, M., McKellar, R. C., Basinger, J. F., and Garrett, A., (2009). A new proposal concerning the botanical origin of Baltic amber. *Proceedings of the Royal Society of London B, Biological Sciences*, 276(1672), 3403–3412.

Yamamoto, S., Otto, A., Krumbiegel, G., and Simoneit, B. R. T., (2006). The natural product biomarkers in succinite, glessite and stantienite ambers from Bitterfeld, Germany. *Review of Palaeobotany and Palynology*, 140(1–2), 27–49.

## CHAPTER 4

## Seasonal stable isotopic composition of modern conifer resins: implications for the use of amber stable isotopes in paleoclimatic reconstruction

### 4.1. Introduction

The carbon and hydrogen isotopic composition of fossil plant organic matter has become a standard tool for reconstructing past climates and past hydrological regimes, as well as ecological systems (*e.g.*, Hou et al., 2008; Li et al., 2009; Sachse et al., 2012). A number of abiotic factors such as water availability, humidity, temperature, light exposure (Vogg et al., 1998; Yang et al., 2009; Zhou et al., 2011; Smith and Freeman, 2006); and biotic factors such as presence of parasites, growth rate and the metabolic pathway that produced terpene (Schmidt et al., 2003; Wolhowe et al., 2009; McKellar et al., 2011) influence the variability in δD and $\delta^{13}C$ of the organic compounds (*e.g.*, Terwilliger and DeNiro, 1995; Dawson et al., 2002). These factors are responsible for the large variability in the δD values of terpenes, the building blocks of terpenoids acids and other biomarkers (*e.g.*, Yakir and DeNiro, 1990; Keppler et al., 2007; Sachse et al., 2012 and references therein), but their individual effect in the stable isotopic composition of resins is yet to be fully constrained. Understanding the relative contribution of abiotic and biotic factors in the δD values of modern resins may provide valuable insights, allowing to more precisely interpret the variability in δD values of their fossilized counterparts, since the δD of fossil resins in particular has been proposed as a potentially sensitive proxy for paleoclimate conditions (Nissenbaum and Yakir, 1995; Nissenbaum et al., 2005).

Recent research conducted on modern plant terpenoids and lipids suggests that the variability in their δD values can be explained by a combination of multiple variables affecting the fractionation factor between plant organic matter and environmental waters. For instance, the correlation between seasonal δD variability of source waters with the δD of plant compounds was used to suggest that precipitation has the strongest influence in the δD of plant organic matter (Polissar and Freeman, 2010; Sachse et al., 2006; Smith and Freeman, 2006; Sachse et al., 2012). On the other hand, seasonal changes in the metabolic pathway of plants have also been explored in order to explain the observed variations in the δD of terpenes compounds (Sessions, 2006; Smith and Freeman, 2006).

Here, I present results from a continuous monitoring of the δD and $\delta^{13}C$ values in modern resins produced by coniferous trees over one growth season from May to November 2011. Because conifers produced most of the amber specimens preserved through time (Tappert et al., 2013), coniferous trees were selected to perform the study. In an effort to examine extrinsic factors, such as local environmental conditions, as well as intrinsic effects on resin isotopic variability (Sachse et al., 2012; Tappert et al., 2013), a number of environmental variables were compared to constrain their seasonal isotopic shift. Some of the trees grew under natural conditions, while others were under care as ornamental trees. Moreover, all of them were in open areas and exposed to variable weather conditions through the seasons, as well as herbivore and pathogen attacks.

Accordingly, the effects of changes in precipitation on resins isotopic

response were examined through the application of a time series evaluation aiming to:

(1) Track and analyze possible seasonal δD variability on conifer resin and its relation to abiotic factors, such as water source deuterium composition.

(2) Compare the δD of resins and precipitiation-water to determine their deuterium isotopic fractionation factor.

(3) Determine the time lapse between changes in δD in precipitation is recorded in the tree's resin.

(4) Constrain potential source of water stress based on stomatal conductance and water use efficiency calculation.

## 4.2. Material and methods

### 4.2.1. Study site, seasonal sampling, and climate data

The fieldwork was conducted within an area of 0.49 $km^2$ at the University of Alberta (North Campus), Edmonton, Alberta, Canada (Fig. 4-1). Resins were sampled from seven randomly selected mature coniferous trees. The studied taxa included: *Picea glauca* (n=1), *Picea mariana* (n=3), *Abies balsamea* (n=1), *Picea pungens* (n=1) and *Thuja occidentalis* (n=1). In addition, a cultivated specimen of *Picea pungens*, which was growing in the proximity to its wild-growing counterpart, was sampled as a control tree (Table 4-1). According to Moss (1955), *Picea mariana* and *Picea glauca* are native species that form part of the Boreal Northern Forest (BNF) dominating the Edmonton river valley (along the North

Saskatchewan River). It should be noted that one of the sampled trees (*Abies balsamea*) was felled during the course of the study because of its poor condition.

Resins were sampled continuously two or three times a month, from May to November 2011. In order to record any change during the growing season (Lombardero et al., 2000), a high sampling density was performed in June (five times). In order to collect newly produced resins and to stimulate resin flow; the bark of the trees was lacerated with a knife creating a wound. The method, however, avoided inducing damage on the tree's phloem or xylem; which potentially would inhibit the supply of water and nutrients from roots through the tree. Relevant biotic stress sources, such as signs or symptoms of insect infestation, disease, or other associate lesions (Gaylord et al., 2007), were considered during the sampling. Since these may exert some constrains on the rate of resin production, they may also have some associated effect on the resin deuterium composition (Table 4-1).

Resins were collected in sample vials, and stored at about 2 °C at the Stable Isotopes Laboratory (University of Alberta), until they were prepared for stable isotope analysis. Parallel to the sampling, a dataset containing temperature, precipitation and monthly average deuterium composition of precipitation was compiled (National climate data and information archive, 2011; IAEA, 1969, 1970; Bowen et al., 2005; Bowen, 2008, 2012).

4.2.2. Isotope analysis

In order to remove the resin's volatile fraction, potentially consisting of monoterpenes, sesquiterpenes and humidity, the samples were placed under vacuum (5 ± 0.5 hours) and heated to 50 ºC. Afterwards, between 5–10 mg of each sample was loaded into a quartz glass tube, together with ~50 mg of $Cu_{(s)}$, ~1 g of $CuO_{(s)}$, and ~50 mg of Ag. Tubes were vacuum-sealed and placed in an oven at 800 ºC. Once the tubes reached ambient temperatures, the combustion products, including $H_2O$ and $CO_2$, were cryogenically extracted. Water of combustion was reduced using Indiana Zinc at 500 ºC to produce $H_{2\ (g)}$ (Coleman et al., 1982). Both $H_{2\ (g)}$ and $CO_{2\ (g)}$ isotopic composition were measured using a dual-inlet Finnigan MAT-252 mass spectrometer. Results are given in the conventional δ notation expressed in per mil:

$$\delta_{(Sample)} = ((R_{Sample}/R_{Standard}) - 1) \cdot 10^3, \qquad \text{Eq. 1}$$

where R is the D/H ratio or $^{13}C/^{12}C$ of the sample and the standard, respectively. Results are reported based on the VSMOW (Vienna Standard Mean Ocean Water) standard for deuterium and the VPDB (Vienna Pee Dee Belemnite) for carbon. Deuterium values are reported with an error of ±4.5‰ of the total value.

In addition, a fractionation factor ($\varepsilon_{Resin\text{-}ppt}$) between the monthly average δD of the resins ($\delta D_{resin}$) and the δD of the precipitation ($\delta D_{ppt}$) was calculated as:

$$\varepsilon_{resin\text{-}ppt} = 1000 * [((\delta D_{resin} + 1000)/(\delta D_{ppt} + 1000)) - 1], \qquad \text{Eq. 2}$$

The fractionation is thereby influenced by factors such as biosynthetic fractionation, leaf evaporation and soil water evaporation (*e.g.*, Chikaraishi et al., 2004, Sachse et al., 2012; Shanahan et al., 2013).

*4.2.2.1. $\delta^{13}C_{resin}$ data evaluation*

The monthly averaged carbon isotopic composition of resins were used to calculate the ratio of intercellular to ambient $CO_{2\,(g)}$ concentration fraction ($c_i/c_a$) using the model of Farquhar et al., (1982) for $C_3$ plants:

$$\Delta = \delta^{13}C_a - \delta^{13}C_{resin} / (1 + \delta^{13}C_{resin}/1000), \quad \text{Eq. 3}$$

wherby,

$$\Delta \cong a + (b - a) * c_i / c_a, \quad \text{Eq. 4}$$

The isotope discrimination $\Delta$ (Eq. 3), was calculated for an average $\delta^{13}C_a$ (atmospheric carbon isotopic composition, -8.25‰, *e.g.*, Cuntz, 2011) and monthly averaged $\delta^{13}C_{resin}$ values (Eq. 4, Saurer et al., 2004). The factors "a" and "b" are constants that represent the diffusional fractionation ($a$ = 4.4‰) and the carboxylation fractionation (b = 27‰) (Farquhar et al., 1982; Cernusak et al., 2013 and references there in). The results were used to:

(1) Compare the values with those of experimentally determined linear relationships between the bulk $\delta^{13}C$ of leaf matter and measured $c_i/c_a$ ratio during photosynthesis (Eq. 5, Cernusak et al., 2013).

$$\delta^{13}C_{resin}\,(‰) = -12.1 - 22.0 * c_i / c_a, \quad \text{Eq. 5}$$

whereby,

$$c_i = ((\Delta - a) / (b - a)) * c_a, \quad \text{Eq. 6}$$

(2) Calculate intercellular $CO_{2\,(g)}$ using atmospheric $CO_{2\,(g)}$ concentration (Eq. 6, data from Saurer et al., 2004 – Keeling et al., 2005), in order to determine the water use efficiency (WUE) per tree (Eq. 7, Ehleringer and Cerling, 1995; Saurer et al., 2004).

$$WUE = A / gH_2O = (c_a - c_i) * 0.62, \quad \text{Eq. 7}$$

The calculations are based on the assumption that the bulk carbon isotopic composition of resins is representative of the bulk carbon isotopic composition of bulk plant/leaf organic matter, as suggested by Tappert et al., (2013). Also, by comparing modeled with calculated $c_i / c_a$ ratios we intended to gain insights into the effect of water stress on the carbon isotopic composition of resins, and its relation to water use efficiency. The latter is defined as fixed carbon per gram of water in terms of the ratio of net photosynthesis (A) per gram of water vapor ($gH_2O$) (Ehleringer and Cerling, 1995; Saurer et al., 2004).

4.2.3. Numerical analysis

The average monthly deuterium composition of precipitation in Edmonton, Alberta was compiled from two sources (IAEA, 1969, 1970; OIPC version 2.2 – Bowen et al., 2005; Bowen, 2008; Bowen, 2012) and compared to recent temperature data collected by the weather station of the Department of Earth and Atmospheric Sciences (EAS) located on top of the Tory Building at the University of Alberta (Fig. 4-1), and with the daily precipitation database from the

National Climate Data and Information Archive, Canada (Canadian Climate Normal, 2011). The datasets were compiled in order to develop a predictor variable dataset that includes relevant abiotic parameters that have a potential to influence the variability of deuterium composition of the resins ($\delta D_{resin}$).

Abiotic variables were compared to the $\delta D_{resin}$ time series in order to identify trends. To better assess predictor and response variable dependence, a general linear regression model (GLM) was also applied to compare mean monthly $\delta D_{resin}$ and $\delta D_{ppt}$ values. Further descriptive statistic analyses allowed us to evaluate variables' distribution and to identify outliers through the use of a box plot graphic tool; which was applied to hydrogen and carbon isotopic composition data (Box, 1976). In addition, a correlation matrix was used to demonstrate possible dependence or relation at a significant level (> 0.5, p-value <0.05) among abiotic and biotic variables ($\delta D_{resin}$). All statistical analyses were performed with the software program 'R'.

## 4.3. Results

### 4.3.1. Edmonton climate

#### *4.3.1.1. General parameters*

Edmonton has a continental climate with short, warm summers and long, cold winters (Olson, 1985). During the seven-month sampling period (May–November 2011) temperature extremes ranged from -3.1°C to 19.5°C; with average daily temperatures ranging from a low of -3°C in November to summer peak of 19.5°C in July. Throughout the year, temperatures rarely

exceed 30°C (typically from late April to mid-September), but can fall below -20°C for an average of 28 days. The meteorological summer generally lasts from late June until early September, and winter lasts from November to March. Spring and fall are both short, but can vary in length. Average relative humidity is about 59.3% (National climate data and information archive, 2011). During the study period total precipitation was about 339 mm, with a monthly maximum of 28.8 mm reported in July, and minimum of 5.2 mm in September. In the area, average annual precipitation is about 500 mm, 25% of which occurs as snow (Anon., 1980) (Table 4-2).

*4.3.1.2. Environmental water deuterium composition in the Edmonton area*

Comparison of monthly mean precipitation deuterium composition from two sources: (1) IAEA (1969, 1970) and (2) Online Isotopes in Precipitation Calculator version 2.2; suggested that the second model fits absolute values representative of the modern dynamic climate and temperature (Bowen, 2012, 2008; Bowen et al., 2005) (Appendix, 2-1). This indicates that the average deuterium composition of precipitation in the region is around -106 ± 55‰, with a maximum of - 87 ± 4‰ during Summer (July) and minimum of -155 ± 10‰ during Winter (November), which parallel both maximum and minimum monthly average precipitation (Fig. 4-2 b).

Since the water source for the studied trees is mostly soil water, an important factor to consider is the soil deuterium composition within the Edmonton area. Soil-water was previously reported to oscillate in the range -136 ± 9‰ (Maulé et al., 1994), and the mean ground-water is -153 ± 1‰ (Maulé et

al., 1994). Although these values are consistent with the meteoric water line of the Edmonton area, occasional storm events can also exert some control over rainwater and soil water deuterium composition and cause considerable deviation from the reported average values (Maulé et al., 1994).

4.3.2. Location of trees under study. Environmental conditions and potential stress sources.

In the Edmonton area, the growing season lasts from May to September. Figure 4-1 shows the types of vegetation and their distribution in the area. In general, coniferous communities are relatively sparse and are associated with the river valley area. In this area, there is a recent history of slope instability and riverbank erosion that is important for the evolution of the riparian forest that exists between the northern boundary of the University of Alberta and the Saskatchewan River. The dynamics of fluvial erosion strongly affect the vegetation and biodiversity in this location, and sporadic landslides are responsible for some of the stress conditions among the trees in this area (*e.g.*, Kathol and McPherson, 1975). The trees sampled at the Emily Murphy Park site (Table 4-1; Fig. 4-1) are located in a steep zone of the embankment, with a slope angle of around 22°. In this area, the trunks of older trees are bent and their roots exposed (Zone 1, Fig. 4-1). By contrast, trees located along the road sample site (n=2) and in the campus area grew under more steady terrain condition (Zone 2 and 3, Fig 4-1). The water sources in the different sampling areas varied according to their location and extent of root system (Strong and Roi, 1983; White et al., 1985).

Spruce specimens located in the Emily Murphy Park site showed signs of beetle infestation, as part of a spruce beetle outbreak (Coleoptera: Curculionidae: Scolytinae) (Table 4-1, Fig. 4-1). The physiological feature observed include: (a) boreholes filled with induced resin exudates and the presence of larvae, presumably from parasites of the bark beetles (*i.e.*, Gara et al., 1995); (b) bark-beetle transported blue-stain fungus associated with resin exudate (Krokene and Solheim, 1997); and (c) internal resin blisters formed from resin accumulation beneath the bark, which created an irregular external surface as part of the bark swelling (*i.e.*, Raczkowski, 1979). For trees exhibiting the latter, a careful sampling was implemented to avoid these sections. Strong signs of infestation were observed on specimen PM-31, which appeared to be a tree that survived a previous infestation. By contrast, tree WS showed signs of active attack during the sampling period (Table 4-1, Fig. 4-1).

4.3.3. δD composition of resins through time and apparent fractionation factor ($\varepsilon_{resin\text{-}ppt}$)

The average $\delta D_{resin}$ for all sampled trees ranged from -254 ± 30‰ in June to -381 ± 15‰ in October-November (Fig. 4-2). This means deuterium-enriched (high) compositions during spring-summer period contrast with relatively depleted (low) compositions during autumn-winter. The difference between monthly minimum and maximum mean deuterium composition of resins ($\Delta D_{max\text{-}min\ resin}$) is up to 61‰, the seasonal shift in precipitation $\Delta D_{max\text{-}min\ ppt}$ = 68‰. Interestingly, after producing the injuries on the bark of trees, freshly produced resins showed a deuterium response in terms of days. In fact, high-resolution

resins sampling during the month of June demonstrated that fluctuation on the response time of $\delta D_{resin}$ to changing $\delta D_{ppt}$ could be constrained to 2–4 days after wounding, and a total recovery $\delta D_{resin}$ to 4 up to 15 days (Fig. 4-2c,e). The response and recovery time is characteristic for each tree, and, as a result, the standard deviation for the June $\delta D_{resin}$ ranges from 5.3 to 47.3‰ (Fig. 4-2c,e). Even though the $\delta D_{resin}$ through time (within each sampled tree and sampling zone) shows similar trends in temporal variation, resins from trees located in different zones produced exudates with distinct $\delta D_{resin}$ values. The difference between specimens located in zone 3, and trees located in zone 1 is about 10 to 30‰ (Fig. 4-2c, e; Fig. 4-3).

The apparent deuterium isotopic fraction between precipitation and resin mean value is about -222‰ as shown in Figure 4-4A. However, the measured values vary between -174‰ and -293‰, with approximately 30‰ variability among trees (Table 4-2). However, a linear regression model between mean monthly deuterium composition of resins and rainwater produced a significant correlation between the predictor and response variables; the slope is representative of a fractionation factor between water and resins ($\alpha_{water\text{-}resin}$) of about 0.7 and a correspondence shift of -228 ± 19‰ (Fig. 4-4 B).

### 4.3.4. Carbon isotopic composition of resins ($\delta^{13}C_{resin}$)

The carbon isotope composition of resins varies from -22.5‰ to -28.8‰. The mean carbon isotopic composition ($\delta^{13}C$ = -25.8‰) is consistent with previously observed resins natural $\delta^{13}C$ range (range $\delta^{13}C_{modern\ resin}$ = -23 to -30% –Tappert et al., 2013. As previously reported by McKellar et al., 2011, trees under

insect attack and associated water stress produce resins with $^{13}C$-enriched carbon isotopic compositions compared to those under low-stress conditions (Fig. 4-5). In this case, stressed trees showed a variability of less than 1‰ in their $\delta^{13}C$, and their maximum values did not exceed an average threshold of -25‰. Trees that produced even more isotopically enriched resins ($\delta^{13}C$ > -25‰) also showed greater variability in their $\delta^{13}C$. These trees typically were prone to succumb due to their poor growth conditions (McKellar et al., 2011). In our study specimen ABM, *i.e.* the specimen that was removed due to poor condition, falls into this category (Fig. 4-1, Fig. 4-5F, Fig. 4-6A). However, specimens PM31 and WS showed similar enriched $\delta^{13}C$ values (Fig. 4-1, Fig. 4-5A, E, F).

The carbon isotopic discrimination for the whole sample population was about $\Delta^{13}C = 18.2 \pm 0.8$‰, with average values of $\Delta^{13}C = 18$‰ calculated from trees under less stress and average low-carbon discrimination, and $\Delta^{13}C = 17$‰ determined for trees related to intense insects attack and stress, such as PM31 and WS (Appendix, 2-2). Minor changes were also determined for the stomatal conductance ratio $c_i / c_a$, ranging between 0.5 and 0.7, with an average value of 0.6 determined for most specimens. Although, the calculated stomatal conductance ratios $c_i / c_a$ fits the linear regression model; this approach may overestimate the $c_i / c_a$ ratio for trees under water stress, as predicted by Cernusal et al., (2013). The values, however, are in accordance with experimental measurements of $c_i/c_a$ based on the $\delta^{13}C_{leaf}$ of the families Cupressaceae and *Pinacea* families ($c_i/c_a = 0.58 - 0.85$, Brodribb and Hill, 1998; Cernusak et al., 2007; Cernusak et al., 2009), and are coherent with an average water use

efficiency value of about 34.7 ± 0.8 μmol/mol (maximum = 42.5 μmol/mol, minimum = 27.7 μmol/mol).

The $c_i/c_a$ ratio reported for *Thuja occidentalis* L. under well-watered conditions showed very depleted $\delta^{13}C$ of bulk leaf matter and relatively high ratio of intercellular to atmosphere fraction ($\delta^{13}C_{leaf}$ = -28.9‰, $c_i/c_a$ = 0.8 – Cernusak et al., 2008). By contrast resins from TOL (*Thuja occidentalis* L.) were more enriched in $^{13}C$, and produced rather high $c_i/c_a$ values ($\delta^{13}C_{resin}$= -26.2‰, $c_i/c_a$ = 0.6). Our observations indicate, that relatively healthy trees have low water use efficiency, whereas trees under water stress, such as PM31, WS and ABM, have high water use efficiency (Appendix, 2-2).

4.3.5. Statistical analyses

*4.3.5.1. Descriptive statistics*

Descriptive statistics of the predictor and signaling variables are summarized in Table 4-2. Dissimilarities among deuterium and carbon isotopic composition from different trees are evident by evaluating the quartiles division, which reflects an asymmetric distribution of the values (Fig. 4-3A, Fig. 4-6A). This shows that the differences in deuterium composition per specimen and their overlap can be correlated with the hydrogen isotopic composition of environmental waters in the area. No outliers were identified. Also, a correlation matrix among the deuterium composition of resins per tree showed a high correlation among the sampled specimens ($> 0.5$, $p < 0.05$), and discrimination of PM-31 and WS (see Table 4-2 and 4-4).

## 4.4. Discussion

Overall, our results point to an important biochemical control that regulates the isotopic fractionation through a kinetic isotopic effect that, among other factors, is constrained by water availability and the timing (season) of resin production. In this regard, Schmidt et al. (2003) suggested that it should be possible to predict the deuterium isotopic composition of compound-specific terpenes based on three factors: (1) hydrogen primary source, (2) plant biosynthesis, and (3) biosynthetic pathway. This study shows that seasonal precipitation, temperature changes, and biological activity are also relevant factors that may strongly affect coniferous resin production, and as a consequence, their $\delta D_{resin}$ values. These parameters, and their relation with the variability of $\delta D_{resin}$, are discussed within the context of the rates of resin biosynthesis using $\delta^{13}C_{resin}$ as an indicator of water source.

### 4.4.1. Hydrogen isotopic fingerprint of resins and their relation with primary water sources

Precipitation and groundwater are the primary water sources for terrestrial plants (White et al., 1985; Flanagan and Ehleringer, 1991; Smith and Freeman, 2006). The spatial and temporal distribution of precipitation not only influence vegetation distribution, but also determines their primary hydrogen isotope pool source (Dansgaard, 1964; Flanagan and Ehleringer, 1991). Physiologically, all of the conifer trees under study are adapted to cope with environmental seasonal changes (Moss, 1955) and also with biotic sources of stress –such as herbivorous and pathogen attack, to which their natural defense response includes the

production of resins (see Levin, 1976; Lombardero et al., 2000; Gaylord et al., 2007; Kolosova and Bohlmann, 2012).

Temperature and precipitation are critical variables during the growth of trees. These determine the photosynthetic rates and the variability of the deuterium composition of terpenoids and resin acids. In fact, the relationship between observed $\delta D_{resin}$ ($\delta D_{resin}$ = -254.05 ± 30‰ to -381.20 ± 15‰, of $\sigma$ = 27.79) and that of $\delta D_{ppt}$ ($\delta D_{ppt}$ = -97‰ to -155‰, $\sigma$ = 29.4) is significant (Fig. 4-4, Table 4-4). This represents the effects of the abiotic factors on the tree's biotic response.

The variability in $\delta D_{ppt}$ creates a fingerprint in $\delta D_{resin}$, and result in comparable seasonal trends in the studied trees (Fig. 4-2, Table 4-2). Precipitation, as the ultimate source of soil-water, is the main water source accessed by most terrestrial plants, but it also controls the δD value of groundwater. Groundwater represents a long-term average isotopic composition of precipitation in the area, and, when available, it influences the deuterium composition of plant-accessed water (Flanagan and Ehleringer, 1991). However, this relationship is not straightforward since the δD of soil-water can be subject to evaporation, which produces some degree of hydrogen isotopic fractionation (see Maulé et al., 1993). In the Edmonton area, the effect of evaporation on soil water is a loss of about 9%, whereby the δD of the first 10-90 cm of soil mostly reflects average monthly precipitation values (Maulé et al., 1993). Therefore, the discrepancy observed when comparing daily and monthly mean $\delta D_{resin}$ values should reflect some additional factors, such as location (Fig. 4-3 A, B).

*4.4.1.1. Location and water source availability as determinant factor on $\delta D_{resin}$*

As previously discussed, source water and its availability influence the deuterium fingerprint of resins produced by trees at different locations within a given geographical region, but different location produces distinct values. Accordingly, trees in zone 1 are less influenced by urban factors, while specimens located in zone 3 may show the influence of watering (Fig. 4-1). Thus, $\delta D_{resin}$ values derived from trees located on campus, and under ornamental care (watered ornamental trees ABM and TOL), differ from trees solely under ambient water influences (BS, WS, PM-31, PM-197, and PM-404)(Fig. 4-3B).

This result is consistent with previous findings by White et al. (1985) that showed a direct relationship between the deuterium composition of sap-water and that of the water source. Based on this observation, it is possible to discriminate between trees that had access to groundwater and those with limited access to groundwater and therefore a reliance upon soil water and soil moisture. By further discriminating this relation, using topographic location and extension of roots within the soil (a factor that in turn controls xylem sap water availability and distribution, see White et al., 1985), the relationship between water source and $\delta D_{resin}$ becomes even more evident.

The influence of soil-water and groundwater access in the $\delta D_{resin}$ provides evidence for the importance of xylem water during the biosynthesis of terpenes. Accordingly, it is clear that the $\delta D_{resin}$ from plants under water stress because of their location is prone to reflect the $\delta D_{ppt}$ (Table 4-2). This also shows whether or

not the tree has access to soil-water and groundwater, as trees with access to a constant water source show less variable $\delta D_{resin}$ values (Fig. 4-2).

Our results may also help to interpret why the deuterium isotopic composition of resins from plants under water stress are more strongly correlated with the seasonal deuterium variability in precipitation (see Table 4-2, Fig. 4-2 and 4-3). Close resemblance and even overlap between hydrogen isotopic composition of plants stem-water and groundwater during long periods of time between rains, contrast with that of stem-water after abundant rain (Flanagan and Ehlringer, 1991). This is comparable with the effect observed on trees located in zone 2, since the $\delta D_{resin}$ of trees clearly depart from that of the groundwater $\delta D$ signature, and are rather comparable with those of precipitation ($\delta D_{ppt}$). Thus, it is clear that resins are also predisposed to rapidly reflect the $\delta D_{ppt}$. The preferential uptake of precipitation or groundwater depends on the tree specimen and its root system.

Previous measurements of the root systems of analogous specimens to those examined here (Strong and Roi, 1983), provided us with the following working values for the average vertical extension of their root systems: (a) black and white spruce (*e.g.*, PM and WS), average 50 cm (0.5 m) vertical extension; (b) balsam fir (*e.g.*, ABM), 100 cm (1 m) vertical extension. By comparing these measurements with the depth variability of the water table in a nearby study area, which yielded 3.7 and 4.4 m depth (Maulé et al., 1994), it is possible to support the assertion that the relative amount of lateral and/or vertical root extension is a

limiting factor in the preferential uptake of rainwater over groundwater, as better evidenced by trees location at topographic heights (ABM, PM).

Furthermore, more recent observations have shown that to overcome water stress, the plant regulatory system produces the hormone ABA (abscisic acid), which is responsible of stomatal regulation and closure (Davies and Zhang, 1991; Broddid and McAdam, 2013). Stomatal closure inhibits water loss, but also increases heating in the leaf surface, and thus leads to leaf water deuterium enrichment. However, the fractionation is balanced by the diffusion of deuterium-depleted xylem-water into sites of evaporation and back to the xylem (Farquhar et al., 2007). This also suggests a likely relation among xylem sap-water, leaf-water and leaf stomatal regulation, which in turns controls the final δD of water within the leaf, and thus, the δD of products later used for the biosynthesis of terpenoids.

Alternatively, it has been observed that trees with constant access to groundwater are capable of redistributing and retrieving water from either deep and shallow layers, which enables a more homogeneous distribution of seasonal water (Burgess et al., 2000). This is in agreement with the observed seasonal variability in tree resins and the significant correlation between monthly average precipitation and $\delta D_{resin}$ (Fig. 4-2, Fig. 4-4). However, the $\delta D_{resin}$ of trees with a constant water supply seems to reflect the deuterium composition of groundwater and its mixture with seasonal precipitation (*i.e.*, TOL – Fig. 4-2E, Fig. 4-3 B, C). Overall, the observed relations explain the 10 to 30‰ difference in the resin's deuterium composition among trees. The variability, however, is not dependent on specific species, but rather on their topographic location and water source (Fig. 4-

3A). More importantly, this explains the relation between environmental waters (specifically precipitation) and $\delta D_{resin}$, which is constrained by their fractionation factor.

4.4.2. Resin's biosynthesis pathway and apparent $\varepsilon_{resin\text{-}ppt}$

Fractionation between the primary water source (soil water, precipitation) deuterium and the primary products of photosynthesis increases with the 'metabolic distance' of each group of secondary compounds (Hayes, 2001; Schmidt et al., 2003; Sachse et al., 2012). As resins are a mixture of terpenoid and resin acids, the fractionation between the polymeric organic molecules and primary cell-water depends on the biosynthesis pathway through which terpenes are produced, as: mevalonic acid (MVA) and methylerythritol phosphate (MEP) (Chappell, 1995; Keeling and Bohlmann, 2006; Zulak and Bohlmann, 2010). As both MVA and MEP pathways occur in different organelles within the cells, they may produce compounds with different hydrogen isotopic composition (Rohmer, 1999; Lichtenthaler, 1999; Schmidt et al., 2003).

The trees studied produce resins that show an ambient water δD fractionation ranging from -184 to -293‰ (Fig. 4-4 A). The MEP pathway is thought to be relevant for resin production, as suggested by the correlation between its gene expression and terpenoids synthesis (monoterpenes, diterpenes, and sesquiterpenes) (Zulak et al., 2009). These MEP products exhibit δD values of about -355‰; whilst triterpenes, and sesquiterpenes produced by MAV-pathway have a δD about - 255‰ (Sessions et al., 1999; Schmidt et al., 2003). Other terpene biomarkers produce comparable values (Sessions et al., 1999;

Hayes, 2001; Schmidt et al., 2003; Sessions and Hayes, 2005; Chikaraishi et al., 2004, 2005). Therefore, these seem consistent with previous observations that cell-water deuterium composition may not differ between organelles (Chikaraishi et al., 2004).

The mean fractionation is around -222 ± 30‰, with -212‰ and -238‰ as mean minimum and maximum (Table 4-2), the linear regression model indicates that the resins deuterium composition can be attributed to a shift from precipitation by 228 ± 19‰ (Fig. 4-4H). This value that can be compared with that obtained through out a mean geometric linear model (-229‰). These values, also, coincided with the values inferred in Early Eocene *Metasequoia* fossilized resins (-229‰ - Wolfe et al., 2012). Thus, a fractionation shift of resins relative to precipitation ($\varepsilon_{ppt\text{-}resin}$) of -228 ± 19‰ represents the combination of metabolic pathways that produce that the constituent terpenoids of coniferous resins.

Although the slope of the general linear regression model that fits the fractionation factor between precipitation and resins ($\alpha_{ppt\text{-}resin} = 0.7$), is lower than that previously report for cellulose ($\alpha_{water\text{-}cellulose} = 0.83$ - Yakir and DeNiro, 1990), lipids ($\alpha_{water\text{-}lipids} = 0.83$) and carbohydrates ($\alpha_{water\text{-}carbohydrates} = 0.93$)(Luo et al., 1991), it is rather similar to the value previously reported for phenylpropanoids synthesis and its kinetic isotopic effect throughout the reduction of phosphoenolpyruvate (PEP) ($D_{methylene}/D_{o-aromate} = 0.70$) by flavoprotein. This can also be related to the reduction of flavoprotein during nicotinamide adenine dinucleotide phosphate (NADPH)-cytochrome P450 oxidoreductase (see Schmidt et al., 2003 and references therein). Similarities between these processes may shed

some light on the effects of environmental conditions on the reactions that induces the isotopic fractionation. While further work is needed to elucidate the significance of this value; it would imply a close relation between the kinetic isotope effects of cellulose and lipids. Hence, the observed fractionation factor and kinetic isotopic effect may clarify the mechanism that regulates the final deuterium fingerprint of terpenoids, providing evidence for the importance of precipitation in the relatively fast traumato-defense synthases.

4.4.3. $\delta D_{resin}$ short-term variability and its correlation with a defense mechanism

Our observations suggest fast environmental water use in resin formation, and that the variation in water availability plays a role in δD values found in resins. This implies not only a close relationship between physiological and biosynthetic responses, it also accounts for the efficiency of the plant defense mechanism in response to stress, and emphasizes the capacity of the plant to concentrate its survival efforts into secondary metabolite production.

The observed deuterium isotope variability can potentially be linked to *de novo* formation of resin ducts in the xylem (Franceschi et al., 2000; Martin et al., 2004; Zulak and Bohlmann, 2010), which stimulate the production and accumulation of inducible resin terpenoids in newly initiated axial resin ducts (Franceschi et al., 2000). Accordingly, the short-term resin deuterium composition variability of coniferous trees under study (Fig. 4-2 C, D, E) should correspond to the time span of terpene acid biosynthesis, particularly because $\delta D_{resin}$ varies in terms of days (between 3 to 15 days). This time lapse is comparable with rates of enzymatic response detected in conifers (Zulak et al., 2009; Lombardero et al.,

2000). The plausibility of fast transport of terpenoids (mono- and diterpenes) from the plastids to the lumen of resin ducts (Martin et al., 2002; Bouvier et al., 2005; Zulak and Bohlmann, 2010) reflects a rapid defense mechanism responds against biotic stress sources (see Kolosova and Bohlmann, 2012). Also, invasive pest attack not only determines the timing of resin production, but also the carbon isotopic fingerprint through induced water stress (McKellar et al., 2011).

4.4.4. $\delta^{13}C$ composition of resins: physiological response and water use efficiency

The carbon isotopic fingerprint has been developed as an important indicator of physiological stress and water stress source. As in the case of $\delta D_{resin}$, a number of abiotic and biotic variables seem to influence the carbon isotopic composition of coniferous tree resins. $\delta^{13}C$ depends on the local conditions, which include: humidity, water availability, nutrient availability, and more importantly local atmospheric $\delta^{13}C$ levels (Tappert et al., 2013). While there are multiple reduction reactions during hydrogen fixation, only one fractionation step can be associated with the fixation of $CO_2$ (see Hayes, 2001; Schmidt et al., 2003). Hence, the $\delta^{13}C$ value of resins is representative of bulk leaf tissue (Tappert et al., 2013 and references therein) (see Fig. 4-1).

Observed mean $\delta^{13}C$ values of resins are consistent with the range of previously reported $\delta^{13}C$values of modern resins (Tappert et al., 2013). Yet, some results deviated from the proposed mean $\delta^{13}C_{resin}$ value of -27‰ (Tappert et al., 2013), by being considerably more enriched in $^{13}C$ ($\delta^{13}C$ < -24‰). Consequently, some other factors and sources of stress may have affected the physiological and thus, photosynthetic fractionation that took place during the formation of

secondary metabolites. One probable influence is that of water stress, which has been reported to produces a $\delta^{13}C$ value increases during intense bark beetle (Coleopterae: Scolytinae) attacks (McKellar et al., 2011). Our water use efficiency calculations show that the main control for such an effect would be the stomatal conductance, and thus, ultimately a result of water stress.

*4.4.4.1. Carbon isotopic discrimination and stomatal conductance*

The relationship between $\delta^{13}C$ and water-stress can be evidenced by the efficiency in plant $^{13}CO_2$ discrimination ($\Delta$), which depends on cellular to atmospheric fraction ratio $c_i/c_a$ (Warren et al., 2001). Stomatal conductance limits this ratio and thus plant water use efficiency (Farquhar et al., 1989; Flanagan et al. 1992; Valentini et al. 1992; Dawson et al., 2002; Cernusak et al., 2013). Moreover, recent research efforts have shown that the relationship between measured bulk $\delta^{13}C$ of leaf tissues from trees strongly correlates with $c_i/c_a$ (Cernusak et al., 2013). In this regard, since $\delta^{13}C_{resin}$ is comparable with $\delta^{13}C_{leaf}$ of bulk leaf tissue (Diefendorf et al., 2012; Tappert et al., 2013), the ratio of intercellular to ambient $CO_2$ mole fraction ($c_i/c_a$) can be calculated based on an experimental geometric linear regression model equation. This model more closely approximates those trees living under relatively low water stress conditions (*i.e.*, PM197, PM404, TOL, and ABM) (see Appendix, 2-2). Although, in general, this model overestimates the response of trees under extremely limited water uptake conditions, when compared with calculated $c_i/c_a$ based on seasonal variability in atmospheric $CO_2$ concentration and $\delta^{13}C_{resin}$ by 0.1 (*i.e.*, WS, and PM31 – Appendix, 2-2).

Importantly, the ratio of intercellular to atmospheric $CO_{2\,(g)}$ ($c_i/c_a$), is also linked to the rate of photosynthesis, which controls the rate of carbon isotopic discrimination against $^{13}CO_{2\,(g)}$. This rate represents the carbon acquired (A) per water vapor losses via stomatal conductance (g) ratio (Farquhar et al., 1989), and it has been found to account for at least 81% of $\delta^{13}C_{leaf}$ variability (Orchard et al., 2010). Experimental measurements conducted on well-watered plants allowed us to elucidate the extent of overestimation of calculated $c_i/c_a$ values, by comparing $c_i/c_a$ values derived from modeled plant response, with ratio $c_i/c_a$ calculated based on atmospheric $^{13}CO_{2\,(g)}$ and $\delta^{13}C_{resin}$ enrichment. This suggests that resin's carbon isotopic composition reflects photosynthetic water use efficiency strategies, which are limited when trees are under physiological stress and under water stress (Figs. 4-3, and 4-6).

*4.4.4.2. Water use efficiency determined by $\delta^{13}C_{resin}$ and its relation with $\delta D_{resin}$*

The relatively enriched $\delta^{13}C_{resin}$ and low stomatal conductance represent the effects of distinct water stress on trees. First, the intrinsic water stress can be related to location. Second, the extrinsic water stress may be related to the effects of insect attack (McKellar et al., 2011). Trees under intrinsic water stress showed water use efficiency comparable with other trees and their derived $\delta D_{resin}$ reflect the isotopic composition of seasonal precipitation better (Appendix, 2-2). On the other hand, trees under extrinsic water stress have high water use efficiency, but even though their resin deuterium composition represents mean monthly $\delta D_{resin}$, they may not accurately represent the deuterium composition of seasonal precipitation (Fig. 4-7, Appendix, 2-2).

Water use efficiency and the deuterium isotopic composition of resin are related, since stomatal conductance and water availability affects: (1) plant's photosynthetic rate and transpiration rate, and (2) as previously discussed, the final deuterium composition of cell-water use for biosynthesis. Therefore, the variability in water use efficiency ratio reflects the response to water stress. Thus, most of the evaluated trees decreased their photosynthetic rate and transpiration rate to reduce water loss. This is diminished, however, when water is available (Fig. 4-7). As a result, $\delta^{13}C_{resin}$ can be correlated with stomatal conductance, as a sensitive index to discriminate a tree's water source.

### 4.4.5. Summary and insights to amber stable isotopic analyses as paleoenvironmental proxy

Results are consistent with previous independent research and show the potential of deuterium composition of resins as a climate proxy. $\delta D_{resin}$ and $\delta^{13}C_{resin}$ values vary as a product of the metabolic response of trees (Fig. 4-7). Also, this process is fast, showing that the hydrogen isotopic fingerprint of resins can change in terms of days, and that it reflects the water source available to the tree. Thus, within the perspective of the geological record, fossilized resin and amber offer a window to past climate.

Understanding this window, however, requires coupling the present knowledge about the physiological response of trees to different environmental stress conditions and their effects on secondary metabolites. Hence, this study shows the importance of precipitation and soil water as primary sources of hydrogen, and demonstrates that the short root systems of coniferous trees lead to

a preferential uptake of precipitation instead of top-soil water, when the water table is not accessible (Fig. 4-7A). Under water stress conditions, cellular water may be used, and would produce resins relatively enriched in deuterium, due to the balance between hydraulic xylem-water uptake and humidity.

Finally, the apparent fractionation between resin and precipitation is ~-228‰. This fractionation factor agrees with values previously determined from exceptional preserved fossil resins (Wolfe et al., 2012) and other terpenes-derived biomarkers (Chikaraishi et al., 2004). Indeed, resins and ambers are capable of recording environmental water's isotopic composition fluctuation and growing conditions such as water stress.

Considering relatively high water stress, the natural variability of hydrogen isotopic composition of resins among trees can be as high as 30‰. When these values are compared with the variability observed in Cretaceous resins from the Edmonton river valley, and Drumheller and Morrin Bridge amber deposits located in Alberta, which are all less than 16‰ (McKellar et al., 2008) (Appendix, 2-3), it is possible to determine the hydrogen isotopic composition of ancient precipitation (Appendix, 2-3). Alternatively, a relatively less-variable hydrogen isotopic distribution of resins could be related to constant water supply, or also, the presence of a relatively constant continental climatic regime.

Additionally, this study also shows that fossil resin's carbon isotopic composition data analysis, coupled with paleotemperature indicators may allow calculation of the stomatal conductance and photosynthetic rate efficiency (Fig. 4-7B). This, coupled with botanical information regarding the resin-producing tree,

may provide us with complementary data useful to evaluate the evolution of this process and its relationship with the hydrogen isotopic composition of ancient water.

### 4.5. Conclusions

The current study provides a model that may help to better constrain the significance of the hydrogen stable isotopic fingerprint of fossil resins, as it has been already achieved for its carbon isotopic composition. The applicability of fossil resin or amber deuterium fingerprint to ancient environmental water reconstructions should consider the following observations:

1. Conifer-resin $\delta D_{resin}$ records seasonal fluctuations of precipitation $\delta D_{ppt}$ as their isotopic shifts occur within ~ 3–15 days of induced resin production.

2. $\delta D_{resin}$ depends on site characteristics and water source that result in up to 30‰ differences between trees in different zones.

3. In general, the sample population showed a coherent seasonal trend in the $\delta D_{resin}$ that reflects a combination of abiotic and biotic controls.

4. $\delta D_{ppt}$ values and (indirectly) temperature, are the main environmental controls over the response observed in $\delta D_{resin}$.

5. Apparent mean $\varepsilon_{resin\text{-}ppt}$ is about -228 ± 19‰, and isotopic fractionation factor ($\alpha_{ppt\text{-}resin}$) about 0.7.

6. Trees under ecophysiological stress (due to water or insects) produce resins that are enriched in $\delta^{13}C_{resin}$. Yet, it is possible to determine carbon discrimination,

stomatal conductance and water use efficiency, and thus detect growth under water stress conditions.

7. Trees under intrinsic water stress produced resins that better represented the seasonal deuterium variability of precipitation.

8. Resins have a natural deuterium composition variability of about 30‰ that can be extrapolated to evaluate the deuterium isotopic composition of amber deposits. Combining this variability with the robust hydrogen isotopic fractionation data here presented, not only proves that resinites and ambers as sensitive paleoclimatic and paleohydrologic indicators, but also offers an avenue to determine the specific contribution of certain terpene biomarkers and plant-derived molecules.

Table 4-1. Description, location and general observation of sampled trees, emphasizing abiotic and biotic stress sources.

| Observed stress source | | Trees under study and their location | | | | Individual observations | |
|---|---|---|---|---|---|---|---|
| **n** | **General observations** | **Location** | **Species** | **Family** | **Sampling code** | **Stress source** | **Observations** |
| 1 | Signs of bark beetle outbreak (*Coleopterae*) | Zone 1 | Picea mariana (Mill.) B.S.P. | Pinaceae | PM31 | 1, 2, 5, 6 | Because of their location these trees are prone to be infleunce solely by environmental waters. PM31 seems to be the tree under extreme ecophysiological stress. |
| 2 | Boreholes fulfilled with resin exudates, presence of larvae | | Picea mariana (Mill.) B.S.P. | Pinaceae | PM196 | 1, 2, 3,4, 6 | |
| 3 | Bark-beetle blue-stain fungi (*Curculionidae*) | | Picea mariana (Mill.) B.S.P. | Pinaceae | PM404 | 1, 2, 3, 6 | |
| 4 | Internal resin lumps formed from resin accumulation outside the tree trunk | Zone 2 | Picea pungens Engelm. | Pinaceae | BS | 1, 2, 3, 6 | These blue and white spruces showed signs of infestation during June, followed by present of parasites. Based on their location, aslo they may be expose to pollution and water stress |
| 5 | Abundant external resin lumps | | Picea glauca (Moench) Voss | Pinaceae | WS | 1, 2, 3, 7 | |
| 6 | Water stress | Zone 3 | Abies balsamea (L.) Mill.+ | Pinaceae | ABM | 5, 6,7 | Trees on campus are under maintainance by ornamental services. As such, these trees are prone to be watered during the summer season. However, because it was in locate over a terrace, ABM was under extreme water stress and exposure to winds, and pollution. This tree was remove in 2012. |
| 7 | Ornamental maintenance | | Thuja occidentalis L. | Cupressaceae | TOL | 5, 7 | |

Table 4-2. Abiotic factors, daily and mean deuterium composition of resins ($\delta D_{resin}$) through time (from May to November). Abiotic factors are average temperature, monthly total precipitation, and monthly mean precipitation deuterium composition ($\delta D_{ppt}$). Biotic responses include daily and mean resin ($\delta D_{resin}$), and calculated monthly mean fractionation ($\varepsilon_{ppt\text{-}resin}$). Descriptive statistics show minimum, maximum, mean and distribution standard deviation of evaluated variables.

| | | | | *Picea mariana* (black spruce) | | | | | | | | |
|---|---|---|---|---|---|---|---|---|---|---|---|---|
| | | | | PM-31 | | | PM-197 | | | PM-404 | | |
| **Month** | **Average temperature (°C)** | **Tppt (mm)** | **$\delta D_{ppt}$ (*) (VSMOW) ‰** | **δD (VSMOW) ‰** | **δDaverage (VSMOW) ‰** | **$\varepsilon_{ppt\text{-}resin}$ (VSMOW) ‰** | **δD (VSMOW) ‰** | **δDaverage (VSMOW) ‰** | **$\varepsilon_{ppt\text{-}resin}$ (VSMOW) ‰** | **δD (VSMOW) ‰** | **δDaverage (VSMOW) ‰** | **$\varepsilon_{ppt\text{-}resin}$ (VSMOW) ‰** |
| May | 9.5 | 15.6 | -97 | - | -301.0 | -226 | - | -303.6 | -229 | - | -277.0 | -199 |
| | 16.1 | | | - | | | - | | | - | | |
| | 15.9 | | | -312.8 | | | -286.3 | | | -276.6 | | |
| | 12.9 | | | - | | | - | | | - | | |
| | 14.5 | | | -293.7 | | | -286.8 | | | -278.4 | | |
| | 13.1 | | | -296.5 | | | -337.6 | | | -276.2 | | |
| June | 7.5 | 128.2 | -87 | -282.8 | -261.1 | -191 | -272.9 | -291.5 | -224 | -286.0 | -270.7 | -201 |
| | 14.9 | | | -258.4 | | | -381.5 | | | -278.0 | | |
| | 12.5 | | | -268.3 | | | -274.6 | | | -262.5 | | |
| | 14.9 | | | -258.6 | | | -286.9 | | | -262.5 | | |
| | 16 | | | -237.5 | | | -241.8 | | | -264.4 | | |
| July | 19.5 | 150.2 | -89 | -264.8 | -268.7 | -197 | -286.7 | -282.5 | -212 | -298.3 | -280.9 | -211 |
| | 17.2 | | | -262.6 | | | -271.8 | | | -265.9 | | |
| | 13.9 | | | -278.8 | | | -288.8 | | | -265.4 | | |
| | 14.3 | | | - | | | - | | | -294.1 | | |
| August | 15.7 | 10.8 | -93 | -389.6 | -338.7 | -271 | -296.2 | -289.7 | -217 | -298.6 | -290.7 | -218 |
| | 12.6 | | | -287.8 | | | -283.2 | | | -282.9 | | |
| September | 17.5 | 5.2 | -101 | -293.6 | -311.6 | -234 | -295.3 | -312.4 | -235 | -292.9 | -304.5 | -226 |
| | 12.2 | | | - | | | - | | | -298.3 | | |
| | 14.6 | | | -329.7 | | | -329.4 | | | -322.3 | | |
| October | 5.2 | 7.4 | -121 | -339.1 | -286.6 | -188 | -334.3 | -333.1 | -241 | -364.0 | -348.2 | -259 |
| | 1.3 | | | -269.3 | | | -338.7 | | | -344.3 | | |
| | 2.1 | | | -251.4 | | | -326.4 | | | -336.5 | | |
| November | -2.3 | 22 | -155 | -312.8 | -323.4 | -199 | -325.0 | -332.4 | -210 | -317.7 | -331.7 | -209 |
| | -3.1 | | | -333.9 | | | -339.8 | | | -345.7 | | |
| Minimum | -3.1 | 5.2 | -155 | -389.6 | -338.7 | -270.9 | -381.5 | -333.1 | -241.3 | -364.0 | -348.2 | -258.5 |
| Maximum | 19.5 | 150.2 | -87 | -237.5 | -261.1 | -188.4 | -241.8 | -282.5 | -210.0 | -262.5 | -270.7 | -199.4 |
| Average | 11.5 | 48.5 | -106 | -293.2 | -298.7 | -215.3 | -304.9 | -306.4 | -224.1 | -297.4 | -300.5 | -217.6 |
| Standard deviatio | 6.2 | 62.5 | 24 | 36.7 | 28.4 | 30.2 | 33.1 | 20.4 | 11.8 | 30.1 | 29.4 | 20.3 |

| | *Picea pungens* (blue spruce) | | | *Picea glauca* (white spruce) | | | *Abies balsamea*+ | | | *Thuja occidentalis* | | |
|---|---|---|---|---|---|---|---|---|---|---|---|---|
| | BS | | | WS | | | ABM | | | TOL | | |
| **Month** | **δD (VSMOW) ‰** | **δDaverage (VSMOW) ‰** | **$\varepsilon_{ppt\text{-}resin}$ (VSMOW) ‰** | **δD (VSMOW) ‰** | **δDaverage (VSMOW) ‰** | **$\varepsilon_{ppt\text{-}resin}$ (VSMOW) ‰** | **δD (VSMOW) ‰** | **δDaverage (VSMOW) ‰** | **$\varepsilon_{ppt\text{-}resin}$ (VSMOW) ‰** | **δD (VSMOW) ‰** | **δDaverage (VSMOW) ‰** | **$\varepsilon_{ppt\text{-}resin}$ (VSMOW) ‰** |
| May | - | -275.1 | -197 | - | - | - | -269.7 | -265.7 | -187 | - | - | - |
| | - | | | - | | | -233.9 | | | - | | |
| | -264.7 | | | - | | | - | | | - | | |
| | - | | | - | | | - | | | - | | |
| | -276.9 | | | - | | | -293.5 | | | - | | |
| | -283.7 | | | - | | | - | | | - | | |
| June | -272.0 | -284.8 | -217 | - | - | - | -257.2 | -276.1 | -207 | -287.7 | -292.6 | -225 |
| | -338.6 | | | - | | | -257.2 | | | -294.6 | | |
| | -265.7 | | | - | | | -291.5 | | | -287.3 | | |
| | -251.7 | | | - | | | -293.1 | | | -293.6 | | |
| | -296.2 | | | - | | | -281.8 | | | -300.0 | | |
| July | -251.1 | -267.2 | -196 | -253.7 | -312.8 | -266 | -277.8 | -280.6 | -210 | -291.7 | -307.9 | -240 |
| | -286.0 | | | - | | | -291.6 | | | -341.7 | | |
| | -266.3 | | | -299.6 | | | -295.8 | | | -279.7 | | |
| | -265.4 | | | -385.2 | | | -257.2 | | | -318.4 | | |
| August | -279.8 | -266.3 | -191 | -341.2 | -331.7 | -263 | -254.8 | -261.9 | -186 | -299.5 | -307.7 | -237 |
| | -252.8 | | | -322.2 | | | -269.0 | | | -315.8 | | |
| September | -269.1 | -314.7 | -238 | -357.9 | -336.7 | -262 | -271.6 | -287.7 | -208 | -338.9 | -334.4 | -260 |
| | -286.0 | | | -327.6 | | | -292.4 | | | -341.5 | | |
| | -389.0 | | | -324.6 | | | -299.0 | | | -322.9 | | |
| October | -317.7 | -327.4 | -235 | - | -327.2 | -235 | -276.3 | -274.3 | -174 | -318.0 | -347.2 | -257 |
| | -334.6 | | | -322.4 | | | -278.5 | | | -359.8 | | |
| | -329.8 | | | -332.0 | | | -268.1 | | | -363.9 | | |
| November | -323.4 | -323.4 | -199 | -274.6 | -336.9 | -215 | -339.0 | -341.9 | -221 | -353.4 | -350.2 | -231 |
| | -323.4 | | | -399.2 | | | -344.7 | | | -346.9 | | |
| Minimum | -389.0 | -327.4 | -237.7 | -399.2 | -336.9 | -265.5 | -344.7 | -341.9 | -221.1 | -363.9 | -350.2 | -259.7 |
| Maximum | -251.1 | -266.3 | -191.1 | -251.7 | -312.8 | -215.3 | -233.9 | -261.9 | -174.4 | -279.7 | -292.6 | -225.2 |
| Average | -294.3 | -294.1 | -210.3 | -322.0 | -329.1 | -248.2 | -284.9 | -284.0 | -199.1 | -319.0 | -323.3 | -241.7 |
| Standard deviatio | 35.6 | 26.9 | 19.4 | 44.9 | 9.9 | 22.3 | 25.6 | 26.9 | 16.7 | 27.2 | 23.8 | 14.0 |

+ Tree removed from the study area

(*) Online Isotopes in Precipitation Calculator version 2.2 (Bowen, 2009; Bowen and Revenaugh, 2003). Temperature data were obtained from the weather station of the Department of Earth and Atmospheric Sciences (EAS) web, and Canadian Climate Normal – Data Base. 2011.

Table 4-3. Daily and mean values of resin carbon isotopic composition ($\delta^{13}C$) through time (from May to November). Descriptive statistics show minimum, maximum, mean and distribution standard deviation of the evaluated variables.

| Month | $\delta^{13}C_{PM-31}$ (VPDB) ‰ | $\delta^{13}C_{average}$ (VPDB) ‰ | $\delta^{13}C_{PM197}$ (VPDB) ‰ | $\delta^{13}C_{average}$ (VPDB) ‰ | $\delta^{13}C_{PM404}$ (VPDB) ‰ | $\delta^{13}C_{average}$ (VPDB) ‰ | $\delta^{13}C_{BS}$ (VPDB) ‰ | $\delta^{13}C_{average}$ (VPDB) ‰ | $\delta^{13}C_{WS}$ (VPDB) ‰ | $\delta^{13}C_{average}$ (VPDB) ‰ | $\delta^{13}C_{ABM}$ (VPDB) ‰ | $\delta^{13}C_{average}$ (VPDB) ‰ | $\delta^{13}C_{TOL}$ (VPDB) ‰ | $\delta^{13}C_{average}$ (VPDB) ‰ |
|---|---|---|---|---|---|---|---|---|---|---|---|---|---|---|
| May | - | -24.2 | - | -26.5 | - | -27.2 | - | -26.7 | - | - | - | -26.7 | - | - |
| | - | | - | | - | | - | | - | | -24.6 | | - | |
| | -24.2 | | -26.5 | | -26.5 | | -26.2 | | - | | - | | - | |
| | - | | - | | - | | - | | - | | - | | - | |
| | -24.3 | | - | | -27.6 | | -26.2 | | - | | -23.2 | | - | |
| | - | | - | | -27.5 | | -27.7 | | - | | - | | - | |
| June | -24.1 | -24.7 | -26.8 | -26.4 | -26.6 | -26.6 | -26.4 | -26.7 | - | - | -23.7 | -26.7 | -24.7 | -26.7 |
| | -24.4 | | -26.9 | | -26.3 | | -26.2 | | - | | -23.5 | | -24.8 | |
| | -24.4 | | -26.7 | | -26.5 | | -26.3 | | - | | -23.8 | | -24.6 | |
| | -26.6 | | -27.4 | | -27.0 | | -27.8 | | - | | -24.9 | | -25.7 | |
| | -24.2 | | -24.1 | | -26.7 | | -26.8 | | - | | -24.8 | | -24.9 | |
| July | -24.5 | -24.3 | -27.2 | -27.2 | - | -26.4 | -26.5 | -25.9 | -28.8 | -26.3 | -22.5 | -25.9 | - | -24.5 |
| | -24.2 | | - | | -26.4 | | -25.9 | | - | | -26.6 | | - | |
| | -24.3 | | - | | -26.5 | | -26.5 | | -24.9 | | -24.3 | | -24.5 | |
| | -24.2 | | - | | -26.5 | | -24.7 | | -25.2 | | -24.3 | | - | |
| August | -24.3 | -24.6 | -26.7 | -26.7 | -26.7 | -26.4 | -26.8 | -26.6 | -24.6 | -24.6 | -24.3 | -26.6 | -24.9 | -24.9 |
| | -24.9 | | -26.7 | | -26.1 | | -26.4 | | - | | -24.3 | | - | |
| September | -24.7 | -24.7 | -27.4 | -27.4 | -25.8 | -25.8 | - | -25.7 | -23.9 | -25.6 | -24.3 | -25.7 | - | - |
| | - | | - | | - | | - | | -26.4 | | -24.5 | | - | |
| | - | | - | | -25.8 | | -25.7 | | -26.4 | | -24.3 | | - | |
| October | -24.7 | -24.7 | - | -27.4 | -25.2 | -25.3 | -26.5 | -25.9 | - | -23.8 | -23.8 | -25.9 | - | - |
| | -24.8 | | - | | - | | -26.5 | | -23.8 | | -23.8 | | - | |
| | -24.6 | | -27.4 | | -25.4 | | -24.6 | | - | | -24.9 | | - | |
| November | - | - | - | - | - | - | -25.2 | -25.2 | -24.8 | -24.6 | -24.3 | -25.4 | -25.2 | -25.2 |
| | - | | - | | - | | - | | -24.4 | | -26.5 | | - | |
| Minimum | -26.6 | -24.7 | -27.4 | -27.4 | -27.6 | -27.2 | -27.8 | -26.7 | -28.8 | -26.3 | -26.6 | -26.7 | -25.7 | -26.7 |
| Maximum | -24.1 | -24.2 | -24.1 | -26.4 | -25.2 | -25.3 | -24.6 | -25.2 | -23.8 | -23.8 | -22.5 | -25.7 | -24.5 | -25.7 |
| Average | -24.6 | -24.6 | -26.6 | -26.9 | -26.4 | -26.3 | -26.3 | -26.1 | -25.9 | -25.0 | -24.4 | -26.2 | -25.0 | -26.2 |
| Standard deviation | 0.6 | 0.2 | 0.9 | 0.5 | 0.6 | 0.7 | 0.8 | 0.6 | 1.4 | 1.0 | 0.9 | 0.4 | 0.4 | 0.4 |

[+] Tree removed from the study area

Table 4-4. Correlation matrix between deuterium composition of seasonally sampled resins, and abiotic factors (temperature and monthly total precipitation). Significant correlation was considered for those values with $R^2 > 0.56$, $p < 0.05$. Abbreviations: Tppt, total monthly precipitation; Ppt, precipitation deuterium composition; Std. Dev., standard deviation.

| | Mean | Std.Dev | Temperature | Tppt | Ppt | PM404 | PM197 | PM31 | WS | BS | ABM | TOL |
|---|---|---|---|---|---|---|---|---|---|---|---|---|
| **Temperature (°C)** | 10.52 | 8.46 | 1.00 | | | | | | | | | |
| **Tppt (mm/month)** | 53.97 | 66.64 | 0.26 | 1.00 | | | | | | | | |
| **Ppt** | -107.67 | 26.28 | **0.81** | **0.51** | 1.00 | | | | | | | |
| **PM404** | -304.46 | 30.13 | **0.60** | **0.71** | **0.81** | 1.00 | | | | | | |
| **PM197** | -306.93 | 22.35 | **0.73** | **0.68** | **0.87** | **0.94** | 1.00 | | | | | |
| **PM31** | -298.37 | 31.10 | 0.08 | **0.80** | 0.41 | 0.33 | 0.29 | 1.00 | | | | |
| **WS** | -324.71 | 19.89 | -0.15 | **0.57** | 0.44 | **0.52** | 0.35 | **0.65** | 1.00 | | | |
| **BS** | -297.29 | 27.96 | **0.65** | **0.60** | **0.76** | **0.85** | **0.96** | 0.15 | 0.25 | 1.00 | | |
| **ABM** | -287.09 | 28.14 | **0.66** | 0.16 | **0.85** | 0.42 | **0.58** | 0.25 | 0.31 | **0.55** | 1.00 | |
| **TOL** | -323.34 | 23.83 | **0.52** | **0.71** | **0.85** | **0.94** | **0.93** | 0.41 | **0.65** | **0.88** | **0.60** | 1.00 |

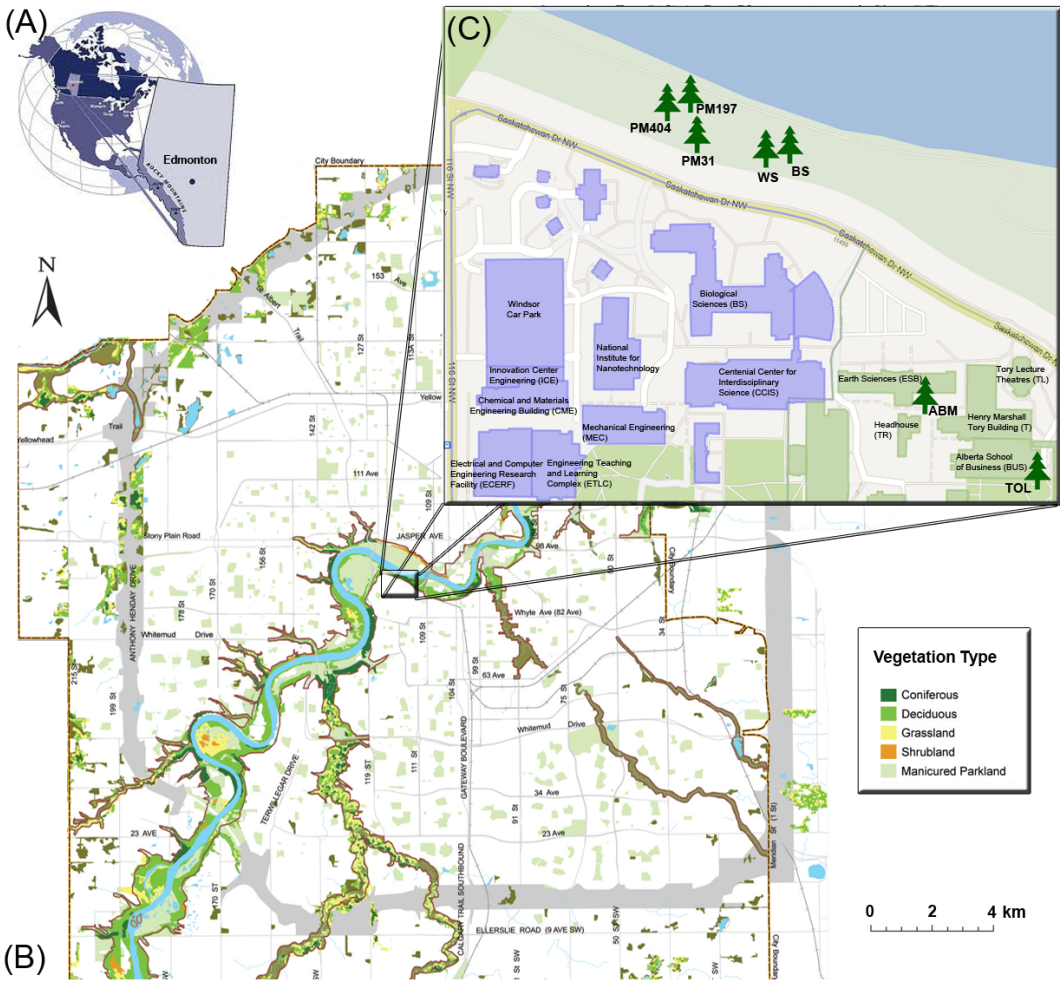


Figure 4-1. Study sites. (A) Relative location of the study sites in Edmonton, Alberta, Canada. (B) Mapped vegetation of the Edmonton area (Map, Office of Natural Areas City of Edmonton, 2006). (C) The study is about 0.49 km$^2$ within the Univerity of Alberta North Campus, northwest Edmonton. The map delimits the location of the three sample zones, and the position of each tree. Zone 1: Emily Murphy Park, river valley (PM31, PM197, and PM404); zone 2: adjacent to Saskatchewan Drive (WS, BS); zone 3: main campus (ABM, CUP) (Map modified from Google Maps, 2011).

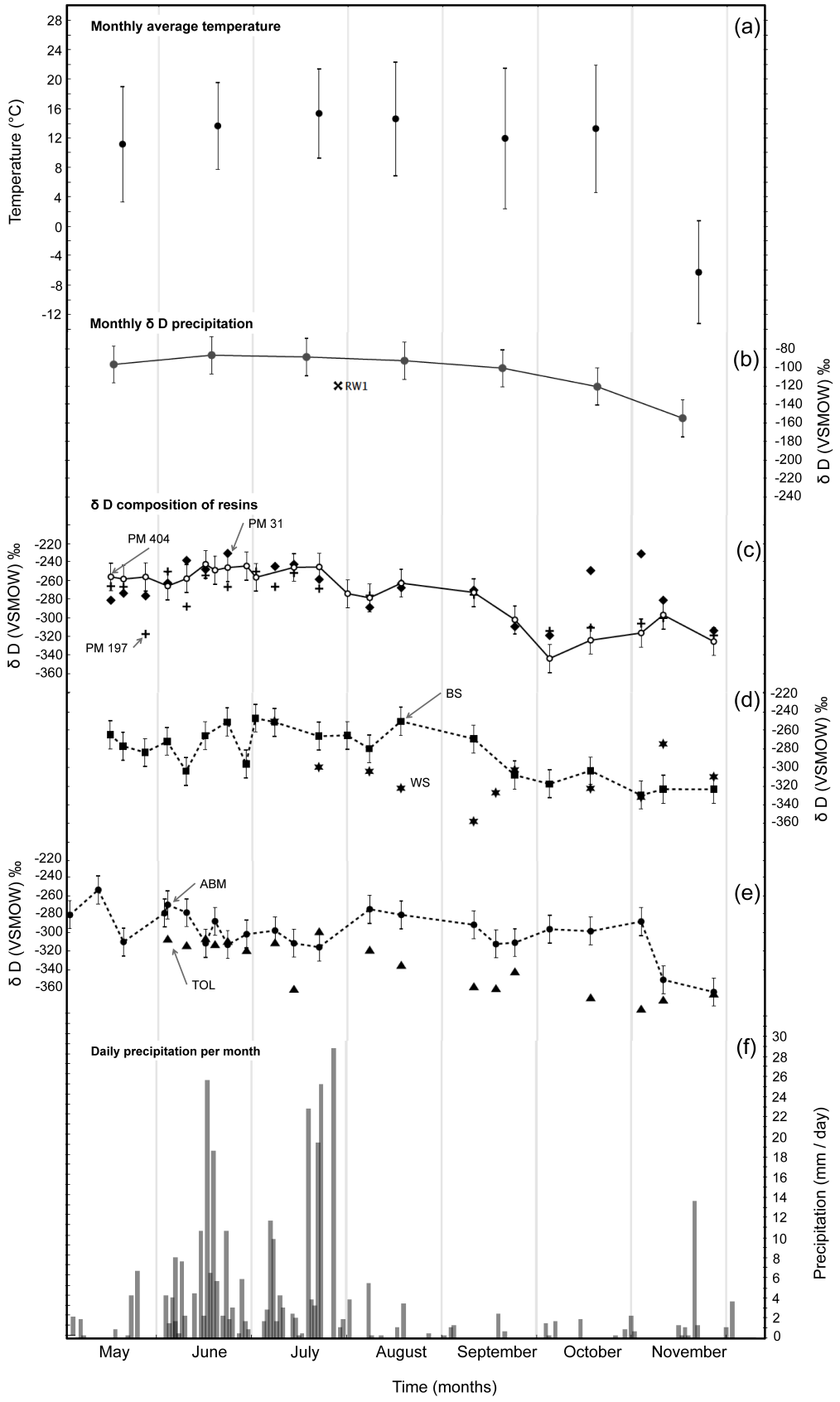
Monthly average temperature
(a)
Temperature (°C)
28
24
20
16
12
8
4
0
-4
-8
-12
Monthly δ D precipitation
(b)
RW1
-80
-100
-120
-140
-160
-180
-200
-220
-240
δ D (VSMOW) ‰
δ D composition of resins
(c)
PM 404
PM 31
PM 197
δ D (VSMOW) ‰
-220
-240
-260
-280
-300
-320
-340
-360
(d)
BS
WS
δ D (VSMOW) ‰
(e)
ABM
TOL
δ D (VSMOW) ‰
Daily precipitation per month
(f)
Precipitation (mm / day)
30
28
26
24
22
20
18
16
14
12
10
8
6
4
2
0
May
June
July
August
September
October
November
Time (months)

Figure 4-2. Deuterium composition of induced resins through time from May to November, coupled with average monthly temperature, hydrogen isotopic composition of precipitation, and daily precipitation. Thus, abiotic factors are represent by: (a) average monthly temperature (EAS weather station), (b) average monthly deuterium composition of precipitation (OIPC version 2.2 – Bowen et al., 2005; Bowen, 2008) and (f) daily precipitation per month (Canadian Climate Normal, 2011). Biotic response was recorded as the daily deuterium composition of resins from trees located in: (c) zone 1 (PM31, PM197, PM404), (d) zone 2 (Bs, WS), and (e) zone 3 (ABM, TOL). Abbreviation: VSMOW, Vienna Standard Mean Ocean Water.

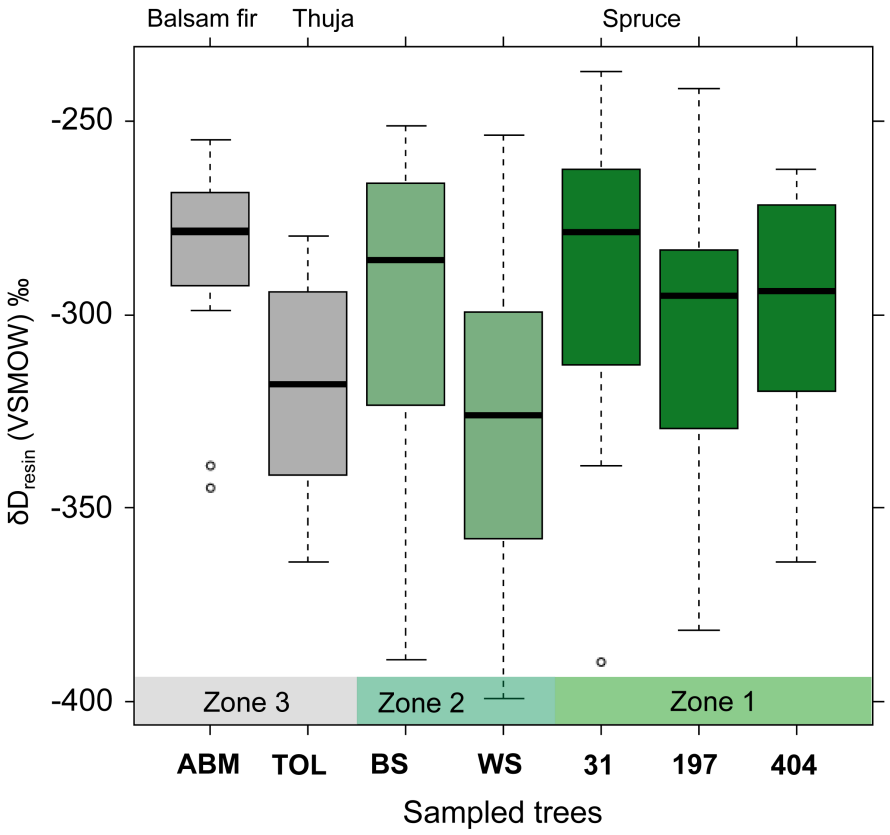


Figure 4-3. Descriptive statistical analyses of biotic and abiotic factors. The biotic factors represent the deuterium content in resins, and the abiotic factors reflect the deuterium content in precipitation, average monthly temperature, and monthly precipitation. (a) Box-plot representing the biotic response variable distribution measured per tree—all trees show an asymmetrical distribution. Abbreviations: VSMOW, Vienna Standard Mean Ocean Water; PM, *Picea mariana*; BS, *Picea pungens*; WS, *Picea glauca*; ABM, *Abies balsamea*; TOL, *Thuja occidentalis*.

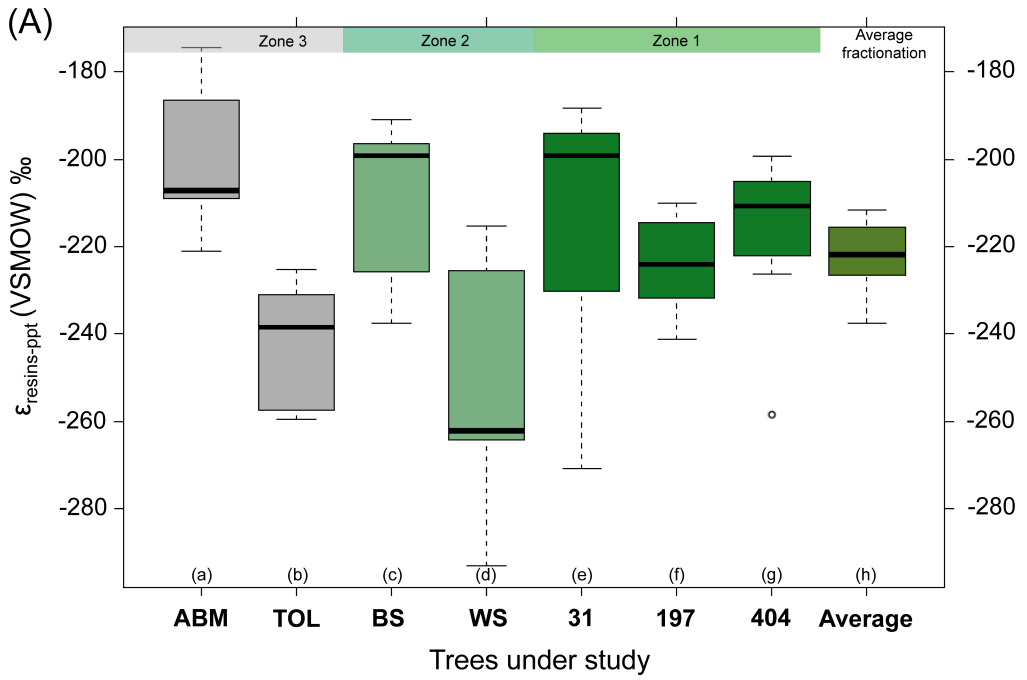
(A)
Zone 3
Zone 2
Zone 1
Average fractionation
-180
-200
-220
-240
-260
-280
$\varepsilon_{resins-ppt}$ (VSMOW) ‰
(a)
(b)
(c)
(d)
(e)
(f)
(g)
(h)
ABM
TOL
BS
WS
31
197
404
Average
Trees under study

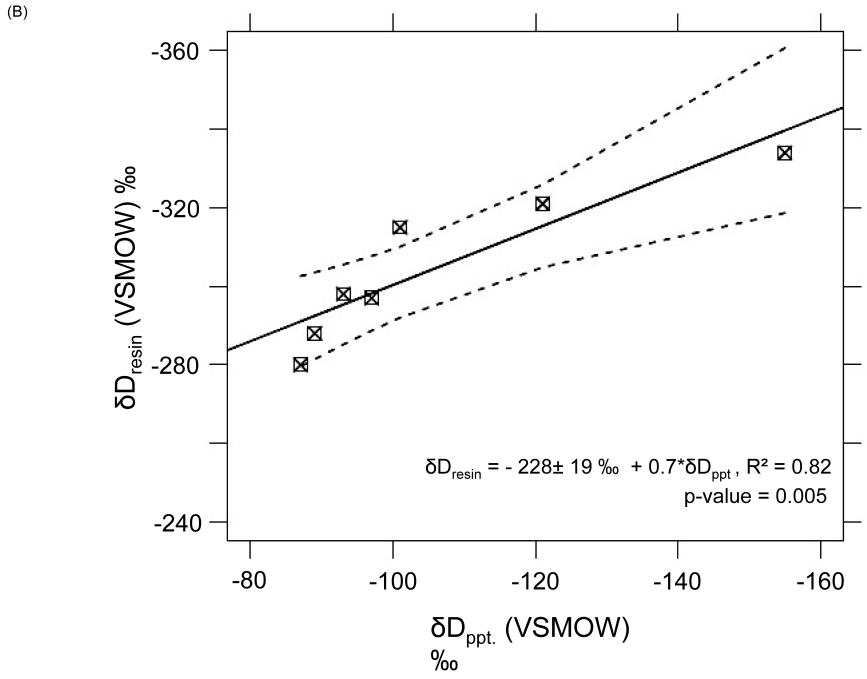
(B)
-360
-320
-280
-240
$\delta D_{resin}$ (VSMOW) ‰
$\delta D_{resin}$ = - 228± 19 ‰ + 0.7*$\delta D_{ppt}$ , $R^2$ = 0.82
p-value = 0.005
-80
-100
-120
-140
-160
$\delta D_{ppt.}$ (VSMOW)
‰

Figure 4-4. Relationships between average resin deuterium values ($\delta D_{resin}$) plotted against mean annual precipitation values ($\delta D_{ppt}$). $\delta D_{ppt}$ values from the area were taken from the Online Isotopes in Precipitation Calculator version 2.2 (Bowen 2009; Bowen and Revenaugh, 2003). (a) Box-plots representing the calculated deuterium fractionation between monthly average precipitation and resin's hydrogen isotopic composition (per tree) in zone 3 (a.a, a.b), zone 2 (a.c, a.d), zone 3 (a.e, a.f, a.g), and the distribution of average fractionation (a.h). (b) General lineal regression model between average monthly deuterium composition of resins and precipitation. The regression parameters are significant ($R^2 = 0.82$, p-value = 0.005) and most of the values fall within the 95% confidence interval. Thus, the slope represents the fractionation factor ($\alpha = (D/H)_{resin}/(D/H)_{ppt} = 0.7$), and the intercept represents initial composition, which is equivalent to the apparent fractionation between precipitation and resin terpenoid compounds ($\varepsilon_{resin\text{-}ppt} = -228 \pm 19‰$ ). Abbreviations listed in Fig. 2-3.

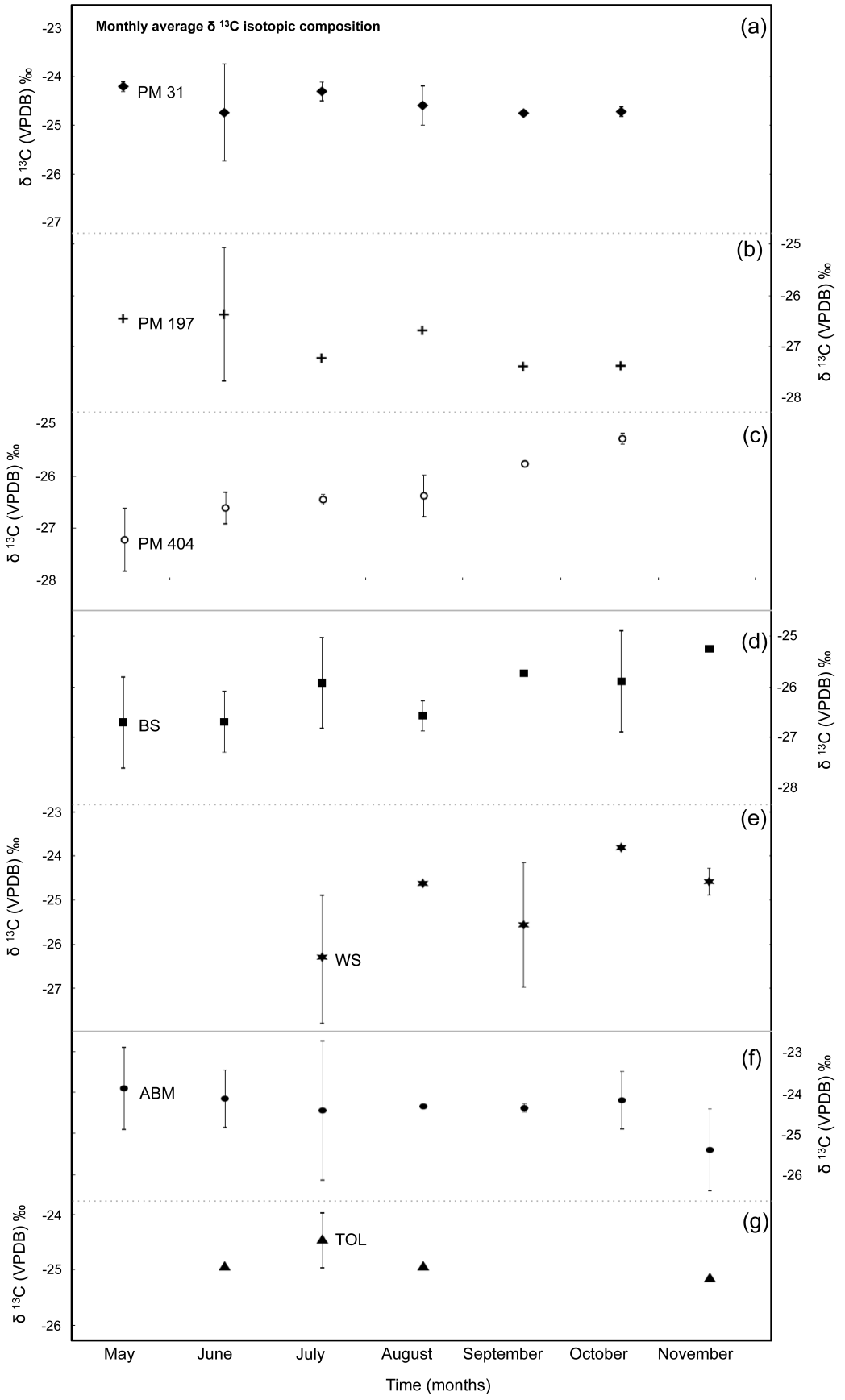
Monthly average δ 13C isotopic composition
(a)
PM 31
(b)
PM 197
(c)
PM 404
(d)
BS
(e)
WS
(f)
ABM
(g)
TOL
δ 13C (VPDB) ‰
May
June
July
August
September
October
November
Time (months)

Figure 4-5. Monthly average carbon isotopic composition of induced resins through time from May to November per tree: *Picea mariana* (a) PM31, (b) PM197, and (c) PM404; *Picea pungens* (d) BS; *Picea glauca* (e) WS; *Abies balsamea* (f) ABM; and *Thuja occidentalis* (g) TOL. Abbreviation: VPDB, Vienna Pee Dee Belemnite.

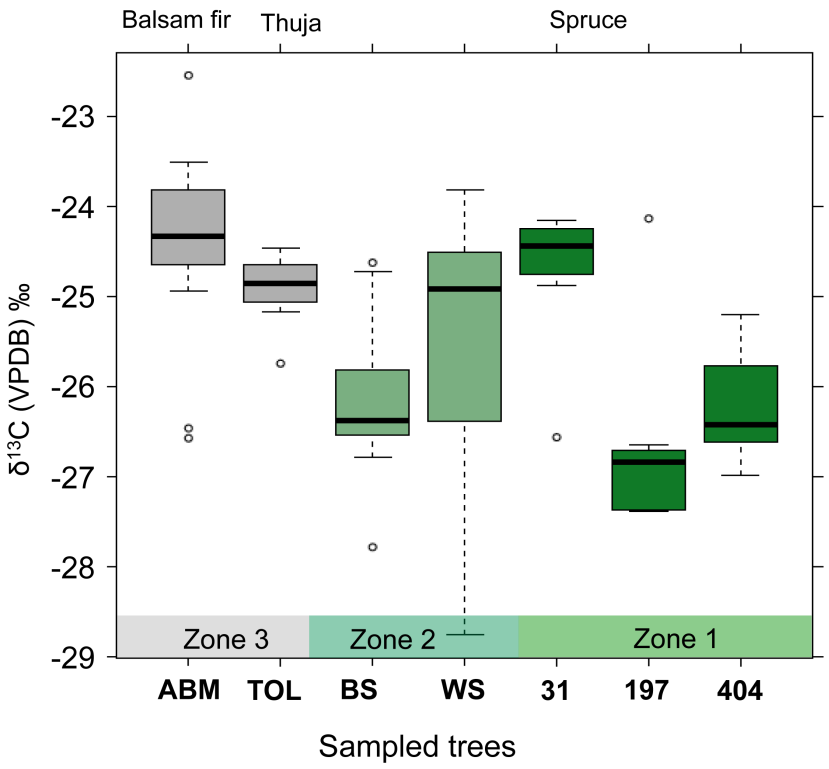


Figure 4-6. Descriptive statistics of carbon data. (a) Box-plot represents the carbon isotopic composition distribution measured per tree in the tree zones. ABM, TOL, WS and PM31 show enrichment characteristic of trees under water stress. Similarly, the quartiles distribution per tree shows asymmetry characteristic of natural systems.

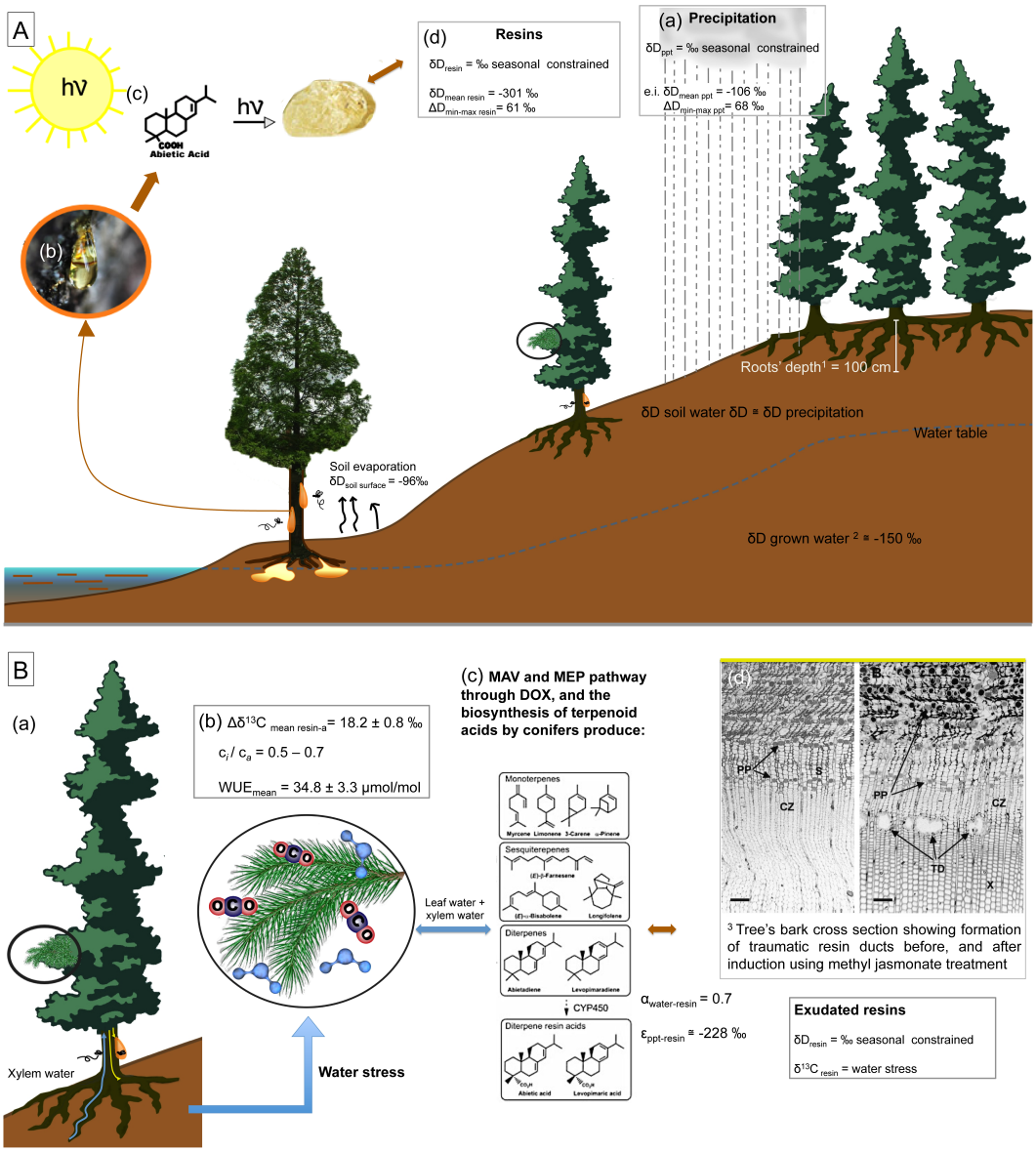


Figure 4-7. Hydrogen and carbon stable isotope respond to stress sources and its relation with primary source pool. The deuterium source pools in the Edmonton area and (A) δD of the different source pools in the Edmonton area and their correlation with the deuterium composition of precipitation (a). Induced resin exudate after insect attack and photo-oxidation process under environmental conditions (b, c and d). (B) Summary of water stress as a control of carbon isotopic discrimination. This shows carbon discrimination between resin and atmospheric carbon (a, b); but also, (a, c) of final cell-water deuterium

composition. Thus, this represents factors controlling carbon and hydrogen isotopic composition controlling processes such as xylem water (a); carbon isotopic discrimination ($\Delta^{13}C_{mean\ resin\text{-}a}$), stomatal conductance ($c_i/c_a$), and also water use efficiency ($WUE_{mean}$) (b); biosynthesis of terpenes through the MAV (mevalonic pathway) and MEP (methoxyletrine through DOX pathway) (modified from Kolosova and Bohlmann, 2012) (c); and final fractionation ($\varepsilon_{ppt\text{-}resin}$), and a fractionation factor ($\alpha_{water\text{-}resin}$) of 0.7 (d) (modified from Franceschi et al., 2002). See text for details. Abbreviations: a, atmosphere; PP, polyphenolic parenchyma cells; S, sieve cells; CZ, cambial zone; TD, traumatic resin ducts; X, xylem. References: [1] Strong and Roi, (1986); [2] Maulé et al., (1993).

## 4.6. References


Anonymous. (1980). Canadian climate normals. 1951-1980. Temperature and precipitation. – Published by Canadian Climate Program, Evironment Canada, Ottawa. p. 126.

Bouvier, F., Rahier, A., and Camara, B. (2005). Biogenesis, molecular regulation and function of plant isoprenoids. *Progress in Lipid Research*, 44(6), 357–429.

Bowen, G. J., (2012), The Online Isotopes in Precipitation Calculator, version 2.2. http://www.waterisotopes.org.

Bowen, G. J. (2008). Spatial analysis of the intra-annual variation of precipitation isotope ratios and its climatological corollaries. *Journal of Geophysical Research*, 113(D5), D05113.

Bowen G. J., Wassenaar L. I. and Hobson K. A. (2005), Global application of stable hydrogen and oxygen isotopes to wildlife forensics. *Oecologia*, 143, 337–348.

Box, G. E. P. (1976). Science and Statistics. *Journal of the American Statistical Association*, 71(356), 791–799.

Brodribb, T., and Hill, R.S., (1998). The photosynthetic drought physiology of a diverse group of southern hemisphere conifer species is correlated with minimum seasonal rainfall. *Functional Ecology*, 12(3), 465–471.

Broddid, T. J., and McAdam, S. A.M., (2013). Abscisic acid mediates a divergence in the drought response of two conifers. *Plant Physiology*, 162, 1370–1377.

Burgess, S.S.O., Pate, J.S., Adams, M.A., and Dawson, T.E., (2000). Seasonal water acquisition and redistribution in the australian woody phreatophyte, banksia prionotes. *Annals of Botany*, 85, 215–224.

Canadian Climate Normal – Data Base. 2011 [Online] Available from: http://www.climate.weatheroffice.gc.ca/climate_normals/results_e.html?stnID=1867&lang=e&dCode=1&StationName=EDMONTON&SearchType=Contains&province=ALL&provBut=&month1=0&month2=12 [Consulted in 2011].

Cernusak, L. A., Ubierna, N., Winter, K., Holtum, J. A. M., Marshall, J. D., and Farquhar, G. D., (2013). Tansley review: Environmental and physiological determinants of carbon isotope discrimination in terrestrial plants. *New Phytologist*, 130, 28–64.

Cernusak, L. A., Winter, K., Aranda, J., Turner, B. L., and Marshall, J. D., (2007). Transpiration efficiency of a tropical pioneer tree (*Ficus insipida*) in relation to soil fertility. *Journal of Experimental Botany*, 58, 3549–3566.

Cernusak, L. A., Winter, K., and Turner, B. L., (2009). Physiological and isotopic ($\delta^{13}C$ and $\delta^{18}O$) responses of three tropical tree species to water and nutrient availability. *Plant, Cell & Environment*, 32, 1441–1455.

Chappell, J., (1995). Biochemistry and molecular biology of the isoprenoid biosynthetic pathway in plants. *Annual Review Plant Physiology and Plant Molecular Biology*, 46, 521–547.

Chikaraishi, Y., Hiroshi N., and Simon, R. P., (2004). Carbon and hydrogen isotopic fractionation during lipid biosynthesis in a higher plant (*Cryptomeria japonica*). *Phytochemistry* 65(3), 323–330.

Chikaraishi, Y., Matsumoto, M., Ogawa, N. O., Suga, S., Kitazato, H., and Ohkouchi, N., (2005). Hydrogen, carbon and nitrogen isotopic fractionations during chlorophyll biosynthesis in C3 higher plants. *Phytochemistry*, 66(8), 911–20.

Coleman, M.L., Shepherd, T.J., Durham, J.J., Rouse, J.E., Moore, G.R., (1982). Reduction of water with zinc for hydrogen isotope analysis. *Analytical Chemistry*, 54(6), 993–995.

Cuntz, M., (2011), Carbon cycle: a dent in carbon's gold standard. *Nature*, 477(7366), 547–548.

Davies, W. J., and Zhang, J. H., (1991). Root signals and the regulation of growth and development of plants in drying soil. *Annual Review Plant Physiology and Plant Molecular Biology*, 42, 55–76.

Dawson, T. E., Mambelli, S., Plamboeck, A. H., Templer, P. H., and Tu, K. P., (2002). Stable isotopes in plant ecology. *Annual Review of Ecology and Systematics*, 33(1), 507–559.

Diefendorf, A.F., Freeman, K.H., and Wing, S.L., (2012). Distribution and carbon isotope patterns of diterpenoids and triterpenoids in modern temperate C3 trees and their geochemical significance. *Geochimica et Cosmochimica Acta*, 85, 342–356.

Ehleringer, J., and Cerling, T., (1995). Atmospheric $CO_2$ and the ratio of intercellular to ambient $CO_2$ concentrations in plants. *Tree Physiology*, 15, 105–111.

Farquhar, G. D., Cernusak, L. A., and Barnes, B., (2007). Heavy water fractionation during transpiration. *Plant Physiology*, 143(1), 11–18.

Farquhar, G.D., Ehleringer, J.R., and Hubick, K.T., (1989). Carbon isotope discrimination and photosynthesis. *Annual Review of Plant Physiology and Plant Molecular Biology*, 40, 503–37.

Farquhar, G., O'Leary, M., and Berry, J., (1982). On the relationship between carbon isotope discrimination and the intercellular carbon dioxide concentration in leaves. *Functional Plant Biology*, 1976, 9, 121–131.

Flanagan, L., and Ehleringer, J. R., (1991). Stable isotope composition of stem and leaf water: applications to the study of plant water use. *Functional Ecology*, *5*(2), 270–277.

Flanagan, L.B., Ehleringer, J.R., Marshall, J.D., (1992). Differential uptake of summer precipitation among co-occurring trees and shrubs in a pinyon-juniper woodland. *Plant, Cell and Environment*, 15, 831–836.

Franceschi, V. R., Krokene, P., Krekling, T., and Christiansen, E., (2000). Phloem parenchyma cells are involved in local and distant defense responses to fungal inoculation or bark beetle attack in Norway spruce (*Pinaceae*). *American Journal of Botany*, 87, 314–326.

Gara, R.I., Werner, R.A., Whitmore, M.C., and Holsten, E.H., (1995). Arthropod associates of the spruce beetle *Dendroctonus rufipennis* (Kirby)(Col., Scolytidae) in spruce stands of south-central and interior Alaska. *Journal of Applied Entomology*, 119(1-5), 585-590.

Gaylord, M.L., Kolb, T.E., Wallin, K.F., and Wagner, M.R., (2007). Seasonal dynamics of tree growth, physiology, and resin defenses in a northern Arizona ponderosa pine forest. *Canadian Journal of Forest Research*, 37(7), 1173–1183.

Google Maps. (2011). [North Campus, University of Alberta. Edmonton, Alberta] [Street map]. Retrieved from: https://maps.google.ca/maps?client=safari&q=university+of+alberta+edmonton&oe=UTF-8&ie=UTF-8&ei=ZceFUqWMBOn0iQK6i4D4Dw&ved=0CAoQ_AUoAg

Hayes, J. (2001). Fractionation of carbon and hydrogen isotopes in biosynthetic processes. *Reviews in mineralogy and geochemistry*, 43(1), 225–277.

Hou, J.Z., D'Andrea, W.J., and Huang, Y.S., (2008). Can sedimentary leaf waxes record D/H ratios of continental precipitation? Field, model, and experimental assessments. *Geochimica et Cosmochimica Acta*, 72, 3503–3517.

International Atomic Energy Agency (IAEA), (1969). Environmental isotope data No. 1, Technical Report Series, 96, IAEA, Vienna.

International Atomic Energy Agency (IAEA), (1970). Environmental isotope data No. 2, Technical Report Series, 117, IAEA, Vienna.

Kathol, C.R., and McPherson, R.A., (1975). Urban geology of Edmonton. *Alberta Research Council*, 32, 55 pp.

Keeling, C. I., and Bohlmann, J., (2006), Diterpene resin acids in conifers. *Phytochemistry*, 67(22), 2415–23.

Keeling, C., Piper, R., Bacastow, R., Wahlen, M., Whorf, T., Heimann, M., and Meijer, H., (2005). Atmospheric $CO_2$ and $^{13}CO_2$ with the terrestrial biosphere and oceans from 1978 to 2000: observations and carbon cycle implications, p. 83–113. [Online] from: http://scrippsco2.ucsd.edu/data/flask_co2_and_isotopic/monthly_co2/monthly_alt.csv

Keppler, F., Harper, D. B., Kalin, R. M., Meier-Augenstein, W., Farmer, N., Davis, S., and Schmidt H., Brown, D.M., and Hamilton, J.T.G., (2007). Stable hydrogen isotope ratios of lignin methoxyl groups as a paleoclimate proxy and constraint of the geographical origin of wood. *New Phytologist*, 176, 600–609.

Kolosova, N., and Bohlmann, J., (2012). Growth and Defence in Plants. In: Matyssek, R., H. Schnyder, W. Oßwald, D. Ernst, J. C. Munch, and H. Pretzsch (Eds.) *Growth and Defense in Plants*, 220, 85–109. Berlin.

Krokene, P., and Solheim, H., (1997). Growth of four bark-beetle-associated blue-stain fungi in relation to the induced wound response in Norway spruce. *Canadian Journal of Botany*, 75(4), 618–625.

Levin, D. A., (1976). The chemical defenses of plants to pathogens and herbivores. *Annual review of Ecology and Systematics*, 7(61), 121–159.

Lichtenthaler, H. K., (1999). The 1-deoxy-D-xylulose-5-phosphate pathway of isoprenoid biosynthesis in plants. *Annual Review Plant Physiology and Plant Molecular Biology*, 50, 47–65.

Lombardero, M.J., Ayres, M.P., Lorio Jr, P.L., and Ruel, J.J., (2000). Environmental effects on constitutive and inducible resin defences of *Pinus taeda*. *Ecology Letters*, 3(4), 329–339.

Luo, Y.-H., Sternberg, L., Suda, S., Kumazawa, S., and Mitsui, A., (1991). Extremely low D/H ratios of photoproduced hydrogen by cyanobacteria. *Plant Cell Physiology*, 32, 897–900.

Martin, D.M., Faldt, J., and Bohlmann, J., (2004). Functional characterization of nine Norway spruce TPS genes and evolution of gymnosperm terpene synthases of the TPS-d subfamily. *Plant Physiology* 135, 1908–1927.

Martin, D.M., Tholl, D., Gershenzonand, J., and Bohlmann, J., (2002). Methyl jasmonate induces traumatic resin ducts, terpenoid resin biosynthesis, and terpenoid accumulation in developing xylem of Norway spruce stems. *Plant Physiology* 129, 1003–1018.

Maulé, C. P., Chanasyk, D. S., and Muehlenbachs, K., (1994). Isotopic determination of snow-water contribution to soil water and groundwater. *Journal of Hydrology*, 155, 73–91.

McKellar R. C., Wolfe, A. P., Tappert, R., and Muehlenbachs, K., (2008). Correlation of Grassy Lake and Cedar Lake ambers using infrared spectroscopy, stable isotopes, and palaeoentomology. *Canadian Journal of Earth Sciences*, 45, 1061–1082.

McKellar, R. C., Wolfe, A. P., Muehlenbachs, K., Tappert, R., Engel, M. S., Cheng, T., Sánchez-Azofeifa, G. A., (2011). Insect outbreaks produce distinctive carbon isotope signatures in defensive resins and fossiliferous ambers. *Proceedings. Biological Sciences / The Royal Society*, 278(1722), 3219–24.

Moss, E., (1955). The vegetation of Alberta. *The Botanical Review*, 21(9), 494-567.

Nissenbaum, A., and Yakir, D., (1995). Stable Isotope Composition of Amber. *In* Amber, resinite and fossil resins (eds. K. B. Anderson & J. C. Crelling), 34–42. Washington, DC: American Chemical Society.

Nissenbaum, A., Yakir, D., and J. H. Langenheim (2005). Bulk carbon, oxygen, and hydrogen stable isotope composition of recent resins from amber-producing *Hymenaea*. *Die Naturwissenschaften*, 92(1), 26–29.

Olson, R., (1985). The climate of Edmonton. Climatological studies (37), The Climate of the Canadian Cities(2). p. 54. Environment Canada, Ottawa, Canada.

Orchard, K. A., Cernusak, L. A., and Hutley, L. B., (2010). Photosynthesis and water-use efficiency of seedlings from Australia monsoon forest, savanna and swamp habitats grown in a common garden. *Functional Plant Biology*, 37, 1050–1060.

Polissar, P. J., and Freeman, K.H. (2010). Effects of aridity and vegetation on plant-wax δD in modern lake sediments. *Geochimica et Cosmochimica Acta*, 74(57), 85–97.

Raczkowski, J., (1979). Swelling properties of bark. *Wood Science and Technology*, 13, 187–196.

Rohmer, M., (1999). A mevalonate-independent route to isopentenyl diphosphate. *In*: Cane, D. (ed.) Comprehensive Natural Product Chemistry, 2, 45–67. Pergamon Press, Oxford, UK.

Sachse, D., Radke, J., and Gleixner, G., (2006). δD values of individual n-alkanes from terrestrial plants along a climatic gradient—implications for the sedimentary biomarker record. *Organic Geochemistry*, 37(4), 69–83.

Sachse, D., Billault, I., Bowen, G.J., Chikaraishi, Y., Dawson, T. E., Feakins, S.J., Freeman, K.H., R. M., Clayton, McInerney, F.A., van derMeer, M.T.J., Polissar, P., Robins, R.J., Sachs, J.P., Schmidt, H-L., Sessions, A.L., White, J.W.C., West, J.B., and Kahmen, A., (2012). Molecular paleohydrology: interpreting the hydrogen-isotopic composition of lipid biomarkers from photosynthesizing organisms. *Annual Review of Earth and Planetary Sciences*, 40(1), 221–249.

Saurer, M., Siegwolf, R., and Schweingruber, F., (2004). Carbon isotope discrimination indicates improving water-use efficiency of trees in northern Eurasia over the last 100 years. *Global Change Biology*, 10(12), 2109–2120.

Shanahan, T. M., Hughen, K., A., and Ampel, L., (2013). Environmental controls on the $^{2}H/^{1}H$ values of terrestrial leaf waxes in the eastern Canadian Arctic. *Geochemica et Cosmochica Acta*. GCA 8289

Schmidt, H. L., Werner, R., and Eisenreich, W., (2003). Systematics of $^{2}H$ patterns in natural compounds and its importance for the elucidation of biosynthetic pathways. *Phytochemistry Reviews*, 2(1/2), 61–85.

Sessions, A., (2006). Seasonal changes in D/H fractionation accompanying lipid biosynthesis in *Spartina alterniflora*, *Geochimica et Cosmochimica Acta*, 70(9), 2153–2162.

Sessions, A. L., and Hayes, J. M., (2005). Calculation of hydrogen isotopic fractionations in biogeochemical systems. *Geochimica et Cosmochimica Acta*, 69(3), 593–597.

Sessions, A. L., Burgoyne, T. W., Schimmelmann, A., and Hayes, J. M., (1999). Fractionation of hydrogen isotopes in lipid biosynthesis, *Organic Geochemistry*, 30, 1193–1200.

Smith, F., and Freeman, K., (2006). Influence of physiology and climate on δD of leaf wax n-alkanes from C3 and C4 grasses, *Geochimica et Cosmochimica Acta*, 70(5), 1172–1187.

Spencer Environmental Management Services. "Mapped Vegetation of the Edmonton Area" [Map]. 1:1000 Edmonton, Alberta: Spencer Environmental Management Services, October 2006.

Strong, W. L., and Roi, G. H. L., (1983). Root-system morphology of common boreal forest trees in Alberta, Canada. *Canadian Journal of Forest Research*, 13, 1164–1173.

Tappert, R., McKellar, R. C., Wolfe, A. P., Tappert, M., Ortega-Blanco, J., and Muehlenbachs, K., (2013). Stable carbon isotopes of resin exudates record responses of C3 plants to changes in atmospheric oxygen since the Triassic. *Geochimica et Cosmochimica Acta*, 121, 240-262.

Terwilliger, V.J., and M.J., DeNiro, (1995). Hydrogen isotope fractionation in wood-producing avocado seedlings: biological constraints to paleoclimatic interpretations of δD values in tree ring cellulose nitrate. *Geochimica et Cosmochimica Acta*, 59, 5199–5207.

Valentini, R., Scarascia Mugnozza, G. E., and Ehleringer, J. R., (1992). Hydrogen and carbon isotope ratios of selected species of a Mediterranean macchia ecosystem. *Functional Ecology*, 6, 627–631.

Warren, C. R., McGrath, J. F., and Adams, M. A., (2001). Water availability and carbon isotope discrimination in conifers. *Oecologia*, 127, 426–86.

Weather station archive – Database. 2011 [Online] Available from: http://easweb.eas.ualberta.ca/weather_archive.php [Consulted in 2011].

White, J. W. C., Cook E. R., Lawrence J. R., and Broeker, W. S., (1985). The D/H ratios of the sap in trees: implications for water source and tree ring D/H ratios. *Geochimica et Cosmochimica Acta*, 49, 237–246.

Wolfe, A. P., Csank, A. Z., Reyes, A. V., McKellar, R. C., Tappert, R., and Muehlenbachs, K., (2012). Pristine Early Eocene wood buried deeply in kimberlite from northern Canada. *PloS One*, 7(9), e45537.

Yakir, D., and DeNiro, M. J., (1990). Oxygen and hydrogen isotope fractionation during cellulose metabolism in *Lemna gibba* L. *Plant physiology*, 93(1), 325–332.

Zhou, Y., Grice, K., Chikaraishi, Y., Stuart-Williams, H., Farquhar, G. D., and Ohkouchi, N., (2011). Temperature effect on leaf water deuterium enrichment and isotopic fractionation during leaf lipid biosynthesis: results from

controlled growth of C3 and C4 land plants. *Phytochemistry*, 72(2-3), 207–213.

Zulak, K. G., and Bohlmann, J., (2010). Terpenoid biosynthesis and specialized vascular cells of conifer defense. *Journal of integrative plant biology*, 52(1), 86–97.

Zulak, K. G., Lippert, D. N., Kuzyk, M. A, Domanski, D., Chou, T., Borchers, C. H., and Bohlmann, J. (2009). Targeted proteomics using selected reaction monitoring reveals the induction of specific terpene synthases in a multi-level study of methyl jasmonate-treated Norway spruce (*Picea abies*). *The Plant Journal*, 60(6), 1015–1030.

# CHAPTER 5

# Conclusions and recommendations for further work on amber stable isotopic composition

## 5.1. Conclusions of this research

In the past twenty years researchers have tried to assess the potential of the stable isotopic composition of amber as a paleoclimatic proxy, yet the isotopic variability in amber's deposits have not been fully constrained. Tappert et al. (2013) showed the applicability and reliability of the carbon isotopic values of ambers through time; but very few studies have used the deuterium content of amber as a paleohydrological indicator (*e.g.*, Wolfe et al., 2012). Before the deuterium isotopic composition of amber could become accepted as a paleoenvironmental proxy, further testing was required to determine the potential for post-depositional hydrogen isotope exchange between basinal waters and resins. Thus, this work achieved to validate amber as a reliable paleoclimatic indicator.

This thesis validates the potential of using amber for paleoclimatic studies in a twofold assessment. First, throughout an experimental approach, the hydrogen exchangeability of resins and ambers was measured under conditions simulating early diagenesis. The second approach included field-based measurements of the isotopic changes in resins over the growth season, in order to determine how these changes reflect the variable deuterium content of rainwater. Insights derived from both approaches are further explained in the following sections of this chapter.

5.1.1. Experimental component: Effects of early diagenetic condition on ambers and resins

A series of thermal hydrous exchange experiments between modern and fossil resins (ambers), and three different deuterated (D-enriched) waters, were conducted in order to simulate their behavior under progressive burial diagenetic conditions. Results of this experiment showed that at 50 ºC, the degree of exchange is 1.5% for resins and 0.5% for ambers. At 90 ºC, equivalent to ~3-4 km of burial, modern resins reported an average post-metabolic [$D_{w\text{-}resin}$] exchange of 1.9%, compared to only 0.5% for mature ambers. At both temperatures, samples reached a maximum saturation and relatively constant concentration after 30 days interacting with deuterated waters. Physical (thermal gravimetric) and chemical (IR spectrometry) analyses provided further evidence that suggested minimal diagenetic changes of initial (metabolic) resin deuterium values. Together these analyses showed that most ambient isotopic exchange occurs prior to the onset of resin polymerization.

Also, detailed analyses of the FTIR spectra from samples subjected to hydrous thermal alteration conditions for 240 days confirm the appearance of early diagenetic alteration compounds. The band ratio analyses (*i.e.*, 3400/3080, 1646/1450 and 924/887) showed an increase in unsaturation and decrease in oxygenated functionalities. Also, the appearance of a peak at 3080(76) $cm^{-1}$, related to aromatic functional groups, suggested the development of secondary acids. These developments were confirmed through cluster analyses between raw and thermally treated samples, together with biogenic and diagenetic derived acids. As a result, thermally treated resins and ambers grouped with diagenetic

derived acids, such as 7-oxodehydroabietic and dehydroabietic acid, which have been previously elucidated as secondary diagenetic products (Otto et al., 2001, 2002, 2007; Qin et al., 2010; 2012).

In addition, when hydrothermally treated samples were reacted with deuterated water; a distinctive peak change in the 1090–1468 $cm^{-1}$ region is considered indicative of deuterium incorporation. This effect, even when minor (<1.9 %), can be identified in the spectra of experimentally treated samples. However, samples that were subjected to temperatures up to 250 ºC showed only minor changes in their fingerprint region. This means that most of the tricyclic diterpenes' structures can be preserved within the polymeric matrix, as has been recently shown (*i.e.*, Dal Corso et al., 2013). Therefore, the experimental outcomes of diagenetic alteration of fossil resins under hydrous- and anhydrous thermal conditions suggested that ambers are reliable recorders of environmental δD of ancient waters.

5.1.2. Hydrogen isotopic composition of resins and their natural variability

The δD composition of plant-derived fossil resins (ambers) has been proven as a valuable paleoenvironmental indicator. However, a degree of uncertainty remained in the interpretation of the broad distribution of δD values that are typically observed within individual amber deposits. In order to obtain a better understanding of the biotic and abiotic (environmental) controls over the deuterium isotope fractionation of resins the fractionation behaviour of resins from modern conifers was further investigated.

Analyses were conducted to evaluate the hydrogen isotope composition of resins ($\delta D_{resin}$) sampled frequently throughout May to November 2011. Seven individual specimens of *Picea, Abies* and *Thuja* were studied in the vicinity of river valley at the University of Alberta North Campus area. Our results indicate that throughout the sampling interval the $\delta D_{resin}$ values showed a maximum variability of around 80‰ ($\delta D_{resin:}$ -261.9 to –341.9‰), which is comparable to the isotopic variability of the precipitation in Edmonton ($\delta D_{ppt:}$ -87 to –155‰). Therefore, the variability of $\delta D_{resin}$ reflects seasonal changes in the hydrogen isotopic composition of rainwater ($\delta D_{ppt}$), which indirectly fluctuates in response to temperature changes. The fractionation factor for hydrogen between resin and precipitation ($\varepsilon_{resin\text{-}ppt}$) is thereby -228 ± 19‰.

The field observations also indicate that injury-induced resins can record short-term weather fluctuations, as reflected by shifts in their isotope values registered within periods of 2–4 days after the injury and lasting from 3–15 days. This is also comparable with the response time after bark beetle attacks. Therefore, the variability in δD values often observed within individual amber deposits, therefore, may simply reflect the natural variation in meteoric events at the time of resin exudation and during the formation of the deposit.

## 5.2. Recommendations

### 5.2.1. Experimental component

This study opens a wide range of research opportunities based on both the experimental and field-based components. Within the experimental component,

molecular characterization can be applied to confirm the synthesis of diagenetically-derived molecules in thermally treated resins and ambers, such as those tentatively identified in Chapter 3 (via spectral FTIR band assignment). Because of the polymeric characteristic of resin and amber specimens, Time-of-Flight Secondary Ion Mass Spectrometry (ToF-SIMS) could be used as a potential technique to identify their molecular arrangement. Measurements using these novel methods can use biogenically-derived acids as standards, and thus compare resulting ionic arrangements with diagenetic compounds (*i.e.*, Sodhi et al., 2012).

5.2.2. Field component

On the other hand, within the field component, improvements in our observations could be achieved by randomly selecting angiosperm and gymnosperm resin producing trees located in an unperturbed area. This may allow us to reduce possible biases in tree response that can be related to their location and stress sources. Also, a bigger population would produce more robust results that can include biotic variables, such as: (1) position of the tree within the canopy; (2) possible effects of crown and bark growth; (3) effects of beetle reproductive cycle; and (4) effects of pathogens. In terms of additional work on abiotic variables, it would be desirable to have simultaneous measurements of the carbon isotopic composition of atmospheric $CO_{2\,(g)}$ and soil water through time, which could be included in the data set of variables evaluated in Chapter 4. In this regard, a simultaneous measurement of these isotopic variables could produce new insights into the likely relation between carbon isotopic fingerprint and individual stress sources, such as water deprivation and possible changes in water

sources. Additionally, this is an important factor to unveil the effects of these stress sources on stomatal conductance, and thus indirectly on plant water deuterium isotopic composition.

Considering all of the aforementioned factors in detail may provide a consistent data set that would allow us to model the possible isotopic responses of tree resins when the trees are subjected to different stress sources. The ability to determine the relationship between the mechanisms that regulate carbon intake and newly synthetized carbohydrate relocation would allow us to better understand the mechanisms that control the stable isotopic fingerprint in resins. Also, utilizing isotopic labeling would help differentiate and trace the possible natural deuterium pools of soil and leaf water, and their relation with primary precipitation deuterium composition, in order to improve the use of amber specimens as valuable paleoenvironmental indicators.

## 5.3. References


Dal Corso, J, Roghi, G., and Ragazzi E., (2013). Physico-chemical analysis of Albian (Lower Cretaceous) amber from San Just (Spain): implications for palaeoenvironmental and palaeoecological studies. *Geologica Acta*, (11), 359–370.

Otto, A., Simoneit, B. R. T., Lesiak, M., Wilde, V., Worobiec, G., (2001). Resin and wax biomarkers preserved in Miocene Cupressaceae s.1. from Belchatow and Lipnica Wielka, Poland. *Acta Palaeobotanica*, 41, 195–206.

Otto, A., Simoneit, B. R. T., and Wilde, V., (2007). Terpenoids as chemosystematic markers in selected fossil and extant species of pine (*Pinus* , *Pinaceae* ). *Botanical Journal of the Linnean Society*, 154, 129–140.

Otto, A., Simoneit, B. R.T, Wilde, V., Kunzmann, L., and Püttmann, W., (2002). Terpenoid composition of three fossil resins from Cretaceous and Tertiary conifers. *Review of Palaeobotany and Palynology*, 120 (3–4), 203–215.

Qin, S. J., Sun, Y. Z., Tang, Y. G., (2010). Long term, low temperature maturation of early diagenetic alterations of organic matter from conifers: aliphatic hydrocarbons. *Geochemical Journal*, 44, 247–259.

Qin, S.J., Sun, Y. Z., Tang, Y. G., and Jin, K., (2012). Early diagenetic transformation of terpenoids from conifers in the aromatic hydrocarbon fraction: a long term, low temperature maturation experiment. *Organic Geochemistry*, 53, 99–108.

Sodhi, R. N. S., Mims, C. A., Goacher, R. E., McKague, B., Wolfe, A. P., (2013). Preliminary characterization of Palaeogene european ambers using ToF-SIMS. *Surface and Interface Analysis*, 45(1), 557–560.

Tappert, R., McKellar, R. C., Wolfe, A. P., Tappert, M. C., Ortega-Blanco, J., Muehlenbachs, K., (2013). Stable carbon isotopes of C3 plant resins and ambers record changes in atmospheric oxygen since the Triassic. *Geochimica et Cosmochimica Acta*, 121, 240–262.

Wolfe, A. P., Csank, A. Z., Reyes, A. V., McKellar, R. C., Tappert, R., and Muehlenbachs, K., (2012). Pristine Early Eocene wood buried deeply in kimberlite from northern Canada. *PloS One*, *7*(9), e45537.

**Appendix 1. Supplementary material of Chapter 2.**

Appendix 1-1. Condition during TGA analyses. Isothermal (3, 4) and non-isothermal (2, 4) analyses of resin and amber products of hydrothermal experiments.

| Method Log (TGA experiment) |
| --- |
| 1: Equilibrate at 30.00 °C |
| 2: 5.00°C/min to 50.00 °C |
| 3: Isothermal for 60.00 min |
| 4: 5.00°C/min to 90.00 °C |
| 5: Isothermal for 60.00 min |
| 6: 5.00°C/min to 250.00 °C |
| 7: End of method |

Appendix 1-2. $\delta^{13}C$ isotopic composition of resins and ambers after time-series hydrous-thermal maturation experiments and thermal anhydrous treatment (TGA).

| | | Deuterated waters | $[D_w]$ 0.25 % | $[D_w]$ 0.5 % | $[D_w]$ 1 % | $[D_w]$ 0.25 % | $[D_w]$ 0.5 % | $[D_w]$ 1 % | Characterization | Sample description and observation (colour, mophology changes) |
|---|---|---|---|---|---|---|---|---|---|---|
| **Sample** | **Replicates*** | **$\delta^{13}C_{resin}$ (VPDB) ‰** | **$\delta^{13}C_{resin}$ (VPDB) ‰** | **$\delta^{13}C_{resin}$ (VPDB) ‰** | **$\delta^{13}C_{resin}$ (VPDB) ‰** | **$\delta^{13}C_{resin}$ (VPDB) ‰** | **$\delta^{13}C_{resin}$ (VPDB) ‰** | **$\delta^{13}C_{resin}$ (VPDB) ‰** | **TGA* $\delta^{13}C_{resin}$ (VPDB) ‰** | |
| HC-BE | 6 | -27.96 | - | - | - | - | - | - | - | Pale yellow (translucide slices). |
| MG-BE | 5 | -27.13 | - | - | - | - | - | - | - | Yellow resin (translucide slices). Chips. |
| DA-BE | 10 | -25.51 | - | - | - | - | - | - | - | Golden yellow (translucide, no inclussions). |
| GLA-BE | 3 | -22.18 | - | - | - | - | - | - | - | Dark orange (translucide, no inclussions). |
| HC-5.DW | 2 | -28.01 | - | - | - | - | - | - | - | Pale yellow (whitish-milky, foamy structure). |
| MG-5.DW | 2 | -27.15 | - | - | - | - | - | - | - | Yellow resin (Opaque, milky, foamy structure). |
| DA-5.DW | 2 | -25.67 | - | - | - | - | - | - | - | Golden yellow (translucide, no inclussions). |
| GLA-5.DW | 2 | -22.30 | - | - | - | - | - | - | - | Dark orange (translucide, no inclussions). |
| HC-5 | 12 | - | -28.00 | -26.68 | -28.00 | -27.91 | -28.78 | -24.86 | - | Pale yellow (whitish-milky, foamy structure). Stalacmite morfology. |
| MG-5 | 15 | - | -26.17 | -26.09 | -25.97 | -27.90 | -25.31 | -27.19 | - | Yellow resin (Opaque, milky, foamy structure). Spherical shape. |
| DA-5 | 12 | - | -25.33 | -25.12 | -25.94 | -25.33 | -25.67 | -25.67 | - | Golden yellow (translucide, no inclussions). |
| GLA-5 | 12 | - | -22.47 | -22.98 | -22.52 | -22.97 | -24.64 | -22.71 | - | Dark orange (translucide, no inclussions). |
| HC-15 | 12 | - | -26.19 | -27.97 | -27.93 | -27.86 | -27.81 | -28.58 | - | Pale yellow (whitish-milky, foamy structure). Spherical shape agregates. |
| MG-15 | 15 | - | -27.53 | -26.79 | -26.45 | -26.09 | -25.58 | -25.97 | - | Yellow resin (Opaque, milky, foamy structure). Spherical shape. |
| DA-15 | 13 | - | -25.49 | -25.22 | -25.24 | -25.29 | -25.26 | -25.44 | - | Golden yellow (translucide). No observed chnages. |
| GLA-15 | 13 | - | -25.19 | -23.56 | -22.97 | -24.97 | -22.43 | -21.66 | - | Dark orange (translucide). |
| HC-30 | 18 | - | -28.70 | -27.76 | -28.35 | -28.62 | -28.58 | -28.07 | - | Pale yellow (whitish-milky, foamy structure). Drop - stalacmite shape. |
| MG-30 | 18 | - | -26.34 | -26.92 | -27.04 | -25.89 | -26.68 | -25.29 | - | Yellow resin (Opaque, milky, foamy structure). Spherical shape. |
| DA-30 | 18 | - | -24.18 | -25.49 | -25.24 | -25.35 | -25.67 | -25.29 | - | Golden yellow (translucide, no inclussions). |
| GLA-30 | 15 | - | -23.39 | -22.30 | -22.21 | -22.83 | -21.41 | -21.17 | - | Dark orange (translucide). |
| HC-60 | 16 | - | -27.86 | -28.23 | -28.62 | -27.99 | -28.28 | -28.35 | - | Pale yellow (whitish-milky, foamy structure). |
| MG-60 | 16 | - | -26.31 | -26.89 | -25.94 | -28.08 | -26.74 | -25.27 | - | Yellow resin (Opaque, milky, foamy structure). |
| DA-60 | 16 | - | -25.26 | -25.10 | -25.41 | -25.44 | -25.94 | -25.52 | - | Golden yellow (translucide). |
| GLA-60 | 16 | - | -20.98 | -21.24 | -23.06 | -20.97 | -24.31 | - | - | Dark orange (translucide). |
| HC-240 | 9 | - | -27.81 | -28.51 | -28.01 | -28.71 | - | -28.78 | -28.73 | Intense yellow resin (Opaque, foamy structure). Spherical shape. After TGA treatment, vitreous aparance, transparent.Glass transition reach after 200 °C |
| MG-240 | 11 | - | -26.94 | -27.23 | -27.34 | -27.10 | -26.63 | -27.10 | -27.43 | Whitish-milky, foamy structure. After TGA treatment, vitreous aparance, transparent. Melting point reach after 200 °C. |
| DAS-240 | 10 | - | -25.43 | -25.22 | -25.43 | -25.15 | -25.41 | -25.42 | -25.22 | Yellow-dark orange (translucide). No observed chnages. Water inclusions. After TGA treatment, vitreous aparance, transparent. Glass transition reach after 200 °C. |
| GLA240 | 18 | - | -23.00 | -21.69 | -21.13 | -21.33 | -23.12 | -23.56 | -23.55 | Dark orange (Milky veins). Alteration surface. After TGA treatment, vitreous aparance, transparent. Glass transition reach after 200 °C. |
| HC-365 | 12 | - | -28.36 | -28.49 | -28.08 | -28.36 | -28.45 | -28.67 | - | Dark orange-yellow (opaque, foamy structure). Spherical shape. |
| MG-365 | 8 | - | -26.94 | -27.09 | -26.17 | -26.60 | -26.55 | -25.35 | - | Whitish-milky, foamy structure. Water inclussions. |
| DA-365 | 8 | - | -25.42 | -25.44 | -25.37 | -25.33 | -25.67 | -25.25 | - | Yellow-dark orange (translucide). Some with alteration foamy surface. |
| GLA-365 | 18 | - | -21.33 | -22.30 | -23.39 | -24.28 | -24.64 | -22.60 | - | Dark orange, whitish veins (development of alteration surface, molten bone, water inclution). |

**Appendix 2. Supplementary material of Chapter 4.**

Appendix 2-1. Mean annual precipitation ($\delta D_{ppt}$) in the Edmonton area. Comparison between estimates data taken from IAEA (1969, 1970) and the Online Isotopes in Precipitation Calculator version 2.2 (Bowen, 2009; Bowen and Revenaugh, 2003).

| | $\delta D_{ppt}$ [1, 2] (VSMOW) ‰ | $\delta D_{ppt}$ [3, 4] (VSMOW) ‰ | $\Delta D_{ppt}$ (VSMOW) ‰ |
|---|---|---|---|
| May | -126 | -97 | 29 |
| Jun | -106 | -87 | 19 |
| Jul | -100 | -89 | 11 |
| Aug | -115 | -93 | 22 |
| Sept | -120 | -101 | 19 |
| Oct | -124 | -121 | 3 |
| Nov | -179 | -155 | 24 |

[1, 2] Data from IAEA (1969, 1970)

[3, 4] Data from Bowen, (2009); Bowen and Revenaugh, (2003)

Appendix 2-2. Calculated carbon isotopic discrimination ($\Delta$), rate of intercellular to ambient $CO_2$ fraction ($c_i/c_a$), and water use efficiency (WUE). Carbon isotopic discrimination was determined between mean monthly resins ($\delta^{13}C_{resin}$) and atmospheric ($\delta^{13}C_a$) (data from Cuntz, 2011). Intercellular $CO_{2(g)}$ was determined using mean monthly atmospheric $CO_2$ (g) concentration in 2011 ($C_a^*$-data taken from Keeling et al., 2005). WUE data per tree were determined using calculate intercellular and atmospheric $CO_2$(g) concentration. Calculated $c_i/c_a$ ratio was compare with instantaneous $c_i/c_a^*$ of seedlings grown under well-watered conditions (Orchard et al., 2010 and references therein).

| | ***Picea mariana* (black spruce), PM31** | | | | | | |
|---|---|---|---|---|---|---|---|
| **Month** | **$\delta^{13}C$** (VPDB)‰ | **$\Delta\delta 13C_{resin\text{-}a}$** (VPDB) ‰ | **$C_i$** (ppm) | **WUE** (ppm) | **WUE** (µmol/mol) | **$C_i / C_a$** | **$C_i / C_a$[(1)]** |
| **(1) May** | -24.2 | 16.6 | 211.2 | 113.4 | 40.8 | 0.54 | 0.6 |
| **(2) June** | -24.7 | 17.1 | 220.5 | 107.0 | 38.5 | 0.56 | 0.6 |
| **(3) July** | -24.3 | 17.7 | 213.0 | 112.4 | 40.4 | 0.52 | 0.6 |
| **(4) August** | -24.6 | 17.0 | 217.5 | 108.6 | 39.1 | 0.60 | 0.6 |
| **(5) September** | -24.7 | 17.1 | 220.6 | 107.0 | 38.5 | 0.60 | 0.6 |
| **(6) October** | -24.7 | 17.1 | 220.7 | 107.6 | 38.8 | 0.60 | 0.6 |
| **(7) November** | - | - | - | - | - | - | - |
| **$C_a^{(*)}$** (ppm) | ***Picea mariana* (black spruce), PM197** | | | | | | |
| 392.7 (1) | -26.5 | 18.9 | 252.3 | 87.8 | 31.6 | 0.61 | 0.7 |
| 391.6 (2) | -26.4 | 18.8 | 250.2 | 88.4 | 31.8 | 0.61 | 0.6 |
| 392.7 (3) | -27.2 | 19.7 | 266.5 | 78.9 | 28.4 | 0.70 | 0.7 |
| 391.2 (4) | -26.7 | 19.2 | 255.6 | 84.8 | 30.5 | 0.70 | 0.7 |
| 391.8 (5) | -27.4 | 19.9 | 268.7 | 77.0 | 27.7 | 0.65 | 0.7 |
| 392.9 (6) | -27.4 | 19.9 | 269.3 | 77.3 | 27.8 | 0.65 | 0.7 |
| 393.8 (7) | - | - | - | - | - | - | - |

| | | | | | | | |
|---|---|---|---|---|---|---|---|
| Zone 1 | ***Picea mariana* (Mill.) B.S.P. (black spruce), PM404** | | | | | | |
| **(1)** | -27.2 | 19.7 | 266.3 | 79.0 | 28.4 | 0.68 | 0.7 |
| **(2)** | -26.6 | 19.1 | 254.6 | 85.6 | 30.8 | 0.65 | 0.7 |
| **(3)** | -26.4 | 18.9 | 252.3 | 87.8 | 31.6 | 0.64 | 0.7 |
| **(4)** | -26.4 | 18.8 | 250.1 | 88.2 | 31.8 | 0.64 | 0.6 |
| **(5)** | -25.8 | 18.2 | 239.3 | 95.4 | 34.3 | 0.61 | 0.6 |
| **(6)** | -25.3 | 17.7 | 231.1 | 101.1 | 36.4 | 0.59 | 0.6 |
| **(7)** | - | - | - | - | - | - | - |
| Zone 2 | ***Picea pungens* (blue spruce), BS** | | | | | | |
| **(1)** | -26.7 | 19.2 | 256.8 | 84.9 | 30.6 | 0.65 | 0.7 |
| **(2)** | -26.7 | 19.2 | 256.0 | 84.8 | 30.5 | 0.65 | 0.7 |
| **(3)** | -25.9 | 18.4 | 242.5 | 93.9 | 33.8 | 0.62 | 0.6 |
| **(4)** | -26.6 | 19.0 | 253.5 | 86.0 | 31.0 | 0.65 | 0.7 |
| **(5)** | -25.7 | 18.2 | 238.6 | 95.8 | 34.5 | 0.61 | 0.6 |
| **(6)** | -25.9 | 18.3 | 242.1 | 94.2 | 33.9 | 0.62 | 0.6 |
| **(7)** | -25.2 | 17.7 | 230.9 | 101.8 | 36.7 | 0.56 | 0.6 |
| | ***Picea glauca* (white spruce), WS** | | | | | | |
| **(1)** | - | - | - | - | - | - | - |
| **(2)** | - | - | - | - | - | - | - |
| **(3)** | -26.3 | 18.7 | 249.3 | 89.7 | 32.3 | 0.63 | 0.6 |
| **(4)** | -24.6 | 17.0 | 217.9 | 108.3 | 39.0 | 0.56 | 0.6 |
| **(5)** | -25.6 | 18.0 | 235.6 | 97.7 | 35.2 | 0.60 | 0.6 |
| **(6)** | -23.8 | 16.1 | 204.1 | 118.0 | 42.5 | 0.52 | 0.5 |
| **(7)** | -24.6 | 16.9 | 218.7 | 109.5 | 39.4 | 0.60 | 0.6 |

| | | | | | | | |
|---|---|---|---|---|---|---|---|
| Zone 3 | ***Abies balsamea*[+] , ABM** | | | | | | |
| **(1)** | -26.7 | 18.5 | 244.1 | 92.9 | 33.4 | 0.70 | 0.7 |
| **(2)** | -26.7 | 18.5 | 243.5 | 92.6 | 33.3 | 0.70 | 0.7 |
| **(3)** | -25.9 | 17.7 | 230.3 | 101.5 | 36.6 | 0.59 | 0.6 |
| **(4)** | -26.6 | 18.4 | 241.5 | 93.6 | 33.7 | 0.62 | 0.7 |
| **(5)** | -25.7 | 17.5 | 226.3 | 103.5 | 37.3 | 0.58 | 0.6 |
| **(6)** | -25.9 | 17.7 | 230.4 | 101.6 | 36.6 | 0.59 | 0.6 |
| **(7)** | -25.4 | 17.1 | 222.1 | 107.3 | 38.6 | 0.56 | 0.6 |
| | ***Thuja occidentalis* L., TOL** | | | | | | |
| **(1)** | - | - | - | - | - | - | - |
| **(2)** | -26.7 | 18.5 | 243.5 | 92.6 | 33.3 | 0.70 | 0.7 |
| **(3)** | -25.9 | 17.7 | 230.3 | 101.5 | 36.6 | 0.59 | 0.6 |
| **(4)** | -26.6 | 18.4 | 241.5 | 93.6 | 33.7 | 0.62 | 0.7 |
| **(5)** | - | - | - | - | - | - | - |
| **(6)** | - | - | - | - | - | - | - |
| **(7)** | -25.2 | 17.0 | 218.7 | 109.5 | 39.4 | 0.56 | 0.6 |

[+] Tree removed from the study area

[(*)] Data taken from Keeling et al., (2005)

[(1)] Data taken from Orchard et al., (2010)

Appendix 2-3. Deuterium isotopic composition of Maastrichtian ambers from Edmonton River Valley, Drumheller Valley and Morrin Bridge deposits locate in Alberta area. See text for details.

| | $\delta D^{(1)}_{amber}$ (VSMOW) ‰ | $\delta D_{mean\ amber}$ (VSMOW) ‰ | σ | $\delta D_{ppt}$ (VSMOW) ‰ |
|---|---|---|---|---|
| Edmonton, River valley | | | | |
| ERV1 | -349 | -344 | 4 | -150 |
| ERV2 | -339 | | | |
| ERV3 | -344 | | | |
| ERV4 | -343 | | | |
| ERV5 | -347 | | | |
| ERV6 | -339 | | | |
| Drumheller Valley amber | | | | |
| DV1 | -321 | -321 | 8 | -120 |
| DV2 | -328 | | | |
| DV3 | -328 | | | |
| DV4 | -315 | | | |
| DV5 | -325 | | | |
| DV6 | -308 | | | |
| Morrin Bridge Crossing amber | | | | |
| MUC1 | -297 | -290 | 16 | -80 |
| MUC2 | -312 | | | |
| MUC3 | -302 | | | |
| MLC1 | -270 | | | |
| MLC2 | -281 | | | |
| MLC3 | -277 | | | |

(1) Data from McKellar et al., (2008)